ISSN 1023-9855

Thoracic Medicine

Volume 37 • Number 4 • December 2022

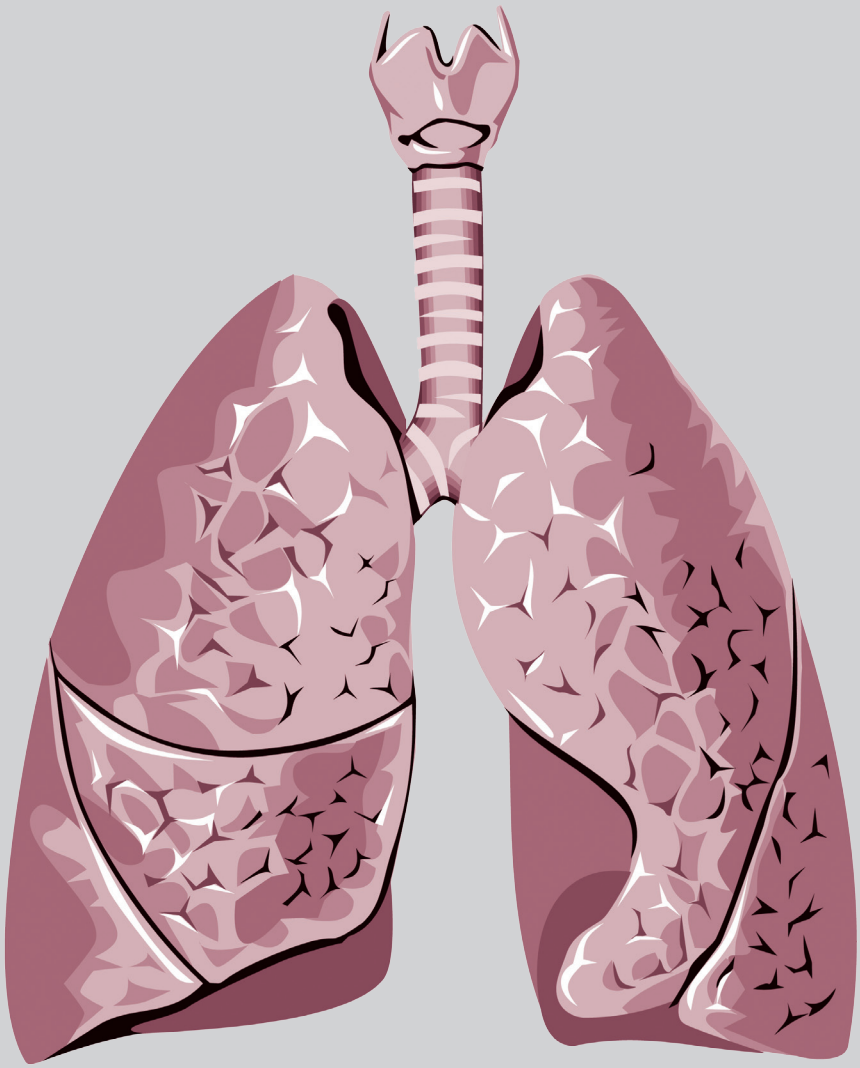

The Official Journal of

Taiwan Society of Pulmonary and Critical Care Medicine

Taiwan Society of Sleep Medicine

Taiwan Society for Respiratory Therapy

Taiwan Society of Tuberculosis and Lung Diseases

Thoracic Medicine

The Official Journal of
Taiwan Society of Pulmonary and Critical Care Medicine
Taiwan Society for Respiratory Therapy
Taiwan Society of Sleep Medicine
Taiwan Society of Tuberculosis and Lung Diseases

Thoracic Medicine

The Official Journal of
Taiwan Society of Pulmonary and Critical Care Medicine
Taiwan Society for Respiratory Therapy
Taiwan Society of Sleep Medicine
Taiwan Society of Tuberculosis and Lung Diseases

Volume 37
Number 4
December 2022

CONTENTS

Clinical Weaning Factors for Prolonged Mechanical Ventilation Patients: A Retrospective Study in Central Taiwan

Tao-An Chen[1], Chang-Sheng Lin[2,3], Chung-Yu Huang[4], Szu-Chi Pai[1], Ya-Ting Chuang[5], Chieh-Hui Lin[2]

Introduction: Mechanical ventilation is the most commonly used short-term life support technique in the world. But, about 5-10% of mechanical ventilation patients will progress from acute to chronic critical illness and require prolonged mechanical ventilation (PMV). Only 50% of these PMV patients are successfully liberated from mechanical ventilation. Therefore, improving the successful weaning rate and determining the influencing factors are important issues. This study aimed to analyze the factors for successful weaning of respiratory care center (RCC) patients and to determine the important weaning factors in PMV patients.

Methods: This was a single-center, retrospective study with 65 patients. This study collected and analyzed patients over the age of 20 in the RCC from October 2019 to August 2020.

Results: We found that patients who were successfully weaned from the ventilator had higher Glasgow Coma Scale (GCS) scores, and higher free thyroid (free T4), albumin and calcium levels on admission. In addition, they had lower APACHE II scores, C-reactive protein (CRP), and aspartate aminotransferase on admission. The patients also had higher systolic blood pressure before extubation, higher arterial carbon dioxide partial pressure ($PaCO_2$) after extubation, and high average albumin and average prealbumin values at the RCC.

Conclusion: We found that APACHE II scores, GCS scores, albumin, calcium, CRP, free T4, GOT are important weaning factors for patients admitted to the RCC. Systolic blood pressure and $PaCO_2$ are important influencing factors before and after the patient is released from the ventilator. In addition to this, average albumin and prealbumin are important weaning maintenance factors when PMV patients are in the RCC. ***(Thorac Med 2022; 37: 256-265)***

Key words: Prolonged mechanical ventilation, weaning, respiratory care center

[1]Division of Respiratory Therapy, Department of Chest Medicine, Show Chwan Memorial Hospital, Changhua, Taiwan, [2]Department of Chest Medicine, Show Chwan Memorial Hospital, Changhua, Taiwan, [3]Department of Nursing, Hung Kuang University, Taichung, Taiwan, [4]Department of Nephrology, Show Chwan Memorial Hospital, Changhua, Taiwan, [5]Surgical Intensive Care Unit, Show Chwan Memorial Hospital, Changhua, Taiwan
Address reprint requests to: Dr. Chieh-Hui Lin, No. 542, Sec. 1, Zhongshan Rd., Changhua City, Changhua County 500009, Taiwan (R.O.C.)

Introduction

Mechanical ventilation (MV) is the most commonly used short-term life support technique in the world, and is used for a wide range of indications [1]. But, about 5-10% of patients will progress from acute to chronic critical illness and require prolonged mechanical ventilation (PMV) [2]. PMV is usually defined as the need for MV for more than 21 days [3]. This progression may be due to some patients having unbalanced respiratory loading and muscle function because of their own disease and physical status while they are being weaned from the ventilator [4]. In the past, these patients would only stay in the intensive care unit (ICU) and use emergency and critical illness resources. The final choice for these patients was to provide longer-term ventilation support at home or in a nursing home.

With the positive ICU management attitude and consideration of overall social cost-effectiveness of recent years, this past procedure may no longer be suitable for patients with certain diseases. As a result, special ventilator-training units, which are more cost-effective and can better meet the needs of certain patients, have been set up [5]. In this specialized and special respiratory care unit, the success rate of ventilator weaning is higher, and the complications and mortality rate are lower [6].

During the 1990s in Taiwan, due to long-term use of ventilators in the ICU, the unequal distribution of emergency and intensive medical resources resulted in many medical difficulties. After years of investigation by experts, a national pilot project was started in Taiwan during the year 2000, namely the Integrated Delivery System (IDS) for patients dependent on the ventilator, which divides patients into 4 stages according to the number of days they use ventilators. With that, the Respiratory Care Center (RCC), which connected acute to chronic critical illness and was specially designed for PMV weaning, was established. But, in 2015, a study specifically pointed out that the pooled mortality of PMV patients at 1 year was 62%, and pooled mortality at hospital discharge was 29%. Only 50% were successfully liberated from MV [7]. As such, improving the successful weaning rate and determining the influencing factors has become an important issue. Unfortunately, various clinical studies are not clear about the prognosis and value of different indicators [8]. Therefore, we used the various clinical values and indicators of RCC patients in our hospital to analyze the factors of successful weaning among PMV patients in the RCC.

Materials and methods

Study population

This retrospective study included patients older than 20 years of age from October 1, 2019 to August 30, 2020 in a regional hospital in central Taiwan. The patients were hospitalized due to PMV and difficult weaning. They transferred to the RCC for active weaning and were screened for enrollment. PMV was defined as MV use for more than 21 days. Meanwhile, we know from the IDS system that RCC care is the second stage for patients at 21–63 days. In the RCC, 24-hour vital sign monitoring and care is performed. The definition of successful weaning from the ventilator is when the patient is liberated from MV for more than or equal to 5 consecutive days. And if, on the first day up to the fifth day, the ventilator is used for less than 6 hours, that day can be regarded as not using the MV. We divided the patients into 2 groups

according to whether they were successfully weaned or not. Conversely, if the patient was reintubated, received non-invasive ventilation, or died within 5 days of being weaned, the patient was designated into a failure group.

In the process of weaning while in the RCC, we did not use a special ventilation mode, and only used a conventional ventilation mode and spontaneous breathing trial for weaning training. And, we did not routinely perform additional chest rehabilitation for patients. Unless the patient had pneumonia or sputum accumulation, we would actively intervene in chest physical therapy. No matter the cause of respiratory failure, our primary goal was that the tidal volume reflected by the patient could reach more than 8 ml/kg (ideal body weight, IBW), and our secondary goal was to avoid hypoxemia or acute respiratory acidosis during weaning. Finally, we adjusted the time appropriately during the spontaneous breathing trial, so that the patient maintained enough respiratory muscle strength that there would be no drastic changes in heart rhythm or breathing pattern, thereby avoiding any possibility of exacerbating respiratory failure.

Data collection and clinical outcomes

We collected the baseline characteristics of the patients during the first 3 days of admission by reviewing the hospital information system. These characteristics included the APACHE II score, Glasgow Coma Scale (GCS) score, age, and laboratory data, which comprised the complete blood count (CBC), electrolytes, liver function, inflammatory biomarkers, renal function and thyroid function. We also recorded the cuff leak test, whether tracheostomy was performed or not, vital signs and weaning parameters before liberation from MV. We made sure that the patient passed the cuff leak test before extubation, and collected arterial blood gas (ABG) after extubation. We ensured that arterial blood was drawn from the patients within 30 to 60 minutes after extubation and placed a sample in an ice bath, and the analysis was performed within no more than 15 minutes from collection. Arterial blood was collected at least 20 minutes from the last suction, and inhaled drugs were considered only after arterial blood analysis. Clinical outcomes included weaning rate and analysis of the good weaning characteristics and indexes of the RCC patients who were successfully weaned from the ventilator in our hospital.

Statistical analysis

All data are expressed as mean ± standard deviation (SD) or percentage. We used the Mann Whitney U test to analyze and compare continuous variables between the 2 groups, and used Pearson's $\chi 2$ test or Fisher's exact test with categorical variables. A p value of <0.05 using a 2-sided test was considered statistically significant. All statistical analyses were performed using SPSS software, version 22.0 (SPSS Inc., Chicago, IL, USA).

Ethics approval and consent to participate

The Institutional Review Board of Show Chwan Memorial Hospital (1091002) approved the study. Since this was a retrospective study, the requirement for informed consent was remitted.

Results

From October 2019 to August 2020, we recruited 65 participants who transferred to the RCC for PMV weaning. The baseline character-

Table 1. Baseline Characteristics

Characteristics	Values
Subject, N	65
Age	
Median y (range)	73(24-91)
Average y	73.8
Sex, n(%)	
Male	38(58.5)
Female	27(41.5)
Main diagnosis, n(%)	
Medical	29(44.6)
Surgical	36(55.4)
Weaning success or not, n(%)	
Success	45(69.2)
Failure	20(30.8)
Duration of RCC	
Median d (range)	22(5-41)
Average d	24.6
Tracheostomy or not while trans out RCC, n(%)	
Yes	13(20)
No	52(80)

istics of the patient population are summarized in Table 1. The etiologies of respiratory failure in these PMV patients were abnormities of the alveoli (56.9%), central nervous system (CNS) conditions (41.5%), and disorders of the peripheral nervous system (1.6%). The average length of time in the RCC for these patients was 24.6 days, and 13 (20%) patients had tracheostomy. The successful weaning rate was 69.2%.

Of the 65 enrolled patients, 45 were successfully weaned (69.2%) and 20 failed weaning (30.8%). We found that the successful weaning group at the time of admission had a higher GCS score (7.27±2.73 vs. 5.22±2.82, p=0.01), a lower APACHE II score (20.44±3.47 vs. 26.3±3.36, p<0.001), a higher than normal free thyroid (free T4) value (0.97±0.25 vs. 0.78±0.17, p=0.027), a higher albumin value (3.09±0.44 vs. 2.6±0.46, p=0.001), higher calcium (8.67±0.77 vs. 8.23±0.81, p=.042), a lower C-reactive protein (CRP) value (3.57±3.34 vs. 6.36±4.25, p=0.02), lower aspartate transaminase (SGOT) (40.63±27.07 vs. 76±41.28, p=0.001), higher systolic blood pressure before extubation (136.07±18.35 vs. 119.71±14.67, p=0.044), normal high arterial carbon dioxide partial pressure after extubation ($PaCO_2$) (41.32±5.08 vs. 32.95±5.19, p=0.012), and higher average albumin (3.17±0.42 vs. 2.64±0.38, p <0.001) and average prealbumin

Table 2. Comparison of the Factors of Weaning

	Weaning success (N=45)	Weaning failure (N=20)	*P* value
Age	70±14.28	74.25±10.42	0.312
APACH-II	20.44±3.47	26.3±3.36	<0.001*
HR (bpm)	86.56±14.86	80.71±14.69	0.321
SBP (mmHg)	136.07±18.35	119.71±14.67	0.044*
DBP (mmHg)	130.49±18.77	134.71±15.17	0.376
RR (bpm)	17.6±5.5	19.57±2.99	0.139
SpO_2 (%)	98.51±1.27	98.86±1.07	1.539
GCS	7.27±2.73	5.22±2.82	0.01*
ABG(after extubation)			
pH	7.45±0.04	7.47±0.04	0.391
$PaCO_2$ (mmHg)	41.32±5.08	32.95±5.19	0.012*
PaO_2 (mmHg)	152.66±58.33	161.6±29.85	0.629
HCO_3- (mmol/L)	27.92±4.14	23.3±4.08	0.051
BE (mmol/L)	3.52±3.99	-0.03±4.01	0.114
SaO_2 (%)	98.42±1.66	99.15±0.17	0.344
Weaning Profile			
Pimax (cmH_2O)	-36.18±13.08	-29.33±12.49	0.092
Pemax (cmH_2O)	44.93±16.91	36.67±16.31	0.134
Spontaneous rate (bpm)	21.55±5.94	22.11±4.01	0.569
MV (L)	5.84±2.35	5.59±2.34	0.615
RSBI	85.13±31.75	96.33±36.25	0.502
Spontaneous Vt (ml)	270.45±84.5	250±85.66	0.302
Cuff leak test (ml)	258.95±129.74	380±90.83	0.058
CBC			
WBC (/uL)	11252.58±5260.7	17100.5±20246.72	0.201
RBC (10^4/uL)	343.58±68.75	346.7±61.75	0.491
Hb (g/dL)	10.33±1.5	9.71±1.56	0.075
Thyroid function			
TSH (ul U/ml)	2.98±3.46	65.44±219.01	0.674
Free T4 (ng/dL)	0.97±0.25	0.78±0.17	0.027*
Cortisol (ug/dL)	10.99±5.88	9.93±4.88	0.589
Liver function			
AST(GOT)(U/L)	40.63±27.07	76±41.28	0.001*
ALT(GPT)(U/L)	37.86±21.73	38.62±30.62	0.811
Bilirubin direct (mg/dL)	0.15±0.07	2.23±2.95	0.374
Bilirubin total (mg/dL)	0.5±0.36	2.3±2.83	0.481
Renal fuction			
BUN (mg/dL)	40.27±30.3	40.63±29.3	0.697
Creatinine (mg/dL)	1.18±1.13	1.47±1.4	0.44
eGFR (ml/min/1.73)	99.51±59.7	86.11±59.59	0.411
Albumin (gm/dL)	3.09±0.44	2.6±0.46	0.001*
average Albumin (gm/dL)	3.17±0.42	2.64±0.38	<0.001*
Prealbumin (gm/dL)	23.74±9.51	19.92±9	0.214
average Prealbumin (gm/dL)	24.09±7.32	18.4±7.53	0.018*
Electrolyte			
Sodium (mmol/L)	139.02±6.32	140.65±8.47	0.413
Potassium (mmol/L)	3.88±0.56	3.94±0.6	0.831
Calcium (mg/dL)	8.67±0.77	8.23±0.81	0.042
Phosphorus (mg/dL)	3.36±1.08	3.48±1.38	0.515
Magnesium (mg/dL)	2.13±0.53	2.3±0.37	0.115
Inflammatory biomarkers			
PCT(Procalcitonin)(ng/mL)	0.36±0.81	1.03±1.42	0.062
CRP(C-Reactive Protein)(mg/dL)	3.57±3.34	6.36±4.25	0.02*
Lactate (mg/dL)	13.73±7.5	11.7±3.82	0.637

Data were expressed as mean ± SD

* $p<0.05$, represented a significant difference between weaning success and failure

(24.09±7.32 vs. 18.4±7.53, p=0.018) (Table 2). In addition, we conducted an analysis of the relationship between successful weaning and tracheotomy, and found that there was no significant (p=0.051) relationship between the 2 factors.

Discussions

In this study, we investigated the important clinical indicators for patients who have required PMV when they are weaning. We determined that a number of factors, including APACHE II score, GCS score, systolic blood pressure, free T4, AST (SGOT), albumin, average albumin and prealbumin during the RCC stay, and calcium and CRP, were significant predictors of successful weaning.

$PaCO_2$

Hypercapnic ventilatory response has been used to predict weaning outcomes in ICU patients on short durations of MV. However, this result may be different in PMV patients. In previous studies, it was found that a higher hypercapnic ventilatory response was more likely to predict successful weaning [9-10]. Our research has substantiated this result. The chemosensitivity determined with the hypercapnic ventilatory response provides a driving motility of the complete respiratory system [11]. The acquired factors that could reduce the hypercapnic drive response in critically ill patients include a dysfunction of either the respiratory center or neural transmission, or both. Excluding the above factors, there is another type of patient who has a low hypercapnic drive response due to insufficient airway occlusion pressure (P0.1). The reason for the insufficient P0.1 is that the level of chemical stimulation is not high enough. P0.1, the negative airway pressure at 0.1 seconds after inspiration is occluded, is measured using a mechanical ventilator [12]. Therefore, low-level $PaCO_2$ may lead to chemoreceptor blunting and insufficient P0.1, which may develop worsening pulmonary mechanics. Thus, eventually, the lung volume becomes close to the total lung volume, rendering the diaphragm unable to act as an inspiratory muscle, and finally leading to weaning failure.

Aspartate aminotransferase (AST)

Aminotransferases are enzymes that catalyze the transfer of an alpha-amino group from an amino acid to an alpha-keto acid. Alanine aminotransferase (ALT) is located only in the cytoplasm, whereas AST is present in both the cytosol (20% of the total) and mitochondria (80% of the total). Because most AST exists in mitochondria, it can be found more easily in highly metabolic tissues such as cardiac and skeletal muscle [13]. Muscle tissue may be damaged following intense prolonged training as a consequence of both metabolic and mechanical factors. At the same time, AST is one of the most useful serum markers for muscle injury, but the apoptosis of muscle tissue after strenuous exercise may also be triggered by an increase of this oxidative stress [14-15]. That is why we speculate from our research that high AST levels may be related to overuse and damage of respiratory muscles. Therefore, PMV patients with abnormal and high AST levels more easily experience weaning failure.

Free thyroxine (free T4)

In the past decade, chronic critical conditions have been associated with reduced serum levels of free triiodothyronine (free T3), free thyroxine (free T4), and thyrotropin, known

as nonthyroidal illness syndrome (NTIS). A recent study found that NTIS was associated with mortality and MV. It was pointed out in the study that ventilatory drive is reduced in hypothyroidism and can be detrimental to patients with hypercapnic respiratory failure [16]. Only those patients with a decreased free T4 value had an increased non-survival risk, indicating that a decrease in free T4 will worsen the course of the disease [17-18]. Low free T4 levels increased the mortality rate.

Low free T4 levels may be due to impaired regulation of hypothalamic-pituitary regulation, including the adrenal axis, leading to relative adrenal insufficiency [19]. Looking back at our analysis, there was indeed no difference in cortisol, but there was a difference in free T4, which prompted us to think about the possibility of the cause of this being outside the hypothalamic–pituitary axis, which is NTIS. NTIS refers to changes in serum thyroid hormone levels observed in critically ill patients in the absence of hypothalamic–pituitary axis dysfunction. This then increased the mortality rate, although the reasons are not fully understood. So far, we only know that a low free T4 level may aggravate the original condition of PMV patients, leading to difficulty in weaning and high mortality.

Calcium

Calcium is known to inhibit sodium channels and repress depolarization of nerve and muscle fibers [20]. Therefore, low serum ionized calcium levels result in a low depolarization threshold for firing action potentials. Lower serum ionized calcium may also reflect the severity of respiratory alkalosis. Ultimately, this results in diaphragmatic fatigue and weakness due to low serum ionized calcium, and work-overloading on the diaphragm by the principal disease [21]. Recent study found that the level of serum ionized calcium might potentially be a good predictor of acute respiratory failure requiring MV in hospitalized patients [22]. In our analysis, we found that the concentration of calcium is significantly related to weaning. But, for our data, we only tested total serum calcium, and did not measure serum ionized calcium in every patient. Therefore, there are certain limitations to the analysis of calcium. Approximately 15% of calcium is bound to organic and inorganic anions, 40% to proteins, especially albumin, and 45% circulates as active ionized calcium [22]. Therefore, with regard to the risk of respiratory failure, we believe that it is meaningful to analyze the association of respiratory muscles, even weaning, with serum ionized calcium in a more accurate manner. This is a point that can be further discussed in the future.

C-reactive protein (CRP)

A recent study reported high inflammatory parameters in patients with failed weaning, and CRP levels that were significantly elevated 48 hours later in patients with failed weaning [23]. The relationship between inflammation and weaning seems to relate to the cardiopulmonary stress of patients during liberation from the ventilator [24]. This process could be considered a stress factor due to the increasing respiratory muscle energy demand and oxygen consumption, which leads to increased cardiac output. Furthermore, this cardiorespiratory stress could activate different response systems, including perhaps the sympathetic nervous system. Activation of this system would result in increased plasmatic catecholamines. Thus, cardiovascular stress could stimulate increased CRP, reflecting the intensity of the inflammation process [25].

In this study, we also found that those who were in the RCC and had abnormally high CRP values were more likely to fail weaning.

Albumin

Over the past 30 years, much of the literature on ventilator weaning has shown that serum albumin levels were a significant predictor of weaning success. Now, we know that patients with albumin concentrations greater than 3.2 g/dL have a higher rate of ventilator weaning, and also that an increase in serum albumin at RCC admission increased the probability of weaning success [26-29]. It is well-known that the concentration of plasma albumin objectively reflects the recent nutritional status of the patient. During MV, the patient is under stress, and there is an increase in energy consumption. Therefore, a high metabolism and decomposition lead to relative malnutrition and a decreased serum albumin level. The body breaks down muscles for compensatory energy. This leads to atrophy of the respiratory muscles and reduced muscle strength, thus increasing the risk of weaning failure [30]. Albumins are known to have a long half-life of about 17 days on average. Depletion of albumin is associated with disease, or renal, gastrointestinal, and catabolic clearances of the body. Therefore, it is difficult to rule out the need for albumin supplementation in patients in the ICU [31]. However, our retrospective review of patient data found that none of the patients had albumin supplementation within 1 week before being transferred to the RCC. However, this may not completely eliminate the bias caused by earlier albumin supplementation, so we collected all of the detected albumin values of patients in the RCC, because we do not supplement the patient with albumin after the patient is transferred to the RCC. Through the method of extended observation, we can determine the changes in albumin in patients to analyze the benefits of albumin for PMV patients. It is certain that having a good albumin status at entry into the RCC and maintaining it during hospitalization is beneficial for patient weaning. In our investigation, we found that when the albumin concentrations were greater than 3.1 g/dL during RCC admission, and the albumin level was maintained at more than 3.0g/dL during the patient's time in the RCC, there was a higher weaning success rate.

Prealbumin

Recent studies have shown that prealbumin can be used to assess nutritional status and inflammation [32-33]. Prealbumin is the earliest serum protein that is altered during conditions of acute malnutrition. In states of systemic inflammation, hepatic production of prealbumin falls and is rapidly reflected in serum levels [34]. Patients with low plasma prealbumin levels are at greater risk for malnutrition and inflammatory conditions. Although we now know that prealbumin may also be a risk factor in MV, the detailed link remains unclear [35]. We suspect it may be related to muscle wasting or cardiorespiratory stress. However, our research data indicates that a higher prealbumin level may be related to a higher weaning rate.

For this study, we used the first blood drawing records and the albumin and prealbumin levels during the patient's RCC stay as the main investigative items. Although we have observed more data after each patient was transferred to the RCC, we did not collect these data completely because of the risk of bias due to the different time points for drawing blood from each patient, but this is something we may be able to do in the future. Observing clinical labora-

tory data for a longer period and comparing this with the initial data upon transfer to the RCC can help us formulate more strategies and better prognoses for PMV patients. Furthermore, numerous recent studies have shown a benefit with chest rehabilitation initiated at every stage of the disease, both during stable disease, and during or after acute exacerbation [36]. Therefore, the effect of chest rehabilitation on RCC patients is a noteworthy focus of future study.

Conclusions

In this study, we found that APACHE II scores, GCS scores, albumin, calcium, CRP, free T4, and GOT are important weaning factors for admission to the RCC. Systolic blood pressure and $PaCO_2$ are important influencing factors before and after the patient is released from the ventilator, and average albumin and prealbumin are important weaning maintenance factors when PMV patients are in the RCC. Apart from this, we found that tracheostomy and weaning appear to be unrelated. Identifying risk factors to achieving success in weaning helps in optimizing weaning strategies.

Acknowledgments

The authors would like to thank all members of the respiratory care community in Show Chwan Memorial who improved the weaning of PMV patients.

References

1. Pham T, Brochard LJ, Slutsky AS. Mechanical ventilation: state of the art. Mayo Clin Proc 2017;92(9):1382 400.
2. Cox CE, Martinu T, Sathy SJ, *et al*. Expectations and outcomes of prolonged mechanical ventilation. Crit Care Med 2009;37(11): 2888-94; quiz 2904.
3. Ghamloush M, O'Connor HH, White AC. Patient-ventilator interaction in the long-term acute-care hospital. Respir Care 2011;56(2): 207-13.
4. Jubran A, Tobin MJ. Pathophysiologic basis of acute respiratory distress in patients who fail a trial of weaning from mechanical ventilation. Am J Respir Crit Care Med 1997;155(3): 906-15.
5. MacIntyre NR. Evidence-based ventilator weaning and discontinuation. Respir Care 2004;49(7): 830-6.
6. Hannan LM, Tan S, Hopkinson K, *et al*. Inpatient and long-term outcomes of individuals admitted for weaning from mechanical ventilation at a specialized ventilation weaning unit. Respirology 2013;18(1):154-60.
7. Damuth E, Mitchell JA, Bartock JL, *et al*. Long-term survival of critically ill patients treated with prolonged mechanical ventilation: a systematic review and meta-analysis. Lancet Respir Med 2015;3(7): 544-53.
8. Hadjitodorov S, Todorova L. Consultation system for determining the patients' readiness for weaning from long-term mechanical ventilation. Comput Methods Programs Biomed 2010;100(1): 59-68.
9. Lee CS, Chen NH, Chuang LP, *et al*. Hypercapnic ventilatory response in the weaning of patients with prolonged mechanical ventilation. Can Respir J 2017;2017: 7381424.
10. Raurich JM, Rialp G, Ibáñez J, *et al*. CO_2 response and duration of weaning from mechanical ventilation. Respir Care 2011; 56(8): 1130-6.
11. Murray and Nadel's Textbook of Respiratory Medicine, W.B. Saunders Company, 1988.
12. Montgomery AB, Holle RH, Neagley SR, *et al*. Prediction of successful ventilator weaning using airway occlusion pressure and hypercapnic challenge. Chest 1987 Apr; 91(4): 496-9.
13. Pilarczyk K, Carstens H, Heckmann J, *et al*. The aspartate transaminase/alanine transaminase (DeRitis) ratio predicts mid-term mortality and renal and respiratory dysfunction after left ventricular assist device implantation. Eur J Cardio-thorac Surg 2017; 52(4): 781-8.
14. Banfi G, Colombini A, Lombardi G, *et al*. Metabolic markers in sports medicine. Adv Clin Chem 2012;56:1-54.
15. Brancaccio P, Lippi G, Maffulli N. Biochemical markers of muscular damage. Clin Chem Lab Med 2010;48(6): 757-67.

16. Butland RJ, Pang JA, Geddes DM. Carbimazole and exercise tolerance in chronic airflow obstruction. Thorax 1982;37(1): 64-7.
17. Plikat K, Langgartner J, Buettner R, *et al*. Frequency and outcome of patients with nonthyroidal illness syndrome in a medical intensive care unit. Metabolism 2007; 56(2): 239-44.
18. Biswas S, Buffery J, Enoch H, *et al*. Pulmonary effects of triiodothyronine (T3) and hydrocortisone (HC) supplementation in preterm infants less than 30 weeks gestation: results of the THORN trial--thyroid hormone replacement in neonates. Pediatr Res 2003;53(1): 48-56.
19. Kaptein EM, Robinson WJ, Grieb DA, *et al*. Peripheral serum thyroxine, triiodothyronine and reverse triiodothyronine kinetics in the low thyroxine state of acute nonthyroidal illnesses. A noncompartmental analysis. J Clin Invest 1982;69(3): 526-35.
20. Armstrong CM, Cota G. Calcium block of Na+ channels and its effect on closing rate. Proc Natl Acad Sci USA 1999;96(7): 4154-7.
21. Moe SM. Disorders involving calcium, phosphorus, and magnesium. Prim Care 2008;35(2): 215-37, v-vi.
22. Thongprayoon C, Cheungpasitporn W, Chewcharat A, *et al*. Serum ionised calcium and the risk of acute respiratory failure in hospitalised patients: a single-centre cohort study in the USA. BMJ Open 2020;10(3): e034325.
23. Forgiarini SGI, Rosa DPD, Forgiarini LF, *et al*. Evaluation of systemic inflammation in patients being weaned from mechanical ventilation. Clinics (Sao Paulo) 2018;73: e256.
24. Lobo SM, Lobo FR, Bota DP, *et al*. C-reactive protein levels correlate with mortality and organ failure in critically ill patients. Chest 2003;123(6): 2043-9.
25. Salazar J, Martínez MS, Chávez M, *et al*. C-reactive protein: clinical and epidemiological perspectives. Cardiol Res Pract 2014; 2014: 605810.
26. Wu YK, Kao KC, Hsu KH, *et al*. Predictors of successful weaning from prolonged mechanical ventilation in Taiwan. Respir Med 2009;103(8): 1189-1195.
27. Chao DC, Scheinhorn DJ, Stearn-Hassenpflug M. Impact of renal dysfunction on weaning from prolonged mechanical ventilation. Crit Care 1997;1(3): 101-104.
28. Mirtallo JM. Assessing the nutritional needs of the critically ill patient. DICP: Ann Pharmacotherap 1990;24(11 Suppl): S20-3.
29. Sapijaszko MJ, Brant R, Sandham D, *et al*. Nonrespiratory predictor of mechanical ventilation dependency in intensive care unit patients. Crit Care Med 1996;24(4): 601-7.
30. Jain MK, Heyland D, Dhaliwal R, *et al*. Dissemination of the Canadian clinical practice guidelines for nutrition support: results of a cluster randomized controlled trial. Crit Care Med 2006;34(9): 2362-2369.
31. Levitt DG, Levitt MD. Human serum albumin homeostasis: a new look at the roles of synthesis, catabolism, renal and gastrointestinal excretion, and the clinical value of serum albumin measurements. Int J Gen Med 2016;9: 229-255.
32. Caccialanza R, Palladini G, Klersy C, *et al*. Serum prealbumin: an independent marker of short-term energy intake in the presence of multiple-organ disease involvement. Nutrition 2013;29(3): 580-2.
33. Lu J, Xu BB, Zheng ZF, *et al*. CRP/prealbumin, a novel inflammatory index for predicting recurrence after radical resection in gastric cancer patients: post hoc analysis of a randomized phase III trial. Gastric Cancer 2019;22(3): 536-545.
34. Mohan A, Arora S, Uniyal A, *et al*. Evaluation of plasma leptin, tumor necrosis factor-α, and prealbumin as prognostic biomarkers during clinical recovery from acute exacerbations of chronic obstructive pulmonary disease. Lung India 2017;34(1): 3-8.
35. Zuo P, Tong S, Yan Q, *et al*. Decreased prealbumin level is associated with increased risk for mortality in elderly hospitalized patients with COVID-19. Nutrition 2020; 78: 110930.
36. Rochester CL, Vogiatzis I, Holland AE, *et al*. An official American Thoracic Society/European Respiratory Society Policy Statement: enhancing implementation, use, and delivery of pulmonary rehabilitation. Am J Respir Crit Care Med 2015;192(11): 1373-1386.

Bradycardia in Patients with COVID-19

Jou-Chun Wu[1], Chao-Hsien Chen[1,2], Yen-Hsiang Tang[2,3], Hsin-Pei Chung[1,2], Yen-Ting Chen[1,2], Kuan-Chih Kuo[1,2], Wen-Kuei Chang[1,2], Chang-Yi Lin[1,2], Chieh-Jen Wang[1,2]

Introduction: Previous studies have reported that COVID-19 infection-related bradycardia is a predictor of a poor prognosis. Remdesivir and tocilizumab were also reported as risk factors for bradycardia. In this study, we aimed to investigate the occurrence of bradycardia among COVID-19 patients and its potential relationship with mortality.

Methods: Adult patients admitted to MacKay Memorial Hospital with COVID-19 infection from May to June 2021 were enrolled for analysis. Patients using medication for rate control, or who developed end-of-life bradycardia, were excluded. Bradycardia was defined as a persistent heart rate of fewer than 60 bpm on 2 separate occasions with a minimum 4-hour gap during hospitalization.

Results: A total of 259 patients were included, and 75 (29%) experienced bradycardia during their hospitalization. Patients in the bradycardia group had a lower lymphocyte count, higher neutrophil/lymphocyte ratio, and increased GOT, GPT, LDH, ferritin, and CRP. Bradycardia was also related to more frequent use of systemic corticosteroids, remdesivir, tocilizumab, and enoxaparin. But after multiple logistic regression, only tocilizumab was recognized as a risk factor for bradycardia (odds ratio [OR]: 2.6512, 95% confidence interval [CI]: 1.3307-5.2823, p=0.0056). There was no significant difference in in-hospital mortality among patients with bradycardia using multivariate logistic regression analysis (OR: 1.0476, 95% CI: 0.3340-3.2857, p=0.9365).

Conclusion: Bradycardia is a frequent phenomenon among hospitalized COVID-19 patients. Patients who had bradycardia events were more likely to receive tocilizumab, but not remdesivir treatment. Bradycardia events were not correlated with mortality in our patient group. Determining the mechanisms of bradycardia among COVID-19 patients requires further study. ***(Thorac Med 2022; 37: 266-276)***

Key words: Bradycardia, COVID-19, mortality, remdesivir, tocilizumab

[1]Division of Pulmonary Medicine, Department of Internal Medicine, MacKay Memorial Hospital, Taipei City, Taiwan, [2]Department of Medicine, MacKay Memorial Collage, New Taipei City, Taiwan, [3]Department of Critical Care Medicine, MacKay Memorial Hospital, Taipei City, Taiwan

Address reprint requests to: Dr. Chieh-Jen Wang, MacKay Memorial Hospital, Tamsui Branch, No. 45, Minsheng Rd., Tamsui District

Introduction

The appearance of coronavirus disease 2019 (COVID-19) led to a worldwide pandemic, beginning in 2019. It was caused by a novel coronavirus, severe acute respiratory syndrome coronavirus-2 (SARS-CoV-2), which is a known cause of respiratory tract infections. Due to its rapid spread, various manifestations, and high mortality in some populations, it has had a significant impact on the health systems of many countries [1].

SARS-CoV-2 infects humans by entering into host cells through angiotensin-converting enzyme 2 (ACE2) receptors, which are expressed in multiple organs [2-3]. Therefore, COVID-19 can not only cause pneumonia, but can also involve multiple organ systems, including the cardiovascular system [4-5]. Arrhythmia, myocarditis, myocardial injury, heart failure, thrombotic events, and pericarditis have been previously reported [4]. In some studies, COVID-19-related bradycardia was found to be related to mortality, and could be a predictor of a poor prognosis [6-7]. However, some COVID-19 treatments may also induce bradycardia, and a suspected association with remdesivir use has often been discussed [8-10]. Tocilizumab-related bradycardia was also reported [11-12].

During the first wave of COVID-19 in Taiwan, we quickly recognized that with the rapidly growing population of infected patients and the limited availability of medical resources, it was important to identify high-risk patients. In this, we observed a significant number of patients who developed bradycardia. Therefore, in this study, we aimed to investigate the occurrence of bradycardia and its potential relationship with mortality in our COVID-19 patient group.

Methods

Design and Patients

This study was a retrospective observational study. All patients admitted to Mackay Memorial Hospital, a tertiary hospital in northern Taiwan, with a diagnosis of COVID-19 from May 1, 2021 to June 30, 2021, were enrolled. Inclusion criteria were: (1) age ≥18 years, and (2) having a diagnosis of COVID-19 confirmed by a positive reverse transcription-polymerase chain reaction (RT-PCR) test at the emergency department. We excluded patients who (1) had repeated admissions, (2) were transferred to/from another hospital, (3) were using medications for rate control, including calcium channel blockers, beta-blockers, and anti-arrhythmic agents, such as amiodarone and mexiletine, or (4) who developed bradycardia just before dying. The patient's electronic medical records were reviewed, and data on their demographic characteristics, co-morbidities, laboratory results, treatments, outcomes during hospitalization, and occurrence of bradycardia were collected. The severity of COVID-19 infection according to Shang's COVID-19 scoring system (CSS) [13] and the Sequential Organ Failure Assessment (SOFA) score [14] was also calculated. Shang's CSS used 5 clinical variables to predict mortality, and patients with a total score >2 were classified as high-risk. This study was approved by the Institutional Review Board of MacKay Memorial Hospital (approval no. 21MMHIS330e) and the need for written informed consent was waived.

Definition of bradycardia

A bradycardia event was defined as a persistent heart rate of fewer than 60 beats per minute on 2 separate occasions, with a minimum of 4

hours apart during hospitalization [7].

Statistical Analysis

All statistical analyses were performed using MedCalc version 20.014 for Windows (MedCalc Software Ltd, Ostend, Belgium). Data were reported as number (percentage) for categorical variables, mean ± standard deviation (SD) for normally distributed continuous variables, and median (interquartile range [IQR]) for non-normally distributed continuous variables. The Shapiro–Wilk test was used to examine the normality distribution of continuous variables. The chi-squared test or Fisher's exact test was used to compare the frequencies of categorical variables, when appropriate. The independent samples t-test was used to compare 2 normally distributed continuous variables, and the Mann-Whitney U test was used for non-normally distributed variables. All reported p values were 2-sided, and a p-value <0.05 was considered to indicate a statistically significant difference.

There were 2 parts to the analysis in this study. First, we wanted to know which patients were more likely to develop bradycardia. Variables with p <0.05 in the univariate logistic regression analysis were considered as confounders, and they then were used in the multivariate logistic regression analysis. Second, to clarify the association between developing bradycardia and mortality, we performed multivariate logistic regression analysis with adjustments for 9 variables. These variables were identified from previous studies as risk factors for mortality, and included older age [15-16], male [15], diabetes [17], hypertension [15,17], chronic kidney disease [15,18], leukocytosis [15], elevated C-reactive protein (CRP) [19], SOFA Score [14], and Shang's CSS score [13].

Results

During the study period, 332 patients were evaluated, and 73 were excluded due to their using medication for rate control, developing bradycardia just before dying, or other logistical reasons (Figure 1). A total of 259 patients were included in the final analysis; 75 patients (29.0%) were included in the bradycardia group and 184 (71.0%) in the no bradycardia group. Patients in the bradycardia group were significantly older (mean age 65.9±10.9 vs. 59.6±16.5 years, p=0.0004).

There was no gender difference between the 2 groups, but there were fewer patients with end-stage renal disease (ESRD) under hemodialysis (0% vs, 8.7%, p=0.0076) in the bradycardia group (Table 1). The bradycardia group had a lower lymphocyte count, a higher neutrophil/lymphocyte ratio, increased aspartate aminotransferase (AST), alanine aminotransferase (ALT), lactate dehydrogenase (LDH), ferritin, and CRP, and a higher SOFA score. The bradycardia group was also associated with more frequent use of systemic corticosteroids (93.3% vs. 73.4%, p=0.0003), remdesivir (52.0% vs. 32.6%, p=0.0036), tocilizumab (52.0 vs. 20.1%, p<0.0001), and enoxaparin (54.7% vs. 28.3%, p=0.0001). Patients with bradycardia were more likely to use supplementary oxygen (93.3% vs. 69.0%, p<0.0001) and mechanical ventilation (42.7% vs. 10.9%, p<0.0001), and to have a longer duration of hospitalization (17.0 [12.0-24.5] vs. 12.0 [9.0-18.0] days, p<0.0001), but there was no significant difference in in-hospital mortality (12.0% vs. 10.9%, p=0.7940) between the 2 groups.

We found that increased age, AST, LDH, and treatment with systemic corticosteroids, remdesivir, tocilizumab, and enoxaparin were

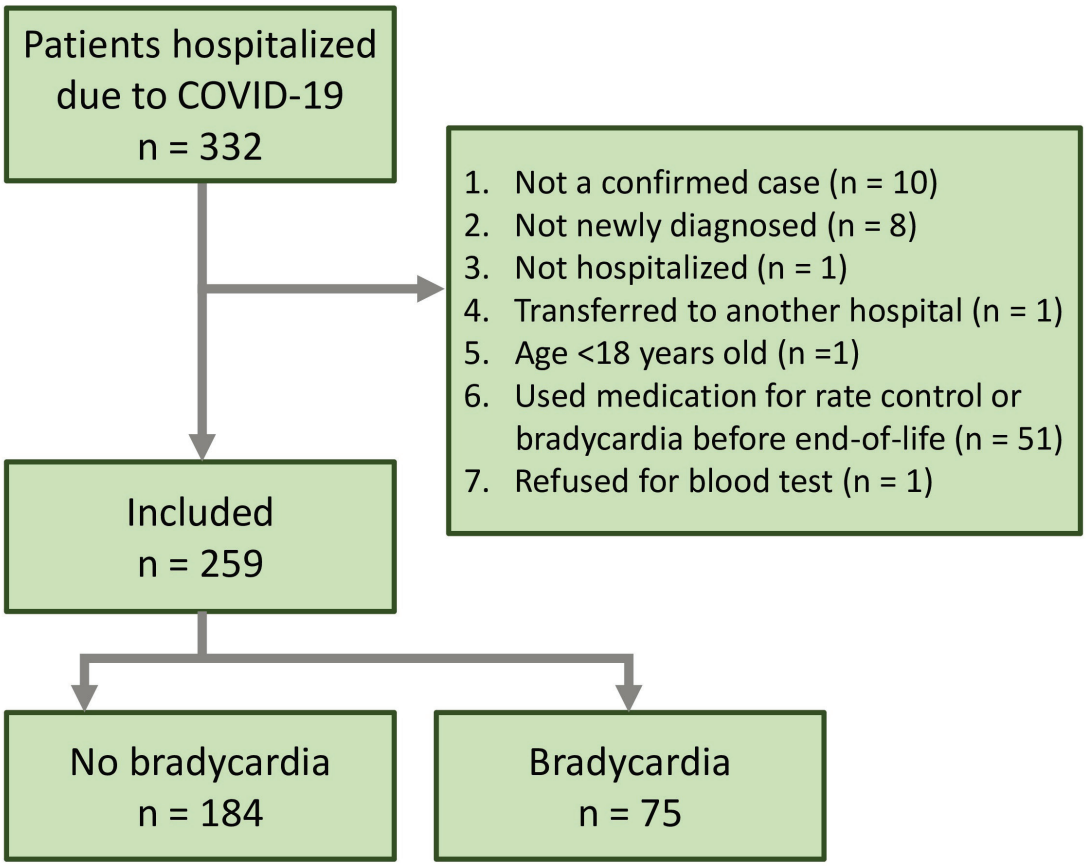

Fig. 1. Flowchart of Patient Inclusion and Exclusion in the Study.

all significant risk factors for bradycardia during univariate regression (Table 2). However, after multiple logistic regression, only tocilizumab was recognized as a significant risk factor for bradycardia (odds ratio [OR]: 2.6512, 95% confidence interval [CI]: 1.3307-5.2823, p=0.0056).

To clarify the relationship between bradycardia and mortality, we performed multivariate logistic regression with adjustment for 9 risk factors (Table 3). Mortality was not associated with bradycardia (OR: 1.0476, 95% CI: 0.3340-3.2857, p=0.9365), but it was associated with hypertension (OR: 3.6796, 95% CI: 1.11369-11.9090, p=0.0297) and a high SOFA score (OR: 1.5303, 95% CI: 1.1852-1.9758, p=0.0011).

Discussions

The influence of COVID-19 on the cardiac system is multifactorial, and cardiac manifestations could be caused by direct viral myocardial damage, downregulation of ACE2 activity, a systemic hyperinflammatory response, critical illness, or drug toxicity [4,20]. Bradycardia is suspected to be related to mortality [6-7], but the pathophysiology of COVID-19-related bradycardia is not fully understood [20]. It was hypothesized that bradycardia might be caused by a direct pathogen effect on the myocardium

Table 1. Basic Characteristics, Comorbidities, Laboratory Results, Treatments and Outcomes between Patients With and Without Bradycardia

Characteristic	Bradycardia (n = 75)	No bradycardia (n = 184)	*p*-value
Age, years	65.9±10.9	59.6±16.5	0.0004
Gender (male/female)	39/36 (52.0%/48.0%)	103/81 (56.0%/44.0%)	0.5603
Body mass index, kg/m^2	24.9 (22.6-27.3)	25.1 (22.7-27.7)	0.4766
Duration of symptoms	7.0 (3.0-8.0)	5.0 (2.0-8.0)	0.0513
High Shang's CSS score	30 (40.5%)	62 (35.8%)	0.4847
SOFA score	2.0 (1.0-3.0)	2.0 (1.0-3.0)	0.0134
Presence of co-morbidities			
Hypertension	32 (42.7%)	61 (33.2%)	0.1485
Diabetes mellitus	20 (26.7%)	52 (28.3%)	0.7954
Cardiovascular disease	3 (4.0%)	7 (3.8%)	> 0.9999
Heart failure	0 (0.0%)	6 (3.3%)	0.1858
Chronic obstructive pulmonary disease	2 (2.7%)	10 (5.4%)	0.5178
Organ transplantation	0 (0.0%)	0 (0.0%)	NA
End-stage renal disease	0 (0.0%)	16 (8.7%)	0.0076
Malignancy	3 (4.0%)	12 (6.5%)	0.5646
WBC count (10^3 / μL)	6000 (4400-8475)	6300 (4500-8600)	0.4865
Total lymphocyte count (10^3 /μL)	774 (505-1076)	972 (630-1367)	0.0098
Neutrophil/lymphocyte ratio	5.74 (4.17-10.23)	4.29 (2.76-8.71)	0.0085
Platelet count (10^3 /μL)	196000 (139500-233500)	191000 (148500-253500)	0.5708
Aspartate aminotransferase (IU/L)	46.0 (33.0-60.8)	32.0 (23.0-50.0)	0.0001
Alanine aminotransferase (IU/L)	41.0 (30.5-68.0)	27.0 (18.0-44.0)	< 0.0001
Serum creatinine (mg/dL)	0.9 (0.7-1.1)	0.9 (0.7-1.2)	0.9093
Creatine kinase (IU/L)	95.0 (60.0-183.0)	103.0 (55.0-198.0)	0.9715
Troponin-I (ng/mL)	0.010 (0.010-0.014)	0.010 (0.010-0.018)	0.9871
D-dimer (ng/mL)	846.5 (639.0-1353.0)	711.0 (446.0-1405.3)	0.1146
Serum LDH (IU/L)	323.0 (233.0-429.0)	239.0 (171.5-317.5)	< 0.0001
Ferritin (ng/mL)	631.5 (344.7-1139.0)	386.1 (171.4-843.2)	0.0003
C-reactive protein (mg/dL)	9.37 (3.43-14.47)	3.57 (1.06-8.49)	< 0.0001
Systemic corticosteroid	70 (93.3%)	135 (73.4%)	0.0003
Remdesivir	39 (52.0%)	60 (32.6%)	0.0036
Tocilizumab	39 (52.0%)	37 (20.1%)	< 0.0001
Enoxaparin	41 (54.7%)	52 (28.3%)	0.0001
NRICM101	16 (21.3%)	41 (22.3%)	0.8674
Oxygen	70 (93.3%)	127 (69.0%)	< 0.0001
Mechanical ventilation	32 (42.7%)	20 (10.9%)	< 0.0001
In-hospital mortality	9 (12.0%)	20 (10.9%)	0.794
Discharged alive	66 (88.0%)	164 (89.1%)	
Duration of hospital stay	17.0 (12.0-24.5)	12.0 (9.0-18.0)	< 0.0001

CSS: COVID-19 scoring system; WBC: white blood cells; SOFA: sequential organ failure assessment; LDH: lactate dehydrogenase.

Table 2. Univariate and Multivariate Logistic Regression of Risk Factors Associated with Bradycardia

Risk factor	Univariate regression OR (CI)	*p*-value	Multivariate regression OR (CI)	*p*-value
Age, years	1.0294 (1.0099-1.0493)	0.0030	1.0213 (0.9988-1.0444)	0.0634
Gender, male	0.8519 (0.4972-1.4597)	0.5597		
BMI	0.9507 (0.8890-1.0167)	0.1401		
Duration of symptoms	1.0409 (0.9697-1.1173)	0.2672		
High Shang's CSS score	1.2207 (0.6983-2.1338)	0.4841		
SOFA score	1.0798 (0.9603-1.2142)	0.1994		
Presence of co-morbidities				
Hypertension	1.5006 (0.8649-2.6035)	0.1488		
Diabetes mellitus	0.9231 (0.5045-1.6888)	0.7951		
Cardiovascular disease	1.0536 (0.2651-4.1879)	0.9409		
Heart failure	NA			
Chronic obstructive pulmonary disease	0.4767 (0.1019-2.2295)	0.3466		
Organ transplantation	NA			
ESRD	NA			
Malignancy	0.5972 (0.1636-2.1799)	0.4352		
WBC count	1.0000 (0.9999-1.0001)	0.9463		
Total lymphocyte count	0.9996 (0.9992-1.0001)	0.1235		
Neutrophil/lymphocyte ratio	1.0000 (0.9727-1.0281)	0.9999		
Platelet count	1.0000 (1.0000-1.0000)	0.6334		
Aspartate aminotransferase	1.0139 (1.0047-1.0232)	0.0031	1.0079 (0.9975-1.0184)	0.1357
Serum creatinine	0.8101 (0.6209-1.0571)	0.1209		
CK	1.0002 (0.9995-1.0010)	0.5760		
D-dimer	1.0000 (0.9999-1.0002)	0.6367		
Serum LDH	1.0029 (1.0011-1.0048)	0.0016	0.9998 (0.9976-1.0020)	0.8765
Ferritin	1.0001 (0.9999-1.0003)	0.4192		
CRP	0.9995 (0.9978-1.0013)	0.6049		
Corticosteroid	5.0815 (1.9371-13.3297)	0.0010	2.6987 (0.8558-8.5099)	0.0902
Remdesivir	2.2389 (1.2944-3.8725)	0.0039	1.2276 (0.6518-2.3117)	0.5255
Tocilizumab	4.3041 (2.4124-7.6791)	<0.0001	2.6512 (1.3307-5.2823)	0.0056
Enoxaparin	3.0611 (1.7547-5.3401)	0.0001	1.3779 (0.6939-2.7361)	0.3597
NRICM101	0.9458 (0.4925-1.8164)	0.8672		

BMI: body mass index; CSS: COVID-19 scoring system; SOFA: sequential organ failure assessment; ESRD: end-stage renal disease; WBC: white blood cells; CK: creatine kinase; LDH: lactate dehydrogenase; CRP: C-reactive protein.

Table 3. Multivariate Logistic Regression with Risk Factors Related to Mortality

Variable	Odds ratio	95% confidence interval	*p*-value
Bradycardia	1.0476	0.3340-3.2857	0.9365
Age	1.0281	0.9828-1.0755	0.2284
Gender, male	1.7068	0.5874-4.9595	0.3260
Diabetes	0.8425	0.2800-2.5349	0.7605
Hypertension	3.6796	1.1369-11.9090	0.0297
Chronic kidney disease	0.8053	0.1668-3.8889	0.7875
White blood count	1.0000	0.9999-1.0001	0.7980
C-reactive protein	0.9998	0.9947-1.0049	0.9279
High Shang's CSS risk score	3.4233	0.7569-15.4840	0.1100
SOFA_score	1.5303	1.1852-1.9758	0.0011

CSS: COVID-19 scoring system; SOFA: sequential organ failure assessment.

or by the effect of an overwhelming inflammatory cytokine storm on cardiac pacemaker cells [20-21]. Circulatory cytokines could also interfere with signal transduction and modulate autonomic activity, resulting in increased vagal tone and further resulting in an imbalance of sympathovagal activation [21]. Bradycardia is very likely the result of cross-talk between the autonomic nervous system and the immune system [22].

The incidence rate of bradycardia in our study was 29%, which is aligned with the findings of previous studies (14.9% to 33%) [7,20,23]. Patients with bradycardia tended to have increased age, lymphopenia, elevated liver enzymes, elevated LDH, higher ferritin, and higher CRP, which have been reported as risk factors for severe illness [1,24]. The SOFA score, which was used to predict the clinical outcomes of patients with multiple organ failure requiring intensive care, has a controversial role in evaluating disease severity and predicting mortality of COVID-19 patients [25-26]. The bradycardia group in our study had significantly higher inflammatory markers, and the SOFA score may indicate that bradycardia is correlated with disease severity. However, the correlations became insignificant after univariate regression. More research and a better tool for assessing disease severity in COVID-19 patients are needed.

Due to the possible correlation with inflammatory status, bradycardia is considered as a potential predictor of a worse outcome [6-7]. In a large multi-center retrospective analysis of 1,053 patients in the USA, 24.9% developed bradycardia, and they were found to have a significant increase in mortality [7]. One European retrospective study also reported that sinus bradycardia was associated with poor outcomes in critically ill patients with COVID-19 of the B1.1.7 lineage [6]. However, Fernando et al found that the degree of bradycardia did not appear to be correlated with clinical outcomes [27]. After adjusting for common risk factors, our study also showed that bradycardia was not significantly correlated with mortality.

Remdesivir, a novel nucleotide analog that

has in vitro activity against SARS-CoV-2 [28], has been previously associated with bradycardia events in clinical studies [8]. The most common side effects of remdesivir include elevated hepatic enzymes, nausea, hypersensitivity and infusion-related anaphylactic reactions [10]. A post-marketing study in a real-world setting suggested that the use of remdesivir was significantly associated with an increased risk of bradycardia, which may be due to the active remdesivir metabolite, a nucleotide triphosphate derivative with similarities to ATP, which is known to slow sinoatrial node automaticity [9]. However, in our study, remdesivir did not have a significant association with bradycardia after multivariate logistic regression.

On the other hand, tocilizumab, an interleukin-6 (IL-6) receptor blocker, is a treatment option for COVID-19 patients who require high-flow oxygen or mechanical ventilation [29]. Tocilizumab, originally used with some rheumatic diseases, such as rheumatic arthritis, was found to improve survival in treating hospitalized COVID-19 patients who have hypoxia and evidence of inflammation [29-30]. The most prevalent adverse event associated with tocilizumab in previous studies was serious infection [31,32,33]. Elevation of lipid levels is also commonly observed, but the clinical significance is unclear, and it may not lead to an increased risk for cardiovascular events [33-34].

Regarding the safety of tocilizumab's use for the treatment of COVID-19, previous studies reported no significant differences in the risk of infections or adverse events compared to the standard-of-care group [35-36]. In an early randomized control trial [11], Stone et al. found that 2 patients in the tocilizumab group, but none in the standard-of-care group, had bradycardia. A single-center, retrospective, observational study found that patients had an average 12 bpm decreased heart rate 12 hours after tocilizumab infusion [12]. To the best of our knowledge, no other evidence of tocilizumab-related bradycardia events have been reported, and the possible mechanism remains unknown. Further investigation is needed.

In our study, no patients with ESRD had bradycardia events. This may be due to the chronic inflammation status of ESRD patients [37]. IL-6 and tumor necrosis factor are found to be retained as uremic toxins in patients with CKD and ESRD [37]. It has been hypothesized that cytokines may interact with the autonomic tone of CKD and ESRD patients [38]. Seibert et al also reported that dialysis patients showed signs of autonomic derangement in their heart rate variability [39]. ESRD patients were found to have a significantly higher baseline heart rate and they were more likely to have a sympathovagal balance that was shifted towards the sympathetic side [39].

Hypertension, Shang's CSS, and the SOFA score were significantly related to mortality in our patient group. As reported in previous studies [40,41], hypertension was found to be associated with higher COVID mortality. Du et al identified hypertension as a predictor of mortality in patients with COVID-19 pneumonia in their prospective cohort study [16]. The CSS originated from a retrospective cohort study of 2,529 patients in Wuhan, China, between January and March 2020 [13]. It identified old age, coronary heart disease, percentage of lymphocytes, procalcitonin, and D-dimer as independent risk factors for mortality. Our patient group supported the correlation between the CSS and mortality. A higher CSS score indicates that the patient is at a high risk of severe illness and a poor prognosis. As mentioned previously, our

study showed that bradycardia might be related to disease severity, but it was not significantly correlated with mortality. The results of the present study suggest that bradycardia could be induced by multiple confounders, instead of being an independent risk factor for disease severity. More research is therefore warranted.

Our study has some limitations: First, it used a single-center, retrospective design. Second, for the protection of the medical staff, we limited their entrance frequency into the ward. Therefore, we did not retrieve 12-lead EKGs for every bradycardia patient if their hemodynamic status was stable. Nevertheless, to the best of our knowledge, this study was the first analysis of bradycardia focusing on an East Asian patient group, and we are the first to find a statistically significant relationship between tocilizumab and bradycardia. It is also worth mentioning that we did not observe any life-threatening events related to bradycardia.

In conclusion, bradycardia was not uncommon in hospitalized COVID-19 patients. Patients who had bradycardia events were more likely to have received tocilizumab treatment, but not remdesivir. Bradycardia events were not significantly correlated with mortality in our patient group, but hypertension and the CSS were. Further studies are needed to investigate the pathophysiology of bradycardia, and its potential association with prognosis.

Acknowledgments

*We thank the medical staffs at Mackay Memorial Hospital who took care of the patients and helped establish the patient database for this study.

References

1. Guan WJ, Ni ZY, Hu Y, *et al*. Clinical characteristics of coronavirus disease 2019 in China. N Engl J Med 2020;382(18): 1708-20.
2. Tang N, Li D, Wang X, *et al*. Abnormal coagulation parameters are associated with poor prognosis in patients with novel coronavirus pneumonia. J Thromb Haemost 2020;18(4): 844-7.
3. Choudhary S, Sharma K, Silakari O. The interplay between inflammatory pathways and COVID-19: A critical review on pathogenesis and therapeutic options. Microb Pathog 2021;150: 104673.
4. Arévalos V, Ortega-Paz L, Rodríguez-Arias JJ, *et al*. Acute and chronic effects of COVID-19 on the cardiovascular system. J Cardiovasc Dev Dis 2021;8(10).
5. Santoso A, Pranata R, Wibowo A, *et al*. Cardiac injury is associated with mortality and critically ill pneumonia in COVID-19: a meta-analysis. Am J Emerg Med 2021;44: 352-7.
6. Chalkias A, Pantazopoulos I, Papagiannakis N, *et al*. Sinus bradycardia is associated with poor outcome in critically ill patients with COVID-19 due to the B.1.1.7 lineage. Toxicol Rep 2021;8: 1394-8.
7. Kumar S, Arcuri C, Chaudhuri S, *et al*. A novel study on SARS-COV-2 virus associated bradycardia as a predictor of mortality-retrospective multicenter analysis. Clin Cardiol 2021;44(6): 857-62.
8. Gubitosa JC, Kakar P, Gerula C, *et al*. Marked sinus bradycardia associated with remdesivir in COVID-19: a case and literature review. JACC Case Rep 2020;2(14): 2260-4.
9. Touafchia A, Bagheri H, Carrié D *et al*. Serious bradycardia and remdesivir for coronavirus 2019 (COVID-19): a new safety concerns. Clin Microbiol Infect 2021;27(5): 791.e5-8.
10. Maheshwari M, Athiraman H. Bradycardia related to remdesivir during COVID-19: persistent or permanent? Cureus 2021 Nov 26;13(11): e19919.
11. Stone JH, Frigault MJ, Serling-Boyd NJ, *et al*. Efficacy of tocilizumab in patients hospitalized with Covid-19. N Engl J Med 2020;383(24): 2333-2344.
12. Staubs A, Noori F, Houshmand F. Bradycardia following tocilizumab administration for COVID-19. Crit Care Med

2022;50(1).

13. Shang Y, Liu T, Wei Y, *et al*. Scoring systems for predicting mortality for severe patients with COVID-19. EClinicalMedicine 2020;24: 100426.
14. Vincent JL, Moreno R, Takala J, *et al*. The SOFA (Sepsis-related Organ Failure Assessment) score to describe organ dysfunction/failure. On behalf of the Working Group on Sepsis-Related Problems of the European Society of Intensive Care Medicine. Intensive Care Med 1996;22(7): 707-710.
15. Chen T, Wu D, Chen H, *et al*. Clinical characteristics of 113 deceased patients with coronavirus disease 2019: retrospective study. BMJ 2020;368: m1091.
16. Du RH, Liang LR, Yang CQ, *et al*. Predictors of mortality for patients with COVID-19 pneumonia caused by SARS-CoV-2: a prospective cohort study. Eur Respir J 2020;55(5).
17. Guan WJ, Liang WH, Zhao Y, *et al*. Comorbidity and its impact on 1590 patients with COVID-19 in China: a nationwide analysis. Eur Respir J 2020;55(5).
18. Ozturk S, Turgutalp K, Arici M, et al. Mortality analysis of COVID-19 infection in chronic kidney disease, haemodialysis and renal transplant patients compared with patients without kidney disease: a nationwide analysis from Turkey. Nephrol Dial Transplant 2020;35(12): 2083-95.
19. Smilowitz NR, Kunichoff D, Garshick M, *et al*. C-reactive protein and clinical outcomes in patients with COVID-19. Eur Heart J 2021;42(23): 2270-9.
20. Amaratunga EA, Corwin DS, Moran L, *et al*. Bradycardia in patients with COVID-19: a calm before the storm? Cureus 2020;12(6): e8599.
21. Ye F, Hatahet M, Youniss MA, *et al*. The clinical significance of relative bradycardia. WMJ 2018;117(2): 73-8.
22. Ye F, Winchester D, Stalvey C, *et al*. Proposed mechanisms of relative bradycardia. Med Hypotheses 2018;119: 63-7.
23. Hu L, Gong L, Jiang Z, *et al*. Clinical analysis of sinus bradycardia in patients with severe COVID-19 pneumonia. Crit Care 2020;24(1): 257.
24. Zhou F, Yu T, Du R, *et al*. Clinical course and risk factors for mortality of adult inpatients with COVID-19 in Wuhan, China: a retrospective cohort study. Lancet 2020;395(10229): 1054-62.
25. Raschke RA, Agarwal S, Rangan P, *et al*. Discriminant accuracy of the SOFA score for determining the probable mortality of patients with COVID-19 pneumonia requiring mechanical ventilation. JAMA 2021;325(14): 1469-1470. doi:10.1001/jama.2021.1545
26. Yang Z, Hu Q, Huang F, *et al*. The prognostic value of the SOFA score in patients with COVID-19: a retrospective, observational study. Medicine (Baltimore). 2021;100(32):e26900. doi: 10.1097/MD.0000000000026900
27. Stancampiano F, Omer M, Harris D, *et al*. Clinical characteristics and outcomes of patients hospitalized for COVID-19 pneumonia who developed bradycardia. South Med J 2021;114(7): 432-7.
28. Wang M, Cao R, Zhang L, *et al*. Remdesivir and chloroquine effectively inhibit the recently emerged novel coronavirus (2019-nCoV) in vitro. Cell Res 2020;30(3): 269-71.
29. RECOVERY Collaborative Group. Tocilizumab in patients admitted to hospital with COVID-19 (RECOVERY): a randomised, controlled, open-label, platform trial. Lancet 2021;397(10285): 1637-45.
30. Khanna D, Lin CJF, Furst DE, *et al*. Tocilizumab in systemic sclerosis: a randomised, double-blind, placebo-controlled, phase 3 trial. Lancet Respir Med 2020;8(10): 963-74.
31. Biggioggero M, Crotti C, Becciolini A, *et al*. Tocilizumab in the treatment of rheumatoid arthritis: an evidence-based review and patient selection. Drug Des Devel Ther 2018 Dec 19;13: 57-70.
32. Navarro-Millán I, Singh JA, Curtis JR. Systematic review of tocilizumab for rheumatoid arthritis: a new biologic agent targeting the interleukin-6 receptor. Clin Ther 2012 Apr;34(4): 788-802.e3.
33. Yazici Y, Curtis JR, Ince A, *et al*. Efficacy of tocilizumab in patients with moderate to severe active rheumatoid arthritis and a previous inadequate response to disease-modifying antirheumatic drugs: the ROSE study. Ann Rheum Dis 2012;71: 198-205.
34. Rao VU, Pavlov A, Klearman M, *et al*. An evaluation of risk factors for major adverse cardiovascular events during tocilizumab therapy. Arthritis Rheumatol 2015;67(2): 372-380.
35. Rezaei S, Fatemi B, Karimi Majd Z, *et al*. Efficacy and safety of tocilizumab in severe and critical COVID-19:

A systematic review and meta-analysis. Expert Rev Clin Immunol 2021 May;17(5): 499-511.

36. Tleyjeh IM, Kashour Z, Damlaj M, *et al*. Efficacy and safety of tocilizumab in COVID-19 patients: a living systematic review and meta-analysis. Clin Microbiol Infect 2021;27(2): 215-227.
37. Cobo G, Lindholm B, Stenvinkel P. Chronic inflammation in end-stage renal disease and dialysis. Nephrol Dial Transplant 2018;33(suppl_3): iii35-iii40.
38. Psychari SN, Sinos L, Iatrou C, *et al*. Relations of inflammatory markers to lipid levels and autonomic tone in patients with moderate and severe chronic kidney disease and in patients under maintenance hemodialysis. Clin Nephrol 2005;64(6): 419-27.
39. Seibert E, Zohles K, Ulrich C, *et al*. Association between autonomic nervous dysfunction and cellular inflammation in end-stage renal disease. BMC Cardiovasc Disord 2016;16(1): 210.
40. Gao C, Cai Y, Zhang K, *et al*. Association of hypertension and antihypertensive treatment with COVID-19 mortality: a retrospective observational study. Eur Heart J 2020;41(22): 2058-66.
41. Mahamat-Saleh Y, Fiolet T, Rebeaud ME, *et al*. Diabetes, hypertension, body mass index, smoking and COVID-19-related mortality: a systematic review and meta-analysis of observational studies. BMJ Open 2021;11(10): e052777.

Congenital Bronchial Atresia – A Case Report

Guo-Zhi Wang[1], Frank Cheau-Feng Lin[1,2]

Congenital bronchial atresia is a rare airway malformation in which a segmental or lobar bronchus is isolated from the main airway, and corresponding lung tissue is hyperinflated via collateral pathways and becomes emphysematous. We reported a young man with congenital bronchial atresia who presented with chronic cough with a borderline restriction of pulmonary function, and was treated successfully with thoracoscopic tri-segmentectomy. Possible differential diagnoses were also discussed. ***(Thorac Med 2022; 37: 277-281)***

Key words: congenital bronchial atresia, pulmonary emphysema, airway malformation, adult

Introduction

Congenital bronchial atresia (CBA) is a rare airway malformation in which a segmental or lobar bronchus is isolated from the main airway. Unlike most congenital anomalies of the airway, CBA is likely to have no or mild symptoms and is discovered incidentally during adulthood. Here, we report a case of CBA in an adult man.

Case Report

A 22-year-old non-smoking young man sought medical care due to a mild dry cough for several years. The symptom was non-specifically related to time, temperature, and posture. There were no accompanying symptoms such as shortness of breath, chest pain, fever, or sputum production. There was no history of asthma, pneumothorax, other systemic diseases, or congenital anomalies. He was healthy and was involved in high-intensity physical activities, such as basketball and swimming. His physical stature and chest wall were normal, but his breathing sound was decreased in the left upper chest region.

Chest radiographs showed hyperlucency and decreased vascular markings in the upper part of the left lung field, and a shifting of mediastinal structures to the contralateral side (Fig. 1). Computed tomography (CT) of the chest showed a well-demarcated region of emphysematous change and a decreased amount

[1]Division of Thoracic Surgery, Department of Surgery, Chung Shan Medical University Hospital, Taichung, Taiwan, R.O.C, [2]College of Medicine, Chung Shan Medical University, Taichung, Taiwan, R.O.C.
Address reprint requests to: Dr. Frank Cheau-Feng Lin, No.110, Sec.1, Jianguo N. Rd., Taichung City 40201, Taiwan

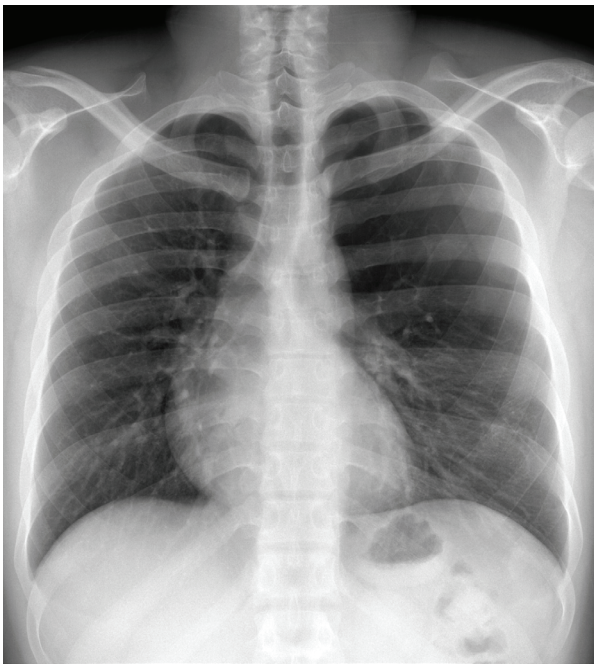

Fig. 1. Chest radiograph showed hyperlucency and decreased vascular markings in the upper half of the left-side lung field and shifting of mediastinal structures to the contralateral side.

of vascular structures in the upper division of the left upper lobe (Fig. 2). There were also several bullae, ranging from 2.5 to 6 cm in diameter, around the apical region. In addition, the upper division bronchus was discontinued at its proximal part (Fig. 3). The bronchus distal to the obliteration was distended without fluid accumulation. There were no cystic lesions or obvious mediastinal vascular anomalies. The spirometry test showed borderline decreased forced expiratory volume in 1 second (FEV1): 3.4 liters, 81% of predicted, borderline decreased forced vital capacity (FVC): 4.15 liters, 83% of predicted, and preserved total lung capacity (TLC): 6.55 liters, 97% of predicted.

Considering the mass effect of the affected lung with the persistent symptom, a thoracoscopic tri-segmentectomy of the left upper division was performed (Fig. 4). The pathology report showed bullae formation and emphysematous change in the lung. No evidence of neoplasm was found. There was prolonged air leakage postoperatively, but otherwise the procedure was uneventful. During the following 3 years, the films and CT scans showed good expansion of the left lung without recurrence of emphysema. His cough improved after the operation.

Discussion

Bronchial atresia is a rare anomaly caused

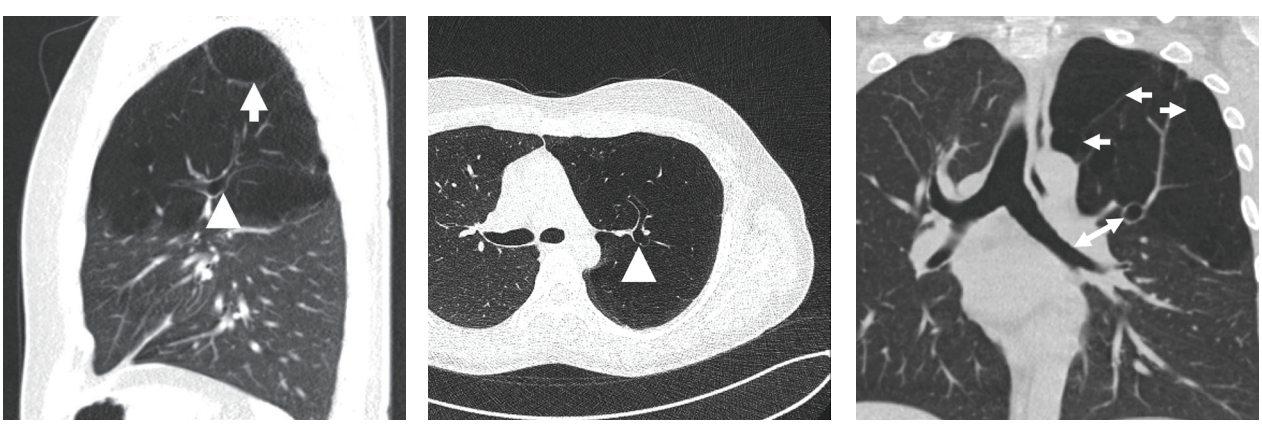

Fig. 2. Chest computed tomography images showed a well-demarcated region of emphysematous change and a decreased amount of vascular structure in the upper division of the left upper lobe. There were also several bullae ranging from 2.5 to 6 cm in diameter around the apical region (arrow). The upper division bronchus (arrowheads) was separated from the proximal part by approximately 3 cm (double-headed arrow).

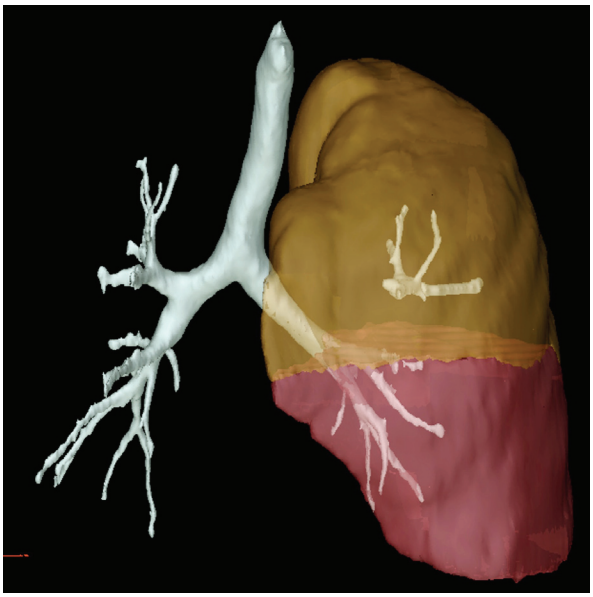

Fig. 3. Three-dimensional reconstruction of a pulmonary computed tomography scan showing the separated left upper division bronchus, the emphysematous region of the lung (brown-colored region), and the remaining left upper lobe that was relatively normal (red-colored region).

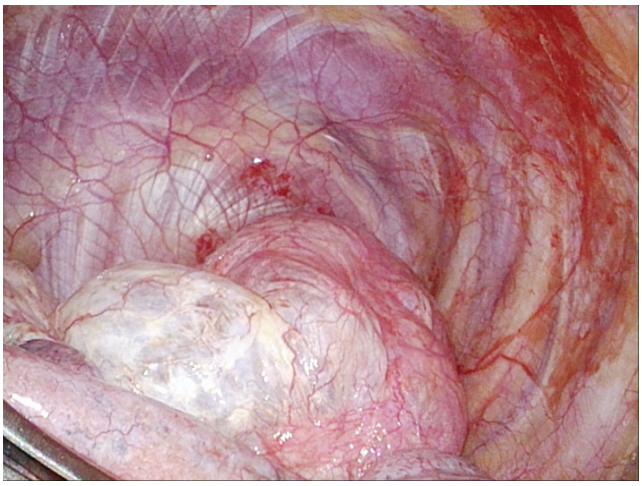

Fig. 4. Emphysematous lung and large bullae at the left upper lobe could be seen during the thoracoscopic surgery with tri-segmentectomy of the left-side upper division.

by focal obliteration of a proximal bronchus. Despite the absence of communication with the central airway, the development of the distal airway and corresponding lung parenchyma is usually normal. A review of published reports revealed that the apicoposterior segment of the left upper lobe is the most frequently involved (approximately two-thirds of patients), followed by the right upper lobe, left lower lobe, right middle lobe, and right lower lobe [1-3].

The exact cause of bronchial atresia is not fully known, but it is commonly considered to be congenital in nature. Two hypotheses have been proposed: The first suggests a repetitive ischemic injury to a segment of the bronchial wall during fetal development, and the second proposes the disconnection of a group of dividing bronchial cells from the bronchial bud [1-2].

Since most patients with bronchial atresia are asymptomatic, the exact prevalence is unknown. An estimated prevalence of 1.2 cases per 100,000 population has been put forth [4]. Approximately two-thirds of diagnoses are incidental, and occur mostly in young men during the second or third decade. However, one-third of patients present with symptoms, including cough, dyspnea, chest pain, and others likely related to recurrent pneumonia. More severe conditions, such as respiratory failure, may prompt the diagnosis at a younger age [4-5].

CT is an option for diagnosing bronchial atresia. A typical finding on CT is tubular or nodular opacities radiating from the hilum, which implies mucoid impaction of the distal bronchus, a bronchocele. The bronchocele may contain air-fluid levels. However, the absence of a bronchocele, but the presence of an air-filled bronchus, has been reported in a minority of cases. Previous articles reported the presentation of both a bronchocele and hyperinflation

in 57% to 83% of cases [3]. There was no bronchocele in the image studies or pathology report for our patient.

Ventilation via collateral pathways (interalveolar pores of Kohn) plays the role of a 1-way valve allowing air to get in, but not out. Secondary to oligemia and air-trapping, the distal lung supplied by an atretic segment may be hyperlucent and hyperinflated. In lobar atresia with complete fissure, hyperinflation may be absent due to the lack of collateral pathways, but atelectasis or a cystic lobe may be present. Severely dilated lung parenchyma may compress normal lung tissue [1,3-6].

There are no current guidelines for the management of bronchial atresia. Management is usually conservative for most asymptomatic patients. Surgery is reserved for those with major clinical symptoms. However, some authors recommend resection to prevent complications, including infection and compromise of adjacent lung regions. Even though the anomaly is more often segmental than lobar, some case series favored lobectomies, rather than sub-lobar resections, because the remaining parenchyma is usually compressed by the abnormal segment, and the obliteration is usually located near the hila [3,5,7,8]. Generally speaking, preserving as much normal lung parenchyma as possible to maintain pulmonary function is the ultimate goal of treatment. The overall prognosis is favorable, with most patients never suffering from severe symptoms, or they will experience excellent outcomes if they undergo surgery [1,8].

Several entities may show features similar to bronchial atresia. Bronchogenic cyst is caused by abnormal budding of the embryonic foregut and tracheobronchial tree. It accounts for 40%-50% of congenital mediastinal cysts, but is sometimes intrapulmonary. The cysts have epithelial lining and contain mucoid material, which may resemble the bronchocele seen in bronchial atresia. An air-fluid level may be seen if intrapulmonary cysts communicate with the tracheobronchial tree. Two-thirds of patients present with symptoms. Symptoms are often caused by compression to the airway, which leads to cough, wheezing, stridor, dyspnea, and pneumonia [2]. There was no cyst-like lesion in our patient.

Congenital lobar emphysema is characterized by progressive overdistension of 1 or 2 lobes. Areas of malacia or stenosis of bronchial cartilage, which contribute to a check-valve mechanism, are considered the most likely etiology. The most affected lobe is the left upper lobe (42.2%), followed by the right middle lobe, and right upper lobe [2]. Chest radiography and CT would show hyperinflation of the affected segment or lobe, which is similar to that in bronchial atresia. Most patients become symptomatic during the neonatal period, with respiratory distress being the most common symptom [2]. However, our patient started with dry cough, but not dyspnea, in his adulthood. Congenital lobar emphysema does not interrupt the continuum of the airway system, which is different from bronchial atresia.

Pulmonary sequestration is defined as a mass of the lung that has no connection to the normal bronchial tree, and its arterial supply arises from systemic arteries. Sequestration is divided into 2 types: intralobar and extralobar. Intralobar sequestration shares visceral pleura with the normal lung, whereas extralobar sequestration has its own. Sequestration is preferably located in the lower lobes. Chest CT may show a soft-tissue mass with an accumulation of air and fluid, bronchiectasis, focal emphyse-

ma, and a hypervascular focus, usually in basal segments of the lung. Due to the development of symptoms, including respiratory distress and recurrent pulmonary infections, sequestration is commonly diagnosed during neonatal periods and childhood. [2] The hyperinflated lung tissue in our patient was found in the left upper lobe, and the dry cough started in his adulthood. Furthermore, the lesion that presented in our patient did not have its own systemic blood supply.

Congenital pulmonary airway malformation (CPAM), also known as congenital cystic adenomatoid malformation, is characterized by multi-cystic lesions of the lung tissue. Overgrowth of bronchioles and interruption of alveolar development during fetal life contribute to this anomaly. In the most common subtype, one that accounts for 75% of cases, the lesion is composed of air-filled thin-walled cysts in variable sizes, with some dominant cysts more than 2 cm in diameter. Cysts are usually air-containing. If the diagnosis is made postnatally, one-half to two-thirds of infants would have respiratory distress or compromise. Older patients often have a recurrent pulmonary infection [2]. Our patient had no respiratory distress or pulmonary infection.

Although bronchocele is a typical finding of bronchial atresia in chest CT, our patient had no bronchocele. The separate upper division of the left-side bronchus was air-filled. Our patient sought medical advice due to chronic mild dry cough. Despite being capable of participating in high-intensity physical activities, his pulmonary function tests have shown obstructive patterns. Thus, we resected the hyper-inflated lung parenchyma and bullae to remove the compression of the normal lung tissue, and relieved his symptom.

Acknowledgment

We thank Mr. Shinji Lo from Nan Kai Corporation for his technical assistance with 3D image reconstruction.

References

1. Gipson MG, Cummings KW, Hurth KM. Bronchial atresia. Radiographics 2009 Sep-Oct; 29(5): 1531-5.
2. Berrocal T, Madrid C, Novo S, *et al*. Congenital anomalies of the tracheobronchial tree, lung, and mediastinum: embryology, radiology, and pathology. Radiographics 2004 Jan-Feb; 24(1): e17.
3. Desir A, Ghaye B. Congenital abnormalities of intrathoracic airways. Radiol Clin North Am 2009 Mar; 47(2): 203-25.
4. Psathakis K, Lachanis S, Kotoulas C, *et al*. The prevalence of congenital bronchial atresia in males. Monaldi Arch Chest Dis 2004 Jan-Mar; 61(1): 28-34.
5. Wang Y, Dai W, Sun Y, *et al*. Congenital bronchial atresia: diagnosis and treatment. Int J Med Sci 2012; 9(3): 207-12.
6. Okuda M, Huang CL, Masuya D, *et al*. Lobar bronchial atresia demonstrating a cystic lesion without overinflation. Eur J Cardiothorac Surg 2006 Aug; 30(2): 391-3.
7. Morikawa N, Kuroda T, Honna T, *et al*. Congenital bronchial atresia in infants and children. J Pediatr Surg 2005 Dec; 40(12): 1822-6.
8. Traibi A, Seguin-Givelet A, Grigoroiu M, *et al*. Congenital bronchial atresia in adults: thoracoscopic resection. J Vis Surg 2017 Nov 30; 3:174.

Intralobar Pulmonary Sequestration with a Significantly Elevated CA 19-9 Level: A Case Report

Kuan-Ming Su[1], Hsao-Hsun Hsu[2], Hao-Chien Wang[1]

Pulmonary sequestration is a rare congenital malformation of non-functioning lung tissue that does not communicate with the airway system and that receives its blood supply from anomalous systemic arteries. An intralobar pulmonary sequestration often presents as an incidental finding on chest computed tomography or is diagnosed via histopathological review of a resected lung tumor. Some cases may have cough, hemoptysis, dyspnea or recurrent pulmonary infections at a certain segment. Over the past 3 decades, there have been several case reports that describe the association between pulmonary sequestration and elevated CA 19-9, which is a widely used tumor marker for gastrointestinal and pancreatobiliary cancers. The underlying mechanism of the elevated CA 19-9 in pulmonary sequestration was thought to be a chronic inflammatory process of the epithelial cells, or an infection, such as Aspergillus or Mycobacterium. In this case report, we present a 50-year-old woman who had a cough with persistent right lower lung opacity for 3 years. An elevated serum CA 19-9 level, up to 3670 U/ml, which was the highest among reported cases, was found in the patient's health exam 1 year prior to her initial presentation. The patient had no evident malignancies. Intralobar pulmonary sequestration was diagnosed by contrast-enhanced computed tomography, and the patient received a right lower lobectomy. Her CA 19-9 level returned to a normal range 4 months after the operation. ***(Thorac Med 2022; 37: 282-287)***

Key words: Pulmonary sequestration, carbohydrate antigen 19-9 (CA 19-9)

Introduction

Pulmonary sequestration is a rare congenital malformation of non-functioning lung tissue that does not communicate with the airway system and that receives its blood supply from anomalous systemic arteries [1]. Pulmonary sequestration comprises 0.15 to 6.4% of all cases of congenital lung malformation. It was first described by Pryce in 1946, and can be divided into 2 types: intralobar and extralobar [2]. Intralobar pulmonary sequestration shares the same visceral pleura as the adjacent normal lung tissue, and the reported incidence was

[1]Division of Pulmonary and Critical Care Medicine, Department of Internal Medicine, National Taiwan University Hospital and College of Medicine, National Taiwan University, Taipei, Taiwan, [2]Division of Thoracic Surgery, Department of Surgery, National Taiwan University Hospital and College of Medicine, National Taiwan University, Taipei, Taiwan
Address reprint requests to: Dr. Hao-Chien Wang, Division of Pulmonary and Critical Care Medicine, Department of Internal Medicine, National Taiwan University Hospital, No. 7, Chung-Shan South Road, Taipei 100, Taiwan

around 75% among all pulmonary sequestration cases. The extralobar type has its own pleura and separates them from the normal lung tissue [3]. Both types have an abnormal systemic blood supply. The arterial supply comes mostly from the thoracic aorta, and may originate from the infradiaphragmatic aorta in approximately 20% of cases [4]. Arterial supply from other systemic arteries, such as the coronary artery, has also been reported [4-7]. The venous return typically drains into the inferior pulmonary vein in the intralobar type. In the extralobar type the venous drainage is often via the azygos vein, although unusual drainage routes, such as into portal veins, have been reported [8].

CA 19-9 (carbohydrate antigen 19-9) is a validated and widely used tumor marker for pancreatic cancer [9]. It is synthesized by normal human pancreatic and biliary ductal cells, and by gastric, colonic, endometrial and salivary epithelia. An elevated CA 19-9 level can be seen in pancreatobiliary and gastrointestinal cancers, but is not specific to those malignancies. There are several case reports describing the association between pulmonary sequestration and elevated serum CA 19-9 levels [10-22]. In this report, we describe a case of intralobar pulmonary sequestration with significantly elevated serum CA 19-9. The serum CA 19-9 level returned to normal after complete surgical resection.

Case Presentation

A 50-year-old female presented to our hospital with intermittent productive cough and persistent right lower lung (RLL) patchy opacity for more than 3 years. She was a non-smoker, and had a history of allergic rhinitis and chronic sinusitis post-left functional endoscopic sinus surgery on 2020/01/30. She recalled that she had an abnormal chest radiograph during a health exam 12 years ago, but she did not receive further exams. Intermittent cough with sputum developed during the past 3 years; she was diagnosed as having had 3 episodes of RLL pneumonia and was treated with antibiotics. The symptoms of pneumonia resolved after treatment, but the RLL opacity persisted. She denied fever, shortness of breath, chest tightness, general malaise or unintentional weight loss. Her physical exam was unremarkable. Her blood tests reported no significant abnormalities in the hemogram, biochemistry profile and autoimmune profile. Her chest radiograph revealed a RLL opacity that had not shown significant interval change during the past 3 years (Figure 1). A contrast-enhanced chest computed tomography (CT) for delayed resolution of the RLL opacity revealed a RLL mass-like patchy consolidation with a feeding artery from the ab-

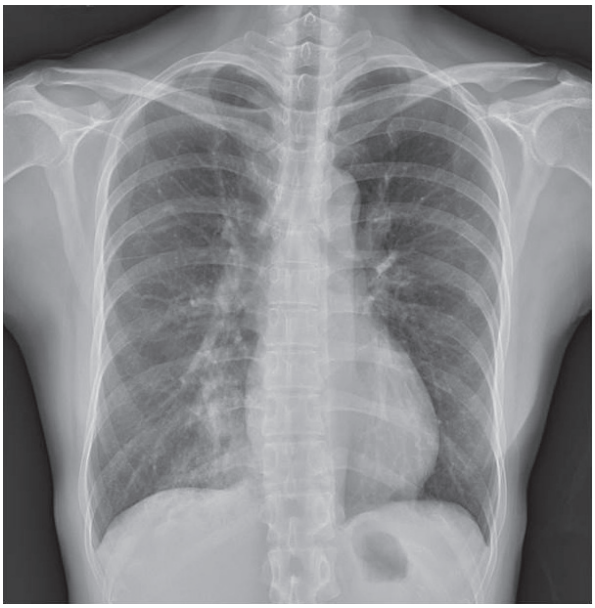

Fig. 1. CXR showed a left upper lung opacity and blunting of the costophrenic angle.

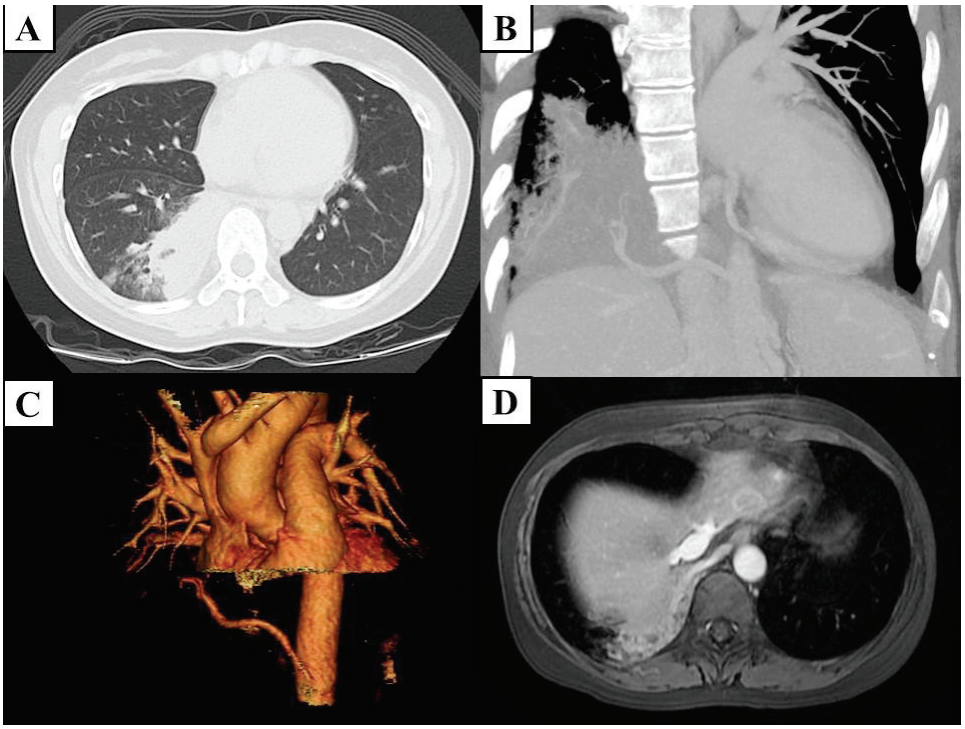

Fig. 2. A. High-resolution chest computed tomography reveals a right lower lung mass-like consolidation with surrounding ground-glass opacities; B. Coronal view of the contrast-enhanced computed tomography shows a feeding vessel from the abdominal aorta entering the right lower lung consolidation; C. 3D reconstructed computed tomography demonstrates the supplying vessels; D. Contrast-enhanced magnetic resonance imaging also reveals a feeding artery from the abdominal aorta.

dominal aorta (Figure 2). Intralobar pulmonary sequestration was therefore suspected.

Our patient was also found to have had elevated serum CA 19-9 level in another health exam about 4years ago; the initial level was 3670 U/ml. The level went as high as > 12000 U/ml at her regular follow-ups in our hospital during the past 3 years (Figure 3). Other tumor markers, including alpha-fetoprotein and CEA, were within normal limits. Surveys of malignancies such as Pap smear, upper gastrointestinal panendoscopy, colon fibroscopy, ultrasonography of the abdomen and pelvis and abdominal magnetic resonance imaging reported no significant abnormalities. A video-assisted thoracoscopic surgery right lower lobectomy then was performed. The histology of the resected lung specimens reported acute and chronic inflammation, with extensive lymphoid aggregates around dilated bronchioles, intraluminal debris and interstitial fibrosis. The resected groups 7, 9 and 11 lymph nodes showed reactive changes. The pathology picture was consistent with an intralobar pulmonary sequestration. Her serum CA 19-9 level returned to normal (6.39 U/ml) 4 months after surgical resection (Figure 3).

Discussion

Our patient was a 50-year-old, never-smoking female who worked as an elementary school teacher. She had no known systemic illness or

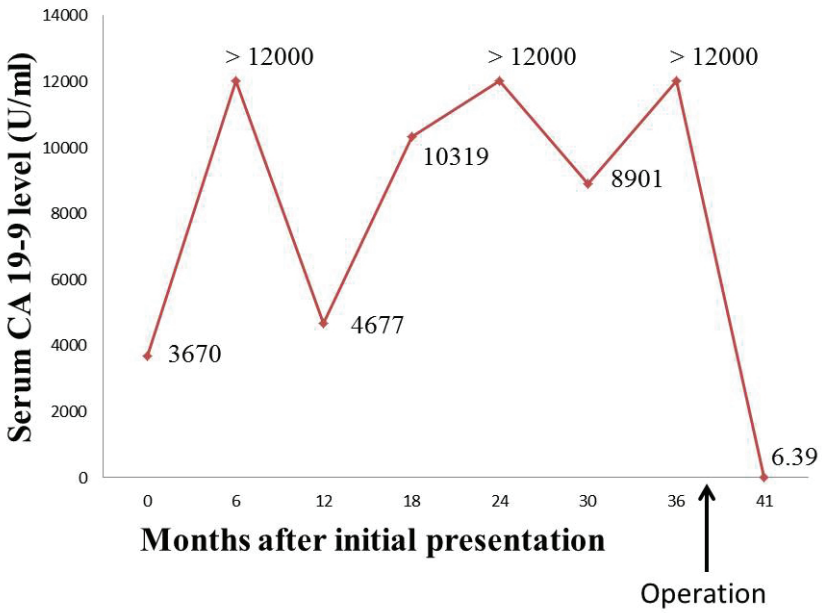

Fig. 3. The increase and decrease in the patient's serum CA 19-9 level over time.

family history of malignancies. She presented with chronic cough and recurrent RLL pneumonia. According to published reports, about 60% of intralobar sequestrations are diagnosed at the age of 20 or younger, and are rarely diagnosed in patients older than 50 years [23]. In a case series reviewing adult patients with pulmonary sequestration from 1997 to 2016, the median age at diagnosis was 42 years; 53% of these patients were male and 47% of them had no relevant symptoms [24].

Asymptomatic intralobar pulmonary sequestrations are often diagnosed incidentally on chest CT. Recurrent pneumonia in a localized segment of the lung is a common clinical presentation of symptomatic intralobar pulmonary sequestration. Cough, hemoptysis and dyspnea on exertion have also been reported in symptomatic cases [25].

CA 19-9 is a widely used tumor marker for gastrointestinal and pancreatobiliary tumors. However, CA 19-9 is not specific to those diseases only. Non-malignant disorders, such as chronic and acute pancreatitis, liver cirrhosis, cholangitis, obstructive jaundice [26], ovarian cyst, heart failure, Hashimoto's thyroiditis, rheumatoid arthritis and diverticulitis have been reported to cause increased CA 19-9 levels [27-28]. Elevated CA 19-9 has also been reported in patients with lung cancer and other non-malignant respiratory disorders, such as idiopathic interstitial pneumonia, diffuse panbronchiolitis, and collagen disease-associated pulmonary fibrosis [29].

Our patient had a significantly elevated CA 19-9 level in a health exam, which raised the concern of undiagnosed cancer. The clinical history, presentation and detailed survey for gastrointestinal cancers reported no evidence of cancer. But clinically, a lung malignancy should be ruled out because of the delayed resolution of RLL opacity with a significantly elevated

tumor marker. Contrast-enhanced CT revealed a feeding artery from the abdominal aorta into the RLL lesion, which is characteristic of pulmonary sequestration. The association between pulmonary sequestration and elevated CA 19-9 is well demonstrated by the normalization of CA 19-9 post operatively, and that there was no evidence of any malignancies.

The underlying mechanism of elevated CA 19-9 levels remains unclear. Some authors thought the mechanism might be due to the effect of the chronic inflammatory process of epithelial cells, because immunohistochemical staining revealedproduction of CA 19-9 in the bronchial and alveolar epithelia of the sequestrated lung [15]. Some others have suggested that a chronic inflammatory process due to infection, such as by Aspergillus or Mycobacterium, may be the cause [18, 22, 30]. Although our patient presented with recurrent pneumonia, and acute and chronic inflammation was found histologically in the resected lung tissue, she was tested several times for sputum cultures and serum galactomannan antigen, all of which were reported to be negative. There was no history or microbiological evidence suggesting that she had aspergillosis or tuberculosis.

In reviewing the published articles, we found 16 case reports that described an association between pulmonary sequestration and elevated serum CA 19-9, including 11 female and 5 male patients with an average age of 40 years (20- 64 years). The reported serum CA 19-9 level had an average of 1060.7 U/ml, ranging from 73.8 U/mL to 3051.1 U/ml [21]. Our patient had the highest initial CA 19-9 level among the published case reports at presentation and was persistently at a very high level during clinical follow-up until the pulmonary sequestration was resected.

In sum, based on our case report and previous articles, pulmonary sequestration can be associated with an elevated serum CA 19-9 level. Suspicion of pulmonary sequestration should be raised in patients with elevated an serum CA 19-9 level plus a persistent lower lung lesion or recurrent pneumonias at the lower lung field.

References

1. Mathew S, Erozan YS. Pulmonary sequestration--a diagnostic pitfall: a case report. Diagn Cytopathol 1997 Apr; 16(4): 353-7.
2. Pryce DM. Lower accessory pulmonary artery with intralobar sequestration of lung; a report of seven cases. J Pathol Bacteriol 1946 Jul;58(3): 457-67.
3. Rosado-de-Christenson ML, Frazier AA, Stocker JT, *et al*. From the archives of the AFIP. Extralobar sequestration: radiologic-pathologic correlation. Radiographics 1993 Mar;13(2): 425-41.
4. Lee EY, Siegel MJ, Sierra LM, *et al*. Evaluation of angioarchitecture of pulmonary sequestration in pediatric patients using 3D MDCT angiography. AJR Am J Roentgenol. 2004 Jul;183(1): 183-8.
5. Van Langenhove G, Convens C, Seynaeve P, *et al*. Intralobar pulmonary sequestration supplied by the right coronary artery. Cathet Cardiovasc Interv 1999; 47: 218-220.
6. Bertsch G, Markert T, Hahn D, *et al*. Intralobar lung sequestration with systemic coronary arterial supply. Eur Radiol 1999; 9: 1324 -1326
7. Grigoryants V, Sargent SK, Shorter NA. Extralobar pulmonary sequestration receiving its arterial supply from the innominate artery. Pediatr Radiol. 2000 Oct; 30(10): 696-8.
8. Kamata S, Sawai T, Nose K, *et al*. Extralobar pulmonary sequestration with venous drainage to the portal vein: a case report. Pediatr Radiol 2000; 30: 492 -494
9. Duffy MJ, Sturgeon C, Lamerz R, *et al*. Tumor markers in pancreatic cancer: a European Group on Tumor Markers (EGTM) status report. Ann Oncol 2010 Mar; 21(3): 441-447.
10. Kodama T, Satoh H, Ishikawa H, *et al*: Serum levels of CA19-9 in patients with nonmalignant respiratory

diseases. J Clin Lab Anal 2007; 21: 103-106.
11. Shiota Y, Kitade M, Furuya K, *et al*: A case of intralobar pulmonary sequestration with high serum CA19-9 levels. Acta Med Okayama 1988; 42: 297-300.
12. Yagyu H, Adachi H, Furukawa K, *et al*. Intralobar pulmonary sequestration presenting increased serum CA19-9 and CA125. Intern Med. 2002 Oct;41(10): 875-8.
13. Morikawa H, Tanaka T, Hamaji M, *et al*. A case of aspergillosis associated with intralobar pulmonary sequestration. Asian Cardiovasc Thorac Ann. 2011 Feb;19(1): 66-8.
14. Matsuoka H, Nohara H: Pulmonary sequestration with high levels of tumor markers tending to be misdiagnosed as lung cancer. Jpn J Thorac Cardiovasc Surg 2006; 54: 117-119.
15. Ambiru S, Nakamura S, Fukasawa M, *et al*. Intralobar pulmonary sequestration associated with marked elevation of serum carbohydrate antigen 19-9. Ann Thorac Surg 2009 Dec;88(6): 2010-1.
16. Komatsu H, Mizuguchi S, Izumi N, *et al*. Pulmonary sequestration presenting elevated CA19-9 and CA125 with ovarian cysts. Ann Thorac Cardiovasc Surg. 2014;20 Suppl: 686-8.
17. Han P, Luo Y, Tian D, *et al*. Pulmonary sequestration presenting with left upper abdominal bloating and marked elevation of serum carbohydrate antigen 19-9: a case report. Oncol Lett 2014 May;7(5): 1493-1496.
18. Ahn YH, Song MJ, Park SH: Intralobar pulmonary sequestration showing increased serum CA19-9. Tuberc Respir Dis (Seoul) 2012; 72: 507- 510.
19. Kugai T, Kinjyo M. [Extralobar sequestration presenting increased serum CA19-9 and associated with lung aspergillosis--an unusual case]. Nihon Kyobu Geka Gakkai Zasshi 1996 Apr; 44(4): 565-9.
20. mbruster C, Kriwanek S, Feichtinger H, *et al*. Intra-abdominal sequestration of the lung and elevated serum levels of CA 19-9: a diagnostic pitfall. HPB (Oxford) 2004; 6(1): 45-8.
21. Dong J, Cai Y, Chen R, *et al*. A case report and a short literature review of pulmonary sequestration showing elevated serum levels of carbohydrate antigen 19-9. J Nippon Med Sch 2015; 82(4): 211-5.
22. Nagaoka H, Taniguchi T, Iesato H, *et al*. Pulmonary sequestration with the elevated serum value of CA19-9: a case report. J Jpn Pract Surg Soc 1996; 57: 571-4.
23. Montjoy C, Hadique S, Graeber G, *et al*. Intralobar bronchopulmonary sequestra in adults over age 50: case series and review. W V Med J. 2012 Sep-Oct; 108(5): 8-13.
24. Alsumrain M, Ryu JH. Pulmonary sequestration in adults: a retrospective review of resected and unresected cases. BMC Pulm Med 2018 Jun 5; 18(1): 97.
25. Mohapatra M, Mishra S, Jena P. Massive hemoptysis in a case of intralobar pulmonary sequestration associated with pulmonary hypoplasia and meandering right pulmonary vein: diagnosis and management. Case Rep Pulmonol 2012; 2012: 960948.
26. Duffy MJ. Role of tumor markers in patients with solid cancers: A critical review. Eur J Intern Med 2007 May;18(3): 175-84.
27. Kim HR, Lee CH, Kim YW, *et al*. Increased CA 19-9 level in patients without malignant disease. Clin Chem Lab Med 2009; 47(6): 750-4.
28. Kim YC, Kim HJ, Park JH, *et al*. Can preoperative CA19-9 and CEA levels predict the resectability of patients with pancreatic adenocarcinoma? J Gastroenterol Hepatol 2009 Dec;24(12): 1869-75.
29. Ventrucci M, Pozzato P, Cipolla A, *et al*. Persistent elevation of serum CA 19-9 with no evidence of malignant disease. Dig Liver Dis. 2009 May; 41(5): 357-63.
30. Ishiura Y, Fujimura M, Minami S, *et al*. Increased CA19-9 level in serum and brochoalveolar lavage fluid from a patient with pulmonary tuberculosis. Nihon Kyobu Shikkan Gakkai Zasshi 1996;34: 477-81.

ROS1-mutated NSCLC with an Uncommon Fusion Partner Treated with Crizotinib – From an Initial Good Response to Acquired Resistance and Rapid Progression

Chien-Yu Lin[1,2], Chia-Hao Hu[1], Che-Wei Hsu[3], Chien-Chung Lin[1,2]

ROS1+ non-small cell lung cancer (NSCLC) is a heterogeneous disease with at least 24 distinct fusion partners and five fusion partners (CD74, SLC34A2, SDC4, ERZ, and TPM3) primarily made up of the ROS1+ patients with NSCLC. A recent study proposed that ROS1 fusion partners may be classified as CD74-ROS1 and non–CD74-ROS1, since these 2 groups have different responses to crizotinib, and a predilection for central nervous system metastasis. Intergenic-breakpoint fusions are defined as 1 or both genomic breakpoints localizing to the intergenic regions; however, whether these intergenic-breakpoint fusions can be activated or not remains unresolved. Here, we reported a case of advanced ROS1 fusion gene rearrangement lung adenocarcinoma, which initially responded to crizotinib, but then recurred within 3 months. The DNA next-generation sequencing for liquid biopsy showed G2032R and L2026M mutations, and an uncommon ROS1 fusion with an intron (ROS1-LOC100505984 rearrangement); however, the patient did not respond to cabozantinib, and instead experienced disease progression. ***(Thorac Med 2022; 37: 288-294)***

Key words: Crizotinib, Cabozantinib, uncommon fusion partner, intergenic-breakpoint fusion, intron

Introduction

ROS1-rearranged non-small cell lung cancer (NSCLC) accounts for around 1.5% of all NSCLC cases in the Asian population [1]. NSCLC patients with ROS1 rearrangement tend to be younger and nonsmokers [2], with lower rates of extrathoracic metastasis, including brain metastasis [3]. Several tyrosine kinase inhibitors (TKIs) have been developed and confirmed to provide survival benefits for these patients [4].

Crizotinib, a TKI-targeting anaplastic lymphoma kinase (ALK), was approved by the FDA (Food and Drug Administration) for treatment of ROS1-rearranged NSCLC in March 2016. Approval was based on its efficacy in an expansion cohort in a phase I study (PROFILE

[1]Department of Internal Medicine, National Cheng Kung University Hospital, [2]Division of Pulmonary Medicine, Department of Internal Medicine, National Cheng Kung University Hospital, [3]Department of Pathology, National Cheng Kung University Hospital.
Address reprint requests to: Dr. Chien-Chung Lin, Department of Internal Medicine and Institute of Clinical Medicine, College of Medicine, National Cheng Kung University Hospital, 138 Sheng-Li Road, Tainan 704, Taiwan.

1001) [5]. Updated results of the study in 2019 showed that crizotinib provided efficient treatment and survival benefits with an objective response rate (ORR) of 72% and a median progression-free survival (PFS) of 19.2 months for patients with advanced ROS1-positive NSCLC [6]. Similar results have been reported in other studies that enrolled East Asian populations [7] and a real-world cohort [8].

Patients with an ALK mutation receiving crizotinib therapy and NSCLC patients with ROS1-rearrangements have developed drug resistance during crizotinib treatment [9]. The G2032R mutation (alteration of another active site residue) is the most frequently identified factor in crizotinib-resistant NSCLC [4], with cabozantinib being reported as a potential agent to target G2032R-mutated NSCLC [10]. The L2026M "gatekeeper" mutation is another acquired resistance that may be sensitive to cabozantinib, as reported in a preclinical study [11].

In addition to the initial- and secondary-resistance mutations that correlate to the response to TKI, evidence has shown that the ROS1 fusion partner is another important factor. A retrospective study with 36 NSCLC patients with ROS1 rearrangements found that the most common ROS1 fusion partner was the CD74 gene, and patients with this fusion partner had a lower ORR and were more likely to present with brain metastases [12]. Intergenic-breakpoint fusions, in which 1 or both genomic breakpoints localize in the intergenic regions, result in a breakpoint between introns of the 2 genes that can be detected by DNA-based next generation sequencing (NGS). Since no chimeric fusion proteins are produced, patients with mutations are unlikely to benefit from the treatment. However, a recent study suggested that RNA-based NGS could improve fusion detection and may also be preferred for intergenic-breakpoint fusions [13].

Herein, we report a case of advanced uncommon ROS1 fusion gene rearrangement lung adenocarcinoma showing an initial response to crizotinib, but then recurring within 3 months. NGS for liquid biopsy was performed during the recurrence and showed G2032R and L2026M mutations and uncommon ROS1 fusion with an intron (ROS1-LOC100505984 rearrangement); however, the patient did not respond to cabozantinib, and instead experienced disease progression.

Case

A 47-year-old woman visited our outpatient clinic with the complaints of general weakness and dyspnea for 1 month. Chest radiography showed massive right pleural effusion. Chest computed tomography (CT) was arranged and revealed a right upper-lung tumor with pleural seeding, superior vena cava (SVC) thombi, and mediastinal and neck lymphadenopathy (Figures 1A, B). Diagnostic thoracentesis was performed and cytology showed malignant cells. A neck lymph-node biopsy showed poorly differentiated adenocarcinoma with positive TTF-1, which was compatible with pulmonary origin (Figure 2). The EGFR mutation RT-PCR test was negative. A further immunohistochemistry test showed a positive result for ROS1 (Figure 3). Although brain MRI did not show brain metastasis, a bone scan indicated multiple bone metastases (Figure 1C), stage IVB (T4N3M1c).

She was then treated with crizotinib (500 mg/day) for ROS1-rearranged NSCLC and apixaban for SVC thrombi. Her dyspnea improved after 1 month of crizotinib use, since the pleural effusion and right upper lobe (RUL) mass had decreased (Figure 4A, before crizo-

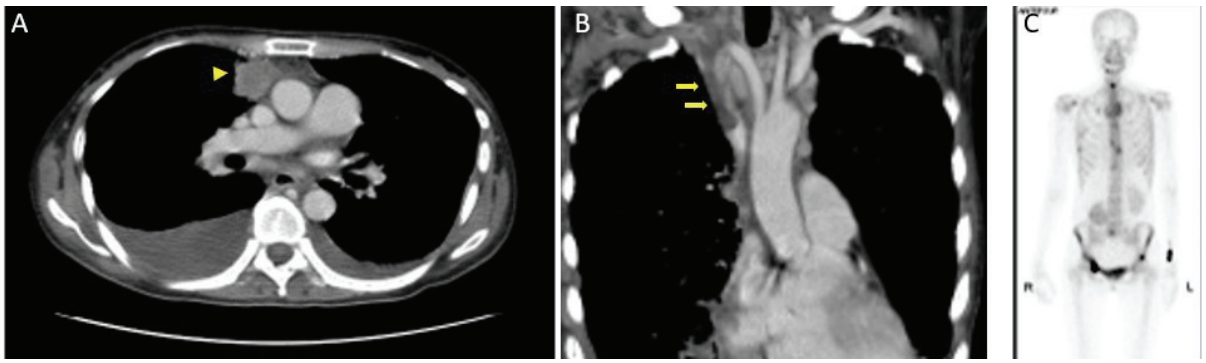

Fig. 1. Image study before and after first-line crizotinib therapy. Chest computed tomography (CT) showed a right upper lung mass (A, arrowhead) with ipsilateral pleural effusion and superior vena cava (SVC) thrombi (B, arrow). A bone scan showed multiple bone metastases (C).

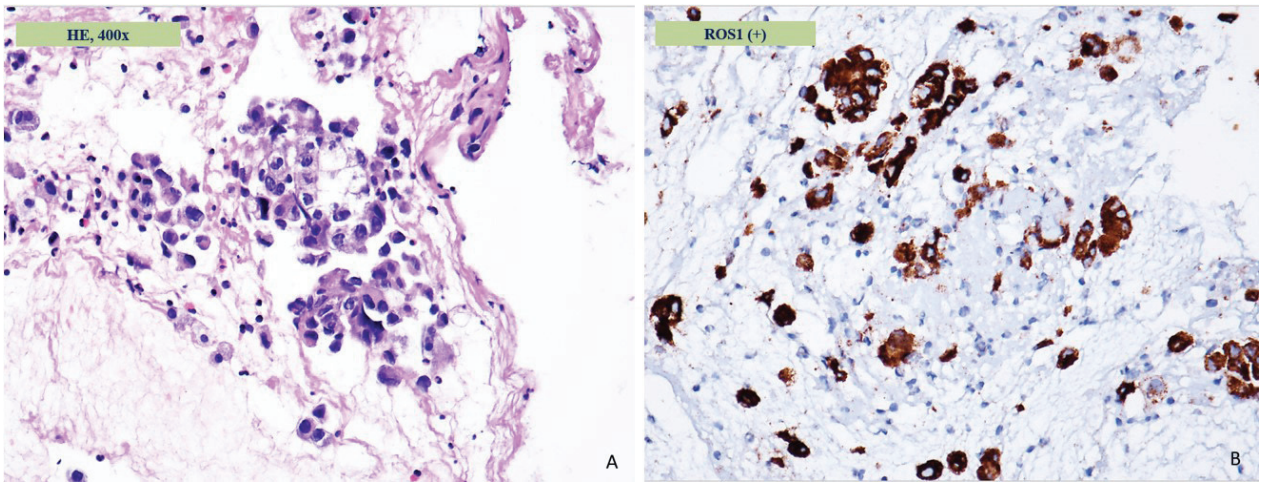

Fig. 2. Microscopic findings of a neck lymph node biopsy.
The glandular structures supported the diagnosis of lung adenocarcinoma (A, hematoxylin and eosin stain, magnification ×400). Immunohistochemical staining showed strong, brown cytoplasmic staining in most tumor cells (B).

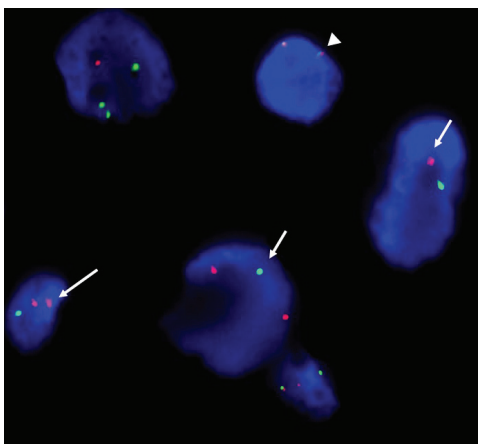

Fig. 3. Fluorescent in situ hybridization (FISH) test for ROS1 gene rearrangement. The FISH test showed a typical ROS1-positive pattern (separated 3′ (red) and 5′ (green) fluorescence) (arrow mark) and normal cells with fused signals (arrowhead).

tinib use; Figure 4B, after crizotinib treatment for 1 month).

However, 2 months later, a brain MRI was arranged because the patient complained of headaches. The chest x-ray and corresponding CT image showed interval progression of RUL cancer with total collapse of the right middle and right lower lobes, progressive lymphadenopathy at the mediastinum, and progressive right pleural seedings with massive pleural effusion (Figure 4C). The MRI image showed nodules in the left parietal lobe and left cerebellar hemisphere compatible with new brain

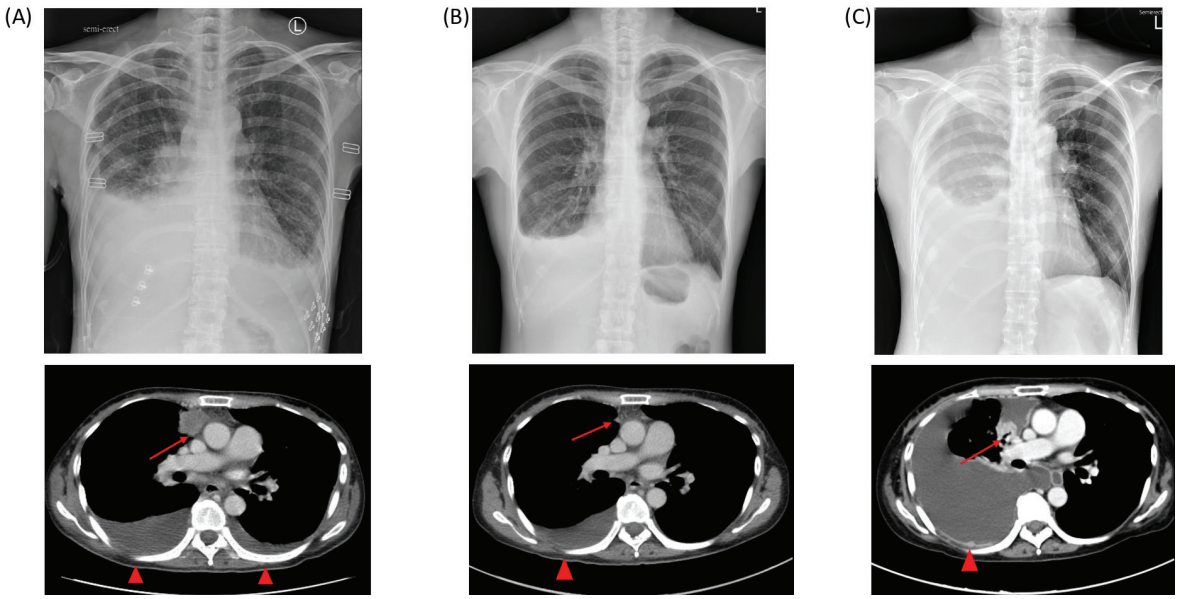

Fig. 4. Chest x-ray and corresponding CT image at diagnosis (A), after treatment with crizotinib for 1 month (B), and after treatment with crizotinib for 3 months (C).

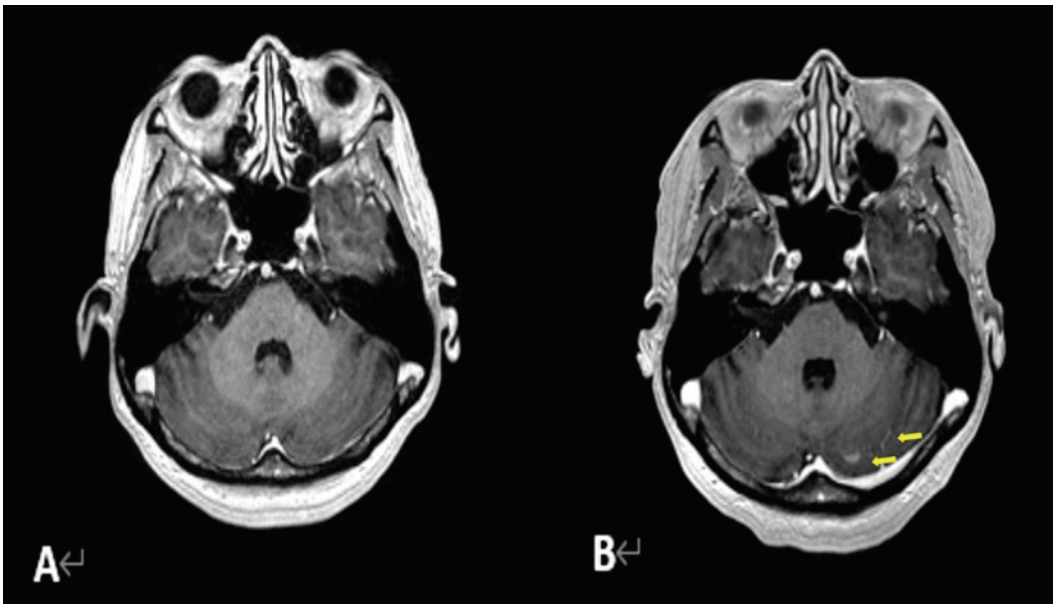

Fig. 5. Brain MRI before and after 3-month crizotinib use: no lesions were identified before crizotinib treatment (A), and new brain metastases (arrow) in the left cerebellar hemisphere developed after 2 months of crizotinib use (B)

metastasis lesions (Figures 5A, B). An DNA NGS study of the peripheral blood samples revealed G2032R and L2026M mutations and uncommon ROS1 fusion with an intron (ROS1-LOC100505984 rearrangement) (Table 1).

Because of the patient's poor performance status, we shifted treatment to cabozantinib 60 mg daily, based on the results of a previous pre-clinical study and a recent phase II study [11,14]. Grade 2 adverse effects, such as headaches and

Table 1. Blood next-Generation Sequencing (NGS) Report

		MAF%
ROS1	L2026M	0.16%
	G2032R	0.51%
	ROS1-LOC10050598 4 rearrangement	present
KRAS	G12S	0.47%
TP53	deletion exons 4-6	present

MAF: mutant allele frequency

paronychia, were noted after cabozantinib use. Two months later, she suffered from worsening headaches, an unsteady gait, nausea and vomiting, and then was sent to our emergency department. The brain MRI image revealed progression of metastases in the bilateral cerebral hemispheres and left cerebellar hemisphere with edema change, as well as newly-found leptomeningeal metastases (Figures 6). A lumbar puncture was performed and increased intracranial pressure was noted. Cerebrospinal fluid cytology showed malignant cells. Thereafter, she received 1 cycle of pemetrexed, but experienced disease progression complicated with pneumonia and respiratory failure. The patient's survival duration was less than 7 months.

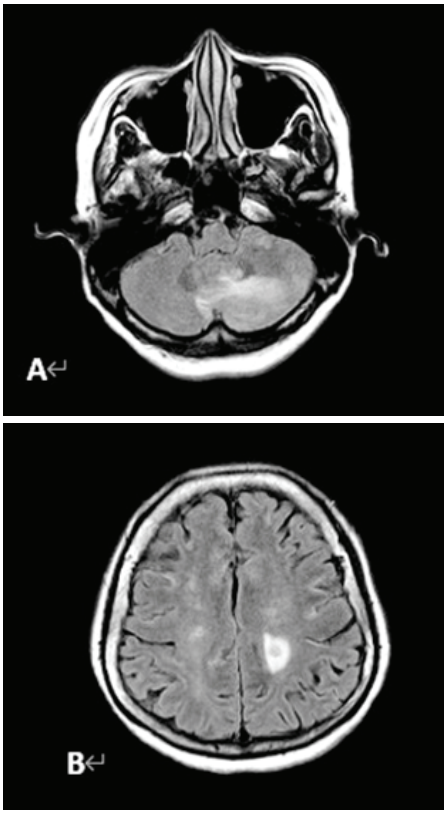

Fig. 6. Brain MRI showed progression of metastasis in the cerebellum (A) and new cerebrum metastasis (B) after 2 months of cabozantinib use.

Discussion

In the PROFILE 1001 study of 52 patients with ROS1-rearranged NSCLC, crizotinib treatment contributed to a median PFS of 19.3 months (5). Previous case reports and in vitro studies have shown that cabozantinib has promising efficacy in treating patients with acquired resistance to crizotinib [11,14].

Different fusion partners may have diverse clinical presentations, efficacy and prognoses. In a study of 49 patients with ROS1 rearrangement, compared with a non–CD74-ROS1 group, the CD74-ROS1 group had low PFS,

low overall survival, and a higher rate of brain metastases after treatment with crizotinib (11).

In our patient, in addition to the G2032R and L2026M mutations, an ROS1 mutation was identified in an NGS blood study. Whether the G2032R mutation was de novo remains unknown, since the biopsied tumor before crizotinib use was too small for an NGS study. Also, to the best of our knowledge, G2032R and L2026M have usually been detected after treatment with crizotinib, and not at the pretreatment stage [4]. However, we cannot exclude the possibility of de novo G2032R/L2026M mutations in this patient.

ROS1 fusion with an intron (ROS1-LOC100505984), which has not been previously reported, was also identified. Unlike previous clinical trials or case reports, our patient showed a short-term response, but then rapid progression of the primary cancer and metastatic brain lesions occurred after taking crizotinib 250 mg twice per day for 3 months. A previous preclinical study demonstrated the efficacy of cabozantinib in overcoming an acquired G2032R mutation, but our patient did not respond to the treatment. We also identified TP53 and KRAS mutations in the blood NGS, which may have contributed to the poor response to crizotinib in our patient [15-16]. Another case report also showed a poor response to crizotinib use in an NSCLC patient with a concurrent ROS1 gene rearrangement and KRAS mutation [15]. Furthermore, a retrospective multicenter study enrolled 94 NSCLC patients with ROS1-rearrangements, and one-third of these patients harbored a concurrent TP53 mutation; these patients had a shorter PFS than those without a TP53 mutation [16]. Therefore, we cannot exclude the possibility that a TP53 or KRAS mutation resulted in a rapid recurrence after crizotinib use and a poor response to cabozantinib.

Sun *et al*. reported that cabozantinib provided a survival benefit, with PFS ranging from 4.9 to 13.8 months, and apparent intracranial activity in 4 patients who developed resistance after first-line crizotinib or ceritinib use [17]. Another phase 2 trial also showed cabozantinib contributed to disease regression (-7% to -92%) in 6 patients who developed resistance to crizotinib [14]. However, a case with a disappointing response to cabozantinib similar to our case was reported by Florian Guisier et al. This ROS1-fusion NSCLC patient developed resistance to crizotinib and subsequent lorlatinib treatment. Though NGS of the pleural biopsy specimen showed a G2032R ROS1 mutation, the patient did not respond to cabozantinib [18].

Recent studies have emphasized that intergenic-breakpoint fusions, in which 1 or both genomic breakpoints localize to intergenic regions, may confound kinase-fusion detection. DNA-based NGS is sufficient to identify actionable mutations and fusions in the majority of cases. When a rearrangement with an intergenic-breakpoint is identified, an RNA-based NGS assay may add value as to whether the functional fusion transcript is being generated or not. However, the clinical significance of these intergenic breakpoints remains unresolved.

Conclusion

We reported a patient with ROS1-rearranged advanced NSCLC who initially responded to crizotinib, but with a shorter PFS of around 3 months. The DNA NGS of the liquid biopsy identified G2032R and L2026M mutations, and an uncommon ROS1 fusion with an intron (ROS1-LOC100505984 rearrangement),

which has not been previously reported. Though cabozantinib was prescribed in accordance with previous preclinical data, the patient did not benefit from this treatment and developed rapid progression of lung cancer. The impact of the rare ROS1 fusion gene of the intron (ROS1-LOC100505984 rearrangement) in this case may be a novel topic of interest for further research.

References

1. Cui M, Han Y, Li P, *et al*. Molecular and clinicopathological characteristics of ROS1-rearranged non-small-cell lung cancers identified by next-generation sequencing. Mol Oncol 2020 Nov; 14(11): 2787-2795.
2. Bergethon K, Shaw AT, Ou SH, *et al*. ROS1 rearrangements define a unique molecular class of lung cancers. J Clin Oncol 2012; 30(8): 863-70.
3. Gainor JF, Tseng D, Yoda S, *et al*. Patterns of metastatic spread and mechanisms of resistance to crizotinib in ROS1-positive non-small-cell lung cancer. JCO Precis Oncol 2017; 2017.
4. D'Angelo A, Sobhani N, Chapman R, *et al*. Focus on ROS1-positive non-small cell lung cancer (NSCLC): crizotinib, resistance mechanisms and the newer generation of targeted therapies. Cancers 2020 Nov; 12(11): 3293.
5. Shaw AT, Ou SH, Bang YJ, *et al*. Crizotinib in ROS1-rearranged non-small-cell lung cancer. N Engl J Med 2014; 371(21): 1963-71.
6. Shaw AT, Riely GJ, Bang YJ, *et al*. Crizotinib in ROS1-rearranged advanced non-small-cell lung cancer (NSCLC): updated results, including overall survival, from PROFILE 1001. Ann Oncol 2019; 30(7): 1121-6.
7. Wu YL, Yang JC, Kim DW, *et al*. Phase II study of crizotinib in East Asian patients with ROS1-positive advanced non-small-cell lung cancer. J Clin Oncol 2018; 36(14): 1405-11.
8. Liu C, Yu H, Chang J, *et al*. Crizotinib in Chinese patients with ROS1-rearranged advanced non-small-cell lung cancer in routine clinical practice. Target Oncol 2019; 14(3): 315-23.
9. Chong CR, Bahcall M, Capelletti M, *et al*. Identification of existing drugs that effectively target NTRK1 and ROS1 rearrangements in lung cancer. Clin Cancer Res 2017; 23(1):204-13.
10. Chong CR, Bahcall M, Capelletti M, *et al*. Identification of existing drugs that effectively target NTRK1 and ROS1 rearrangements in lung cancer. Clin Cancer Res 2017; 23(1): 204-13.
11. Katayama R, Kobayashi Y, Friboulet L, *et al*. Cabozantinib overcomes crizotinib resistance in ROS1 fusion-positive cancer. Clin Cancer Res 2015; 21(1): 166-74.
12. Li Z, Shen L, Ding D, *et al*. Efficacy of crizotinib among different types of ROS1 fusion partners in patients with ROS1-rearranged non-small cell lung cancer. J Thorac Oncol 2018; 13(7): 987-95.
13. Li W, Liu Y, Li W, *et al*. Intergenic breakpoints identified by DNA sequencing confound targetable kinase fusion detection in NSCLC. J Thorac Oncol 2020; 15(7): 1223-31.
14. Guo R, Preeshagul I, Schoenfeld A, *et al*. P1. 14-50 A phase 2 trial of cabozantinib in ROS1-rearranged lung adenocarcinoma. J Thorac Oncol 2019; 14(10): S574-S575.
15. Zhu YC, Lin XP, Li XF, *et al*. Concurrent ROS1 gene rearrangement and KRAS mutation in lung adenocarcinoma: A case report and literature review. Thorac Cancer 2018 Jan; 9(1): 159-163.
16. Gen L, Xu HM, Zhao J, *et al*. Concurrent TP53 mutation adversely impact the efficacy of crizotinib in ROS1-rearranged lung cancer patients. J Clin Oncol 2019; 37(15): e20535-e20535.
17. Sun TY, Niu X, Chakraborty A, *et al*. Lengthy progression-free survival and intracranial activity of cabozantinib in patients with crizotinib and ceritinib-resistant ROS1-positive non–small cell lung cancer. J Thorac Oncol 2019; 14(2): e21-e24.
18. Guisier F, Piton N, Salaun, M, *et al*. ROS1-rearranged NSCLC with secondary resistance mutation: case report and current perspectives. Clin Lung Cancer 2019 Nov; 20(6): e593-e596.

Drainless Uniportal Thoracoscopic Pneumonectomy for Carcinoid Tumors — A Case Report

Tzu-Ning Kao[1], Mong-Wei Lin[1], Jin-Shing Chen[1]

Drainless uniportal thoracoscopic pneumonectomy for lung cancer has not been reported. Here, we reported 2 patients with centrally located carcinoid tumors who underwent drainless uniportal thoracoscopic pneumonectomy. A 49-year-old woman and a 38-year-old woman were diagnosed with carcinoid tumor and were treated using minimally invasive uniportal thoracoscopic surgery. The surgery resulted in small wounds, less pain, and fewer infection sites, leading to better postoperative recovery. Without the drainage tube, complications related to tube placement and imbalanced thoracic cavity pressure could be avoided. The successful outcomes of our 2 patients suggest that drainless uniportal thoracoscopic pneumonectomy is safe, technically feasible, and can be used in selected patients. ***(Thorac Med 2022; 37: 295-300)***

Key words: carcinoid tumor, minimally invasive surgery, uniportal thoracoscopic pneumonectomy

Background

To the best of our knowledge, the use of drainless uniportal thoracoscopic pneumonectomy has not been reported. However, uniportal thoracoscopic pneumonectomy has been performed previously and has shown positive results in selected cases with tumors involving central structures [1-6]. We report the successful application of drainless uniportal thoracoscopic pneumonectomy in 2 patients with carcinoid tumors.

Case presentation

A previously healthy 49-year-old woman working as a factory accountant had dry cough for half a year. She visited our hospital, where an initial chest radiograph (CXR) and computed tomography (CT) scan revealed a 4-cm right hilar mass with a hilar convergence sign (Fig. 1A). Trans-bronchial biopsy confirmed the diagnosis of a carcinoid tumor. Brain magnetic resonance imaging and bone scan showed no distant metastasis. The clinical stage was

[1]Department of Surgery, National Taiwan University Hospital and National Taiwan University College of Medicine, Taipei, Taiwan.
Address reprint requests to: Dr. Mong-Wei Lin, Department of Surgery, National Taiwan University Hospital and National Taiwan University College of Medicine, No. 7, Chung-Shan South Road, Taipei 10002, Taiwan.

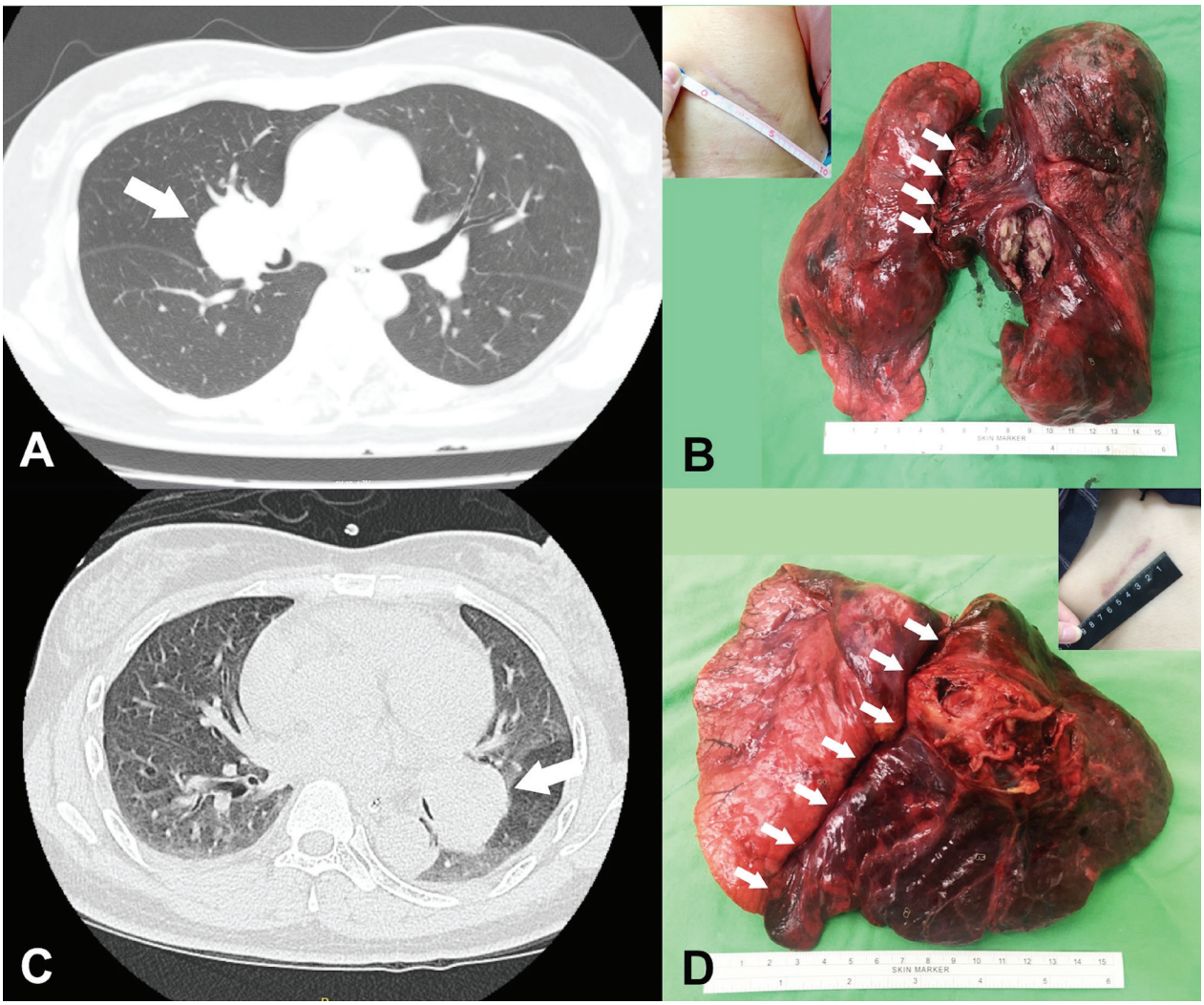

Fig. 1. (A) Preoperative chest CT image of the first case showing a hilar carcinoid tumor. (B) A 5-cm single port incision was made via the 5th intercostal space. Illustration showing the surgical specimen of the right lung in the first case. Arrows indicate the staple line for the intracorporeal stapled lobectomy. (C) Preoperative chest CT image of the second case showing a hilar carcinoid tumor. (D) Illustration showing the skin incision and surgical specimen of the left lung in the second case. Arrows indicate the staple line for the intracorporeal stapled lobectomy. CT, computed tomography.

cT2N0M0, and right pneumonectomy with mediastinal lymph node dissection was indicated.

The patient was placed in the lateral decubitus position after general anesthesia with double lumen intubation, and the pulmonary artery was catheterized. A 5-cm single port incision was created in the right 5th intercostal space along the anterior axillary line (Fig. 1B). The surgery was conducted in 3 steps. First, the non-tumor part of the lung was removed. We identified and dissected the structures with endostaplers using a single-direction approach in the following order: the inferior right pulmonary vein, superior right pulmonary vein, right main bronchus, and right main pulmonary artery. To remove the whole right lung through the small 5-cm single incision, we performed intracorporeal stapled lobectomy for the initial removal of the non-tu-

mor part. Second, the tumor was removed. The residual lung with the tumor was then resected and retrieved (Fig. 1B). Third, group 3, 4, and 7 mediastinal lymph node dissection was performed. After the surgery, the bronchus stump was checked for air leaks. No further drainage system was used after the pneumonectomy. The postoperative pathologic report confirmed a carcinoid tumor, stage pT2aN0M0, stage IB. After surgery, the patient was transferred to the intensive care unit for postoperative care, and then was transferred to the general ward on postoperative day 4. She was discharged on postoperative day 11. The patient's follow-up was uneventful. CXR showed good expansion of the remaining left lung. Postoperative chest CT scans showed no tumor recurrence 18 months after the surgery.

The second case was that of a 38-year-old woman, in whom a 5-cm, homogenously enhanced tumor in the left upper lung was accidently detected by CXR during her hospital admission for an episode of intracranial cerebral hemorrhage. Initially, she had experienced a sudden onset of right-side weakness, consciousness disturbance, and slurred speech, without previous trauma history or medication use. Brain CT revealed spontaneous intracerebral hemorrhage at left basal ganglion with a midline shift to the right side. Craniectomy was performed initially for the intracranial cerebral hemorrhage, and the patient showed postoperative muscle power of 3 in the right upper and lower limbs. The CXR and CT revealed a mass in the left lung (Fig. 1C). Trans-bronchial biopsy confirmed the diagnosis of a left upper lung carcinoid tumor. After staging work-up using whole-body positron emission tomography and brain CT, the clinical stage was determined to be cT2N0M0, stage IB.

Drainless uniportal thoracoscopic left pneumonectomy was performed 51 days after her brain surgery (Fig. 1D). Overall, the operative technique was the same as that for the first patient. A 5-cm single-port incision was created in the left 5th intercostal space along the anterior axillary line. We used the single direction method and the same 3 steps as with the first patient to complete the surgery. First, we identified and dissected the inferior left pulmonary vein, left main bronchus, superior pulmonary vein, and left main pulmonary artery. Second, we performed an intracorporeal stapled lobectomy for removal of the non-tumor part. Third, group 5, 6, and 7 mediastinal lymph node dissection was performed. No drainage system was used. The postoperative pathologic report confirmed a carcinoid tumor, stage pT2bN0M0, stage IIA. Her postoperative course was uneventful. She was transferred to the general ward on postoperative day 7, and then to the rehabilitation department on postoperative day 19. The follow-up chest CT scans revealed no recurrence 2 years after surgery.

Discussion and Conclusions

Minimally invasive thoracoscopic surgery has multiple benefits, including decreased early postoperative pain, shortened hospital stay, and fast recovery. Video-assisted thoracoscopic surgery (VATS) has been widely adopted for lung lobectomy with proven feasibility and safety. However, for patients with a centrally located tumor, pneumonectomy is a more appropriate option [1]. Thoracoscopic pneumonectomy has been reported recently as a feasible surgical technique for some cases [1]. A few papers have reported pneumonectomy through a uniportal VATS, which yielded achievable and safe

Table 1. Summary of Reported Surgical Outcomes in lung Cancer Patients with Thoracoscopic Pneumonectomy

Peri-operation parameters	First Case	Second Case	Conlan *et al*. Ref. 1	Gonzalez-Rivas *et al*. Ref. 2	Domjan *et al*. Ref. 4
	Current study				
Case number	2		1	10	1
Operative time (minutes)	140	106	180	201±40 (130-250)*	102
Blood loss (mL)	< 30	< 30	200	NM+	NM
Port number /size (cm)	1/5	1/5	3/NM	1/4-6	1/5
Wound extension	No need	No need	Dilate 1 incision to accept three fingers.	Enlarge if needed; may use a rib retractor.	NM
ICU stay (days)	3	6	NM	NM	NM
Hospital stay (days)	11	19	2 weeks	Median 4 days (range 3-12)	5 days

*Values were presented as average ± standard deviation (range)

+NM=Not mentioned

results as well when performed by surgeons with broad VATS experience [2-6]. Considering the evolution of the techniques and equipment, selected patients with centrally located tumors could still benefit from uniportal thoracoscopic pneumonectomy, as shown in the 2 cases in the present study.

Table 1 summarizes reported surgical outcomes of lung cancer patients using thoracoscopic pneumonectomy [1,2,4]. The criteria to discharge a patient after drainless uniportal thoracoscopic pneumonectomy are similar to those after conventional thoracoscopic pneumonectomy, and include a stable hemodynamic status without intravenous medication, and recovery from major postoperative complications.

A single-port approach for thoracoscopic pneumonectomy was used for our patients; this resulted in fewer wounds, which led to less pain and fewer sites of infection. This in turn resulted in better recovery. One of the major complications of this procedure is injury to the hilar structures involving the great vessels. The uniportal approach helped provide geometrically parallel access for instruments, mimicking the maneuvers performed during open surgeries, which enabled better hilar dissection and possible bleeding control [7].

Post-pneumonectomy bronchopleural fistula formation is a severe complication. Many studies have been done to explore ways to prevent this condition, such as using a stapler suture, reinforced sutures, or flap coverage. However, controversy exists. Although some studies sug-

gested that flap reinforcement of the bronchial stump would reduce the risk of bronchopleural fistula, different outcomes were reported in other studies.

Klepetko et al. discussed outcomes of different ways of protecting the bronchial stump, including no reinforcement; the group without reinforcement did not experience a higher bronchopleural fistula rate [8]. Similarly, Caushi et al reported a cohort of 558 patients that underwent lung resection with up to a 12-year follow-up, but flap reinforcement did not significantly reduce the rate of developing bronchopleural fistula [9]. Our experience also showed similar results, in that no bronchial stump buttressing had to be done routinely in all patients. Bronchial stump buttressing with pericardial fat or an intercostal muscle flap was used only if the patient received neoadjuvant therapy, radiotherapy, or a steroid or immunosuppressant.

In both of our cases, we performed intracorporeal staple lobectomy for the non-tumor parts after completing the pneumonectomy procedures. The non-tumor part can be removed at first. Then, the centrally-located main tumor, together with the hilum structure and the residual lobes, can be retrieved from the small incision without damaging the integrity of the tumor itself (Figure 1B, D). This also highlights the feasibility of uniportal thoracoscopic pneumonectomy.

A common complication after lung surgery is air leakage, which was avoided in our cases because we performed pneumonectomy rather than segmentectomy or lobectomy in patients without neoadjuvant therapies. Considering post-pneumonectomy space management, a drainless setting was introduced. To drain or not to drain after pneumonectomy has long been debated [10]. As long as the surgeon performs careful and comprehensive intra-operative surgical hemostasis, hemothorax can be prevented and a chest tube insertion becomes unnecessary. Here, the drainless system provided better maintenance of stable pressure in the post-pneumonectomy cavity. Some chest tube-related complications, such as kinks or occlusions can be avoided, as well. Moreover, without the drainage tube, postoperative wound care became easier. The wound could heal faster with a lower risk of infection. The cosmetic results were also better since the alignment was more even and smooth. In our second case, the patient with intracranial hemorrhage could start the rehabilitation program sooner, without the whole drainage system, including water-sealed bottles. Overall, the pros of the absence of a drainage system may outweigh the cons.

In conclusion, using the uniportal thoracoscopic approach in pneumonectomy helps the surgical process geometrically, reduces unnecessary complications, and speeds recovery. Furthermore, a drainless setting after surgery results in better quality of postoperative care in terms of safety, healing, cosmetic appearance, and rehabilitation. Our results suggest that drainless uniportal thoracoscopic pneumonectomy is technically feasible; however, further studies are required to validate the indications, safety, and efficacy of this novel procedure.

List of abbreviations

CXR: chest radiography; CT: computed tomography; VATS: video-assisted thoracoscopic surgery.

Declarations

Ethics approval and consent to participate

Given that this manuscript is a case report and does not contain the patients' personal data, the need for approval was waived by the Research Ethics Committee at National Taiwan University Hospital.

Consent for publication

Written consent for publication of personal or clinical details along with any identifying images was obtained from the 2 patients included in the case report.

Availability of data and materials

The datasets used and/or analyzed during the current study are available from the corresponding author on reasonable request.

Competing interests: The authors declare no conflicts of interest.

Funding: This study was supported by National Taiwan University Hospital, Taipei, Taiwan (NTUH NTUH109-S4659, MS-419). The funding was used only for financial subsidies for English editing.

Authors' contributions

T.N.K. and M.W.L analyzed and interpreted patient data regarding lung cancer and surgery. M.W.L performed the surgery. T.N.K was a major contributor in writing the manuscript. M.W.L. and J.S.C. supervised the writing of the manuscript and revised the manuscript. All authors read and approved the final manuscript.

References

1. Conlan AA, Sandor A. Total thoracoscopic pneumonectomy: indications and technical considerations. J Thorac Cardiovasc Surg 2003; 126: 2083-5.
2. Gonzalez-Rivas D, Delgado M, Fieira E, *et al*. Uniportal video-assisted thoracoscopic pneumonectomy. J Thorac Dis 2013; 5: S246-52.
3. Gonzalez-Rivas D. Uniportal thoracoscopic surgery: from medical thoracoscopy to non-intubated uniportal video-assisted major pulmonary resections. Ann Cardiothorac Surg 2016; 5: 85-91.
4. Domjan M, Mavko A, Štupnik T. Single-port video-assisted thoracoscopic surgery (VATS) right pneumonectomy: a case report. J Vis Surg 2017; 3: 130.
5. Yang C, Abu Akar F, Chen J, *et al*. Right sleeve pneumonectomy via uniportal video-assisted thoracoscopic approach. J Thorac Dis 2018; 10: E391-6.
6. Yu PSY, Ng CSH. Left uniportal VATS pneumonectomy. In: Gonzalez-Rivas D, Ng C, Rocco G, D'Amico T, ed. Atlas of Uniportal Video-Assisted Thoracic Surgery. Singapore: Springer; 2019; 165-168.
7. Bertolaccini L, Rocco G, Viti A, *et al*. Geometrical characteristics of uniportal VATS. J Thorac Dis 2013; 5: S214-6.
8. Klepetko W, Taghavi S, Pereszlenyi A, *et al*. Impact of different coverage techniques on incidence of post-pneumonectomy stump fistula. Eur J Cardio-Thorac Surg 1999; 15: 758-763.
9. Caushi F, Qirjako G, Skenduli I, *et al*. Is the flap reinforcement of the bronchial stump really necessary to prevent bronchial fistula? J Cardiothorac Surg 2020; 15: 248.
10. Morcos K, Shaikhrezai K, Kirk AJB. Is it safe not to drain the pneumonectomy space? Interact Cardiovasc Thorac Surg 2014; 18: 671-5.

Mediastinal Schwannoma Diagnosed by Endobronchial Ultrasound Transbronchial Needle Aspiration (EBUS-TBNA) – A Case Report

Yueh-Lin Lee[1], Chieh-Mo Lin[1], Chun-Hsien Lin[1], Jing-Lan Liu[1], Yu-Ching Lin[1], Meng-Jer Hsieh[2,3]

Schwannoma is a peripheral nerve sheath tumor. Schwannomas arising from mediastinal lymph nodes are extremely rare. We reported a 62-year-old male patient who was referred to our chest department due to a 2.7-cm mediastinal nodule that was incidentally found using low-dose computed tomography. Bronchoscopic endobronchial ultrasound (EBUS) revealed a hypoechoic and well-defined tumor surrounded by a hyperechoic capsule. A definite diagnosis of schwannoma was made later based on a specimen obtained by EBUS-guided transbronchial needle aspiration. ***(Thorac Med 2022; 37: 301-305)***

Key words: mediastinal schwannoma, endobronchial ultrasound-guided transbronchial needle aspiration (EBUS-TBNA), elastography

Introduction

Schwannomas (also called neurilemomas) are encapsulated tumors that originate from Schwann cells. They are the most common tumor of the peripheral nerves. The majority of schwannomas, with the exception of atypical types, do not transform to malignancy [1]. Forty-five percent of schwannomas occur in the head and neck, and only about 9% occur in the mediastinum. When located in the mediastinum, the schwannoma usually originates from the posterior mediastinum. Schwannomas arising from mediastinal lymph nodes are extremely rare [2-3].

Case Presentation

A 62-year-old man was referred to our chest department for evaluation of a mediastinal nodular lesion. The patient had been suffering from lumping throat and an intermittent cough during the most recent half year. There were no fever episodes, purulent sputum, wheezing breathing

[1]Division of Pulmonary and Critical Care Medicine, Chang Gung Memorial Hospital, Chiayi Branch, Chiayi, Taiwan, [2]Division of Pulmonary and Critical Care Medicine, Chang Gung Memorial Hospital, Linkou, Taoyuan, Taiwan, [3] Department of Respiratory Therapy, School of Medicine, Chang-Gung University, Taoyuan, Taiwan.
Address reprint requests to: Dr. Meng-Jer Hsieh, Department of Pulmonary and Critical Care Medicine, Linkou Chang-Gung Memorial Hospital, Chang-Gung Medical Foundation. No.5, Fu-Xin St. Guishan District, Taoyuan City, 333, Taiwan.

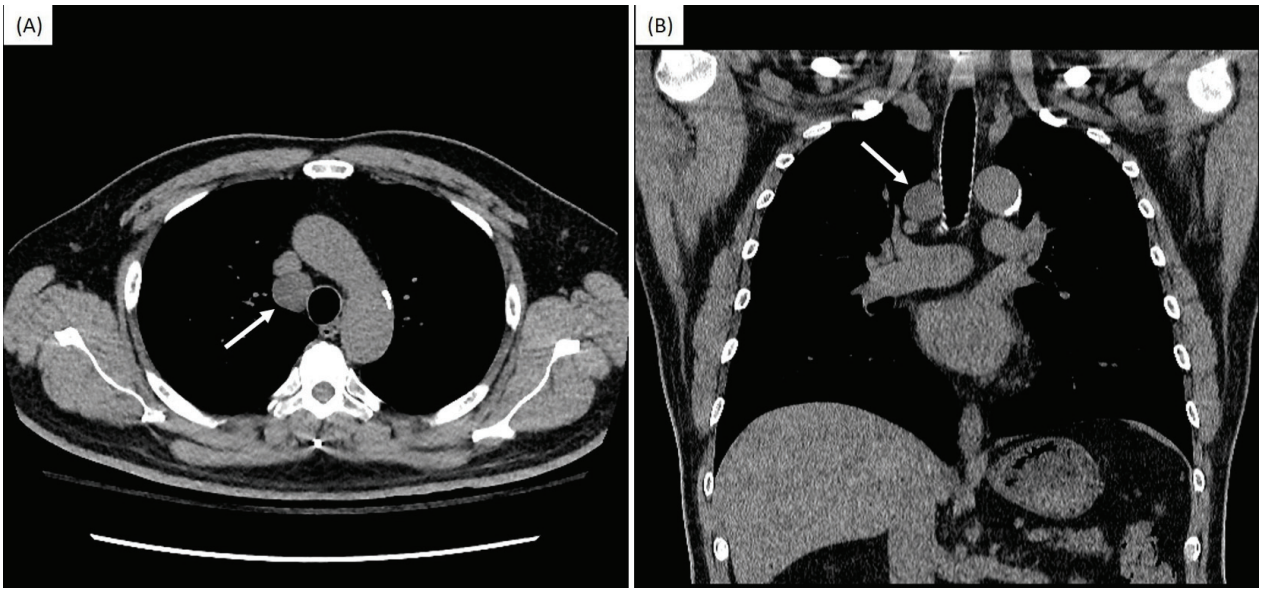

Fig. 1. Low-dose CT (LDCT) of the chest revealed a paratracheal, round, well-defined nodule at the right side of the middle mediastinum (white arrow). It was below the aortic arch but above the azygos vein, located in station 4R of the mediastinum. (A) axial view, (B) coronal view of the LDCT.

sounds, or shortness of breath. He was a non-smoker, and was receiving regular outpatient department follow-up for hypertension, dyslipidemia, and prediabetes. Low-dose computed tomography (LDCT) of the chest during a health exam revealed a round, well-defined 2.7-cm nodule at the right lower paratracheal area in mediastinal station 4R (S4R) (Figure 1 A, B). His baseline biochemistry, hematological tests, and physical examinations were unremarkable.

Bronchoscopy with conscious sedation was performed. Convex-probe endobronchial ultrasound (CP-EBUS) showed a well-defined hypoechoic tumor, with an echogenic capsule and posterior acoustic enhancement. Elastography revealed the texture of the tumor to be hard, and there was no central vasculature. EBUS-transbronchial needle aspiration (EBUS-TBNA) was performed for sampling (Figure 2 A~D), with the largest specimen measuring 0.3 x 0.3 x 0.1 cm. The sample showed areas of compact spindle cells called Antoni A areas, and fewer cellular areas of a fibrillar collagen known as Antoni B areas (Figure 3 A, B). Immunohistochemical staining of S-100 protein was positive (Figure 3 C), and a diagnosis of schwannoma was confirmed.

The patient was referred to the chest surgeon for surgical resection, but he was hesitant about further interventions due to the surgical risks and the possible long-term complications. As of this writing, he has been receiving regular follow-up at our chest outpatient department, and there was no progressive change in nodular size as determined by CT 6 months after tissue proof.

Discussion

Mediastinal schwannoma is a slow-growing nerve sheath tumor arising from Schwann cells of the spinal or thoracic nerves. The overall incidence rate of nerve sheath tumor is about 1.1 per 100,000 person-years, and less than 10%

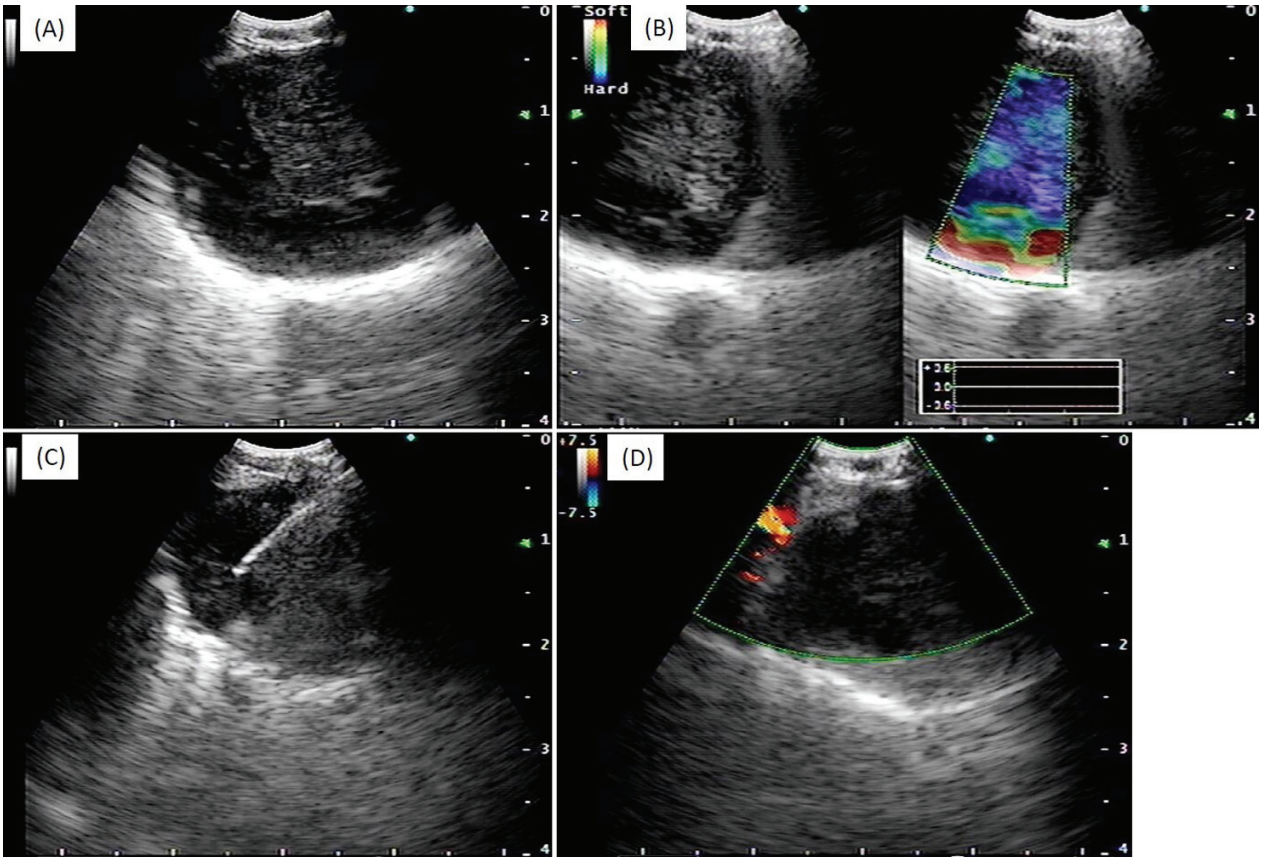

Fig. 2. Convex-probe endobronchial ultrasound (CP-EBUS) revealed (A) a hypoechoic nodule with echogenic capsule and posterior acoustic enhancement. (B) EBUS-elastography of the lymph node revealed a heterogeneous appearance with a blue area (hard rigidity) and a few green infiltrations (intermediate rigidity). (C) Endobronchial ultrasound-guided transbronchial needle aspiration (EBUS-TBNA). (D) Color Doppler mode showed a few vasculatures inside the lymph node.

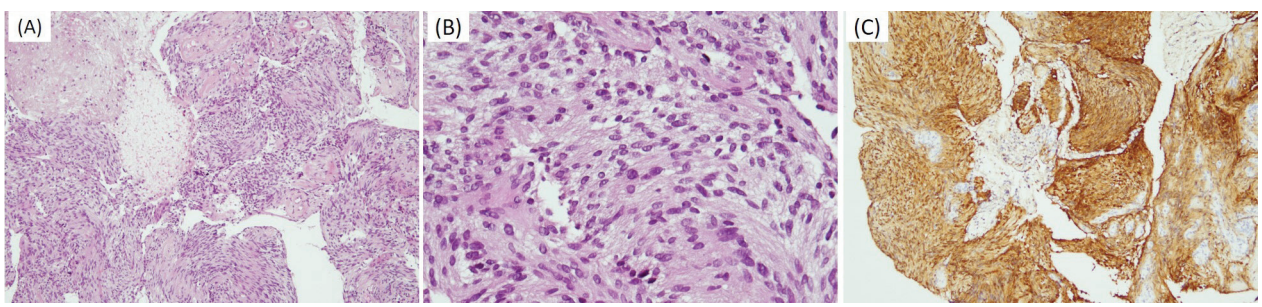

Fig. 3. Pathologic images. Spindle mesenchymal cells of a benign character forming irregular bundles within a collagenized matrix. (A) H&E stain, x100, (B) H&E stain, x400. (C) Immunohistochemical stain was positive for S-100, x100.

of these tumors are located in the mediastinum [2, 3]. Those located in the mediastinum usually originate from the posterior mediastinum. Schwannomas arising from mediastinal lymph nodes are extremely rare [4]. In adult patients, approximately two-thirds of mediastinal benign schwannomas are asymptomatic and found incidentally. Schwannomas may cause symptoms related to compression of adjacent anatomical structures, including pain, dyspnea, cough, par-

esthesia, and Horner syndrome. As seen radiologically, schwannomas located in the mediastinum are well-circumscribed homogeneous or heterogeneous and spherical masses that mimic enlarged lymph nodes. Punctate calcifications are occasionally detected, and low attenuation correlates with areas of hypocellularity.

Schwannomas are histologically characterized by the presence of a highly organized cellular component of compact spindle cells (Antoni A), and a loosely myxoid component (Antoni B), with palisading nuclei termed Verocay bodies. In immunohistochemical staining, polyclonal antibody S-100 will strongly stain schwannomas [5]. Though the majority of schwannomas do not transform to malignancy, they are difficult to distinguish from metastatic lymph nodes using positron emission tomography (PET) due to the high uptake of 2-deoxy-2-fluoro-d-glucose (18F-FDG) in some cases [6]. Melanotic schwannomas and malignant peripheral nerve sheath tumors (MPNST) are pathological variants that transform to malignancy. They both account for less than 1% of primary peripheral nerve sheath tumors [7].

The diagnosis is usually based on histological examination. Biopsy for intranodal schwannoma can be performed via surgical mediastinoscopy, EBUS-TBNA or endoscopic ultrasound-guided fine needle aspiration (EUS-FNA) [8]. Compared to mediastinoscopy, EBUS-TBNA is a minimally invasive modality for use in mediastinal or pulmonary disease sampling, with a lower complication rate (1.23%), lower cost, and similar accuracy for the diagnosis of mediastinal lesions (sensitivity and specificity are 94.1% and 94.3%, respectively) [9, 10, 11]. Despite the benign nature of the tumor and the low risk of malignant change, surgical resection may be required for diagnosis and relief of symptoms. Surgical resection is usually performed by video-assisted thoracoscopy or thoracotomy. In cases with benign neoplasms, complete excision of the lesion itself is generally sufficient. For malignant lesions, surgical resection and adjuvant radiation therapy is used to control residual disease. Unfortunately, the 5-year survival of patients with malignant schwannoma is below 20%, and there are no known chemotherapeutic regimens that are effective against these tumors [7,12].

The EBUS elastography images, when analyzed semi-quantitatively or quantitatively, have been proved to be a useful tool in differentiating intrathoracic lymph nodes [13]. Type classification is a method with very high sensitivity, specificity and accuracy. A type 1 (predominantly non-blue) appearance tends to be benign, while a type 3 (predominantly blue) appearance tends to be malignant. The sensitivity, specificity, positive predictive value, negative predictive value and diagnostic accuracy rate were 100%, 92.3%, 94.6%, 100% and 96.7%, respectively. [13]. In our case, EBUS elastography showed a type 3 appearance, but the texture of the node was much harder than that of metastatic lymph nodes, in our experience, when doing EBUS-TBNA. Thus, in this case, a mediastinal nodule with a type 3 EBUS elastography appearance turned out to be a benign schwannoma.

In summary, we presented the case of a schwannoma that originated from a rare location in the upper mediastinal lymph node, which was diagnosed using the safer endoscopic EBUS-TBNA examination. Ultrasound findings together with the application of elastography might be helpful in the diagnosis of mediastinal schwannomas.

References

1. Bhattacharyya AK, Perrin R, Guha A. Peripheral nerve tumors: management strategies and molecular insights. J Neurooncol 2004; 69: 335.
2. Strollo DC, Rosado-de-Christenson ML, Jett JR. Primary mediastinal tumors: Part II. Tumors of the middle and posterior mediastinum. Chest 1997; 112: 1344-57.
3. Takeda S, Miyoshi S, Minami M, et al. Intrathoracic neurogenic tumors - 50 years' experience in a Japanese institution. Eur J Cardiothorac Surg 2004; 26(4): 807-12.
4. Piana S, Gelli MC, Cavazza A, et al. Ancient schwannoma arising in a lymph node: report of a case and review of literature. Pathol Res Pract 2002; 198(1): 51-54.
5. Kurtkaya-Yapicier O, Scheithauer B, Woodruff JM. The pathobiologic spectrum of schwannomas. Histol Histopathol 2003; Jul;18(3): 925-34.
6. Beaulieu S, Rubin B, Djang D, et al. Positron emission tomography of schwannomas: emphasizing its potential in preoperative planning. Am J Roentgenol 2004; 182: 971-4.5.
7. Kapoor A, Singhal MK, Narayan S, et al. Mediastinal schwannoma: A clinical, pathologic, and imaging review. South Asian J Cancer 2015 Apr-Jun; 4(2):104–105.
8. Kang LH, Shin DH, Yoon SH. Schwannoma arising in mediastinal lymph node diagnosed by endobronchial ultrasound. Respirol Case Rep 2019; 7(8).
9. Verdial FC, Berfield KS, Wood DE, et al. Safety and costs of endobronchial ultrasound-guided nodal aspiration and mediastinoscopy. Chest 2020; 157(3): 686-93.
10. Sehgal IS, Dhooria S, Aggarwal AN, et al. Endosonography versus mediastinoscopy in mediastinal staging of lung cancer: systematic review and meta-analysis. Ann Thorac Surg 2016; 102(5): 1747-55.
11. Zhi X, Chen J, Xie F, et al. Diagnostic value of endobronchial ultrasound image features: a specialized review. Herth FJF Endosc Ultrasound 2021; 10(1): 3-18.
12. Chen XF, Ma QY, Wang SH, et al. Surgical treatment of posterior mediastinal neurogenic tumors. J Surg Oncol 2019 May; 119(6): 807-813.
13. Chen YF, Mao XW, Zhang YJ, et al. Endobronchial ultrasound elastography differentiates intrathoracic lymph nodes: a meta-analysis. Ann Thorac Surg 2018 Oct; 106(4): 1251-57.
14. Lin CK, Yu KL, Chang LY, et al. Differentiating malignant and benign lymph nodes using endobronchial ultrasound elastography. J Formos Med Assoc 2019; 118: 436-443.

Stridor in a 24-year-old Male Treated with Bronchoscopic Electrocautery: A Case Report

Hsuan Feng Wu[1], Yi-Hsi Wang[1], Wen-Feng Fang[1]

Stridor is an important sign suggestive of central airway stenosis warranting emergency treatment. We present the case of a 24-year-old male with acute stridor, who was diagnosed with severe upper airway obstruction based on his past acute respiratory failure history, physical examination, spirometry, radiographic imaging, and bronchoscopy. A critical subglottic upper airway obstruction was identified via bronchoscopy. Bronchoscopic electrocautery was performed in the intensive care unit. The patient tolerated this alternative treatment method, rather than undergoing surgical treatment, and had a good outcome. ***(Thorac Med 2022; 37: 306-312)***

Key words: stridor, post-intubation tracheal stenosis, bronchoscopy, electrocautery

Introduction

Stridor is an abnormal, high-pitched sound produced by turbulent airflow through a partially obstructed airway at the central airway including the supraglottis, glottis, subglottis, or trachea. This symptom is widely variable from mild to fatal, and it is important to classify the severity of airway narrowing, extent, cause and shape of stenosis. Bronchoscopy plays a role in not only diagnosis of central airway obstruction but also treatment.

Case presentation

A 24-year-old healthy male with no history of cigarette smoking, alcohol consumption, or betelnut chewing, but with a history of pneumonia complicated with acute respiratory failure requiring mechanical ventilation for approximately 2 weeks during his childhood, presented to our clinic. Of note, he had no sequelae after this earlier mechanical ventilation.

He presented to our outpatient clinic with a sudden onset of dyspnea after exertion, accom-

[1]Division of Pulmonary and Critical Care Medicine, Department of Internal Medicine, Kaohsiung Chang Gung Memorial Hospital, Kaohsiung, Taiwan.
Address reprint requests to: Dr. Wen-Feng Fang, Division of Pulmonary and Critical Care Medicine, Department of Internal Medicine, Kaohsiung Chang Gung Memorial HospitalNo.123, Dapi Rd. Niaosong Dist, Kaohsiung City 83301 Taiwan, R.O.C.

panied by hoarseness and cough. He previously sought medical help at different local clinics, where bronchodilator inhalation was prescribed for suspected asthma attacks; however, these treatments did not help. Therefore, he visited our outpatient department for further evaluation. He denied fever, headache, myalgia, chest pain, abdominal pain, and oliguria. Physical examination revealed stridor during breathing, but without hoarseness, wheezing, or crackles. Laboratory examinations, including complete blood count, were all within normal range.

We performed spirometry to determine if there were obstructive lung diseases, and found a fixed and decreased flow in both the expiratory and inspiratory phases (Figure 1). The most recent chest radiograph on 14 December 2020 showed no active lung lesions (Figure 2). Chest computed tomography (CT) 3 weeks later revealed no obvious tracheal lesions, and showed relatively good caliber for most of the airways, including the trachea, larynx, and hypopharynx. Mild bilateral wall indentation at the subglottic region was noted, with the narrowest diameter of approximately 1.2 cm (Figure 3). Using a flexible bronchoscope, we found severe tracheal

Date of Birth:		02/27/1997		Age:		23 Years		
Sex:		male		Height:		172 cm		
				Weight:		58 kg		
		Pred	pre	%(pre/Pr	post	%(post/P	Change	%change
FVC	L	4.92	2.51	51.0	2.80	56.9	0.29	11.52
FEV 1	L	4.18	0.84	20.0	0.76	18.1	-0.08	-9.41
FEV 1 % FVC	%		33.38		27.12		-6.27	-18.77
FEV 3	L		1.94		1.75		-0.19	-9.77
FEV6	L		2.50		2.72		0.21	8.53
PEF	L/s	9.64	0.93	9.7	0.81	8.4	-0.12	-13.06
MMEF 75/25	L/s	4.96	0.57	11.4	0.47	9.4	-0.10	-17.62
MEF 25	L/s	2.50	0.40	16.0	0.38	15.2	-0.02	-5.00
MEF 50	L/s	5.39	0.62	11.4	0.44	8.2	-0.18	-28.65
MEF 75	L/s	8.20	0.79	9.6	0.70	8.5	-0.09	-11.51
PIF	L/s		0.54		0.59		0.05	9.67
FIF25	L/s							
FIF 50	L/s		0.39		0.44		0.05	13.55
FIF75	L/s							
FEF50 % FIF50	%		159.14		100.00		-59.14	-37.16
V backextrapolati	L		0.01		0.01		0.00	22.77
FET PEF	s		0.13		0.15		0.02	15.03
Date			12/14/20		12/14/20			
Time			12:03:30		12:26:39			

Comment:

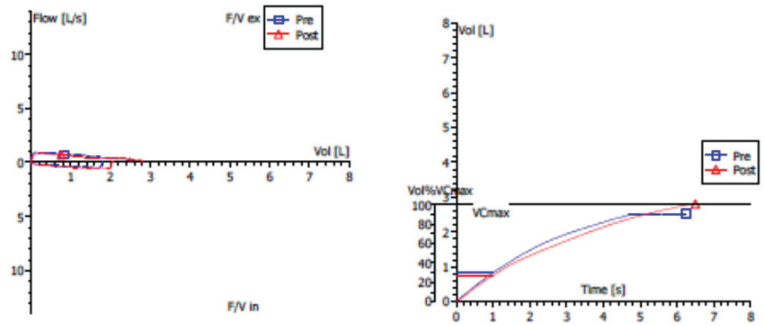

Fig. 1. Spirometry revealed a severely restricted lung, and the flow-volume loop was compatible with a fixed airway.

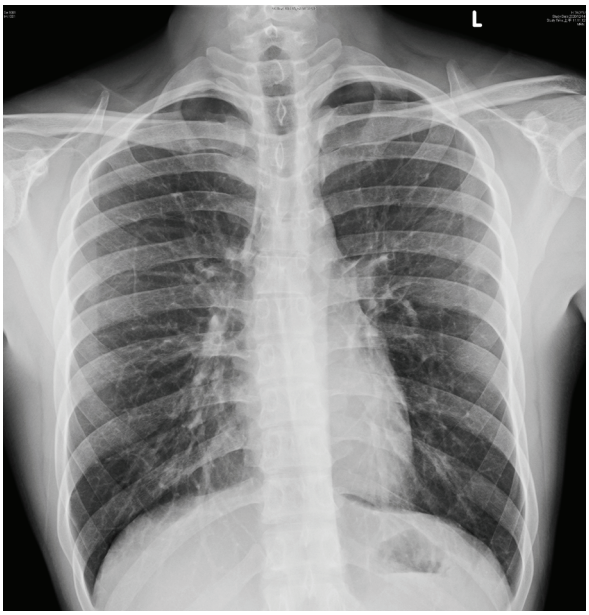

Fig. 2. Chest X-ray showed no active lung lesions.

stenosis, consistent with the circular granulation tissue and membrane, at 1.5 cm below the vocal cord (Figure 4).

As the patient was at high risk of acute respiratory failure due to severe subglottic tracheal stenosis, we admitted him to the medical intensive care unit (ICU) and arranged bedside therapeutic bronchoscopy. We inserted the fiberscope through the right nostril and held the tip 1 cm above the vocal cord. We then used the electrocauterization catheter to cut the stenotic membrane, resulting in an increase of approximately 50% in the area of the trachea (Figure 5). All procedures were performed and monitored in the ICU, and were uneventful. Midazolam (5

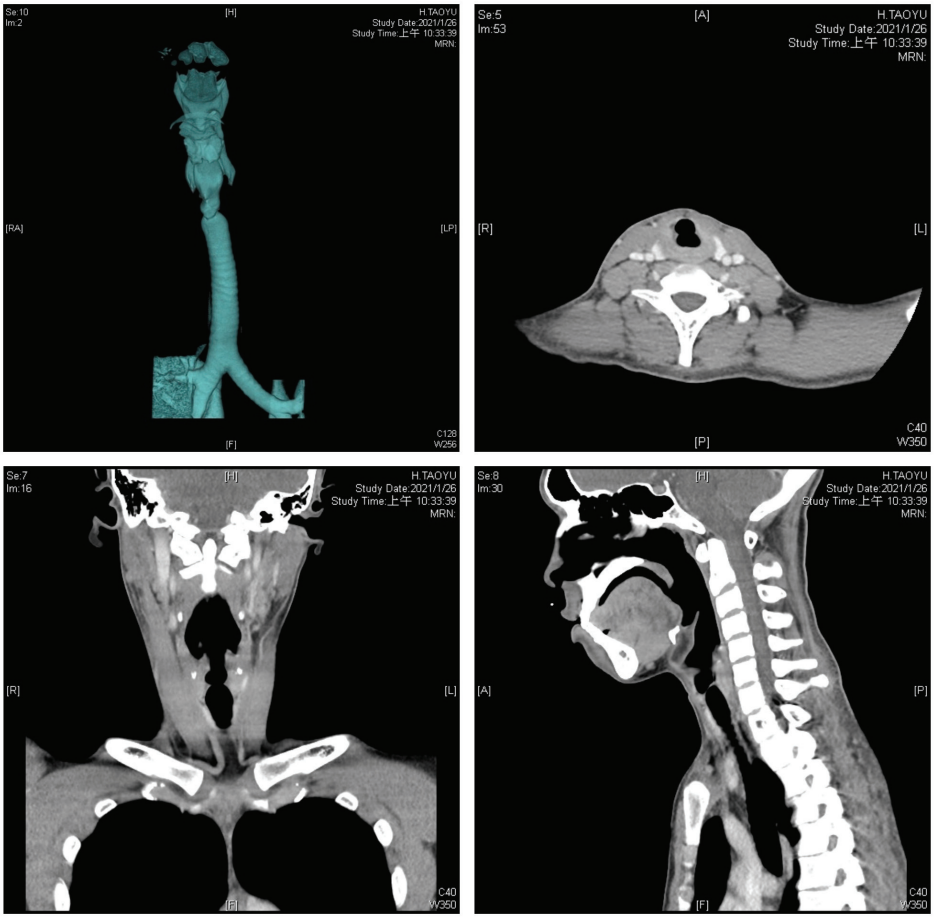

Fig. 3. CT showed only a granulation-like lesion at the subglottis; there was no obvious lesion in the reconstruction picture.

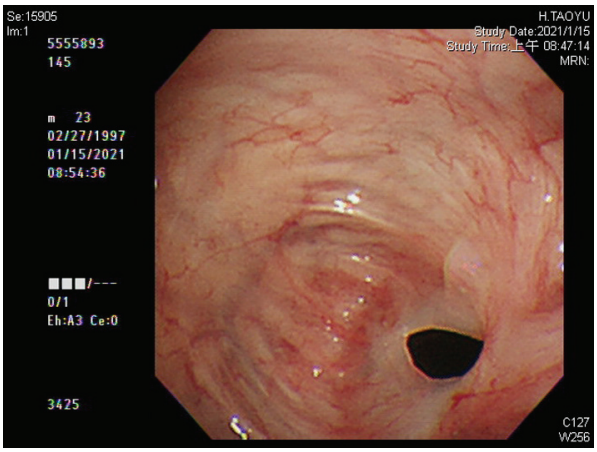

Fig. 4. Diagnostic bronchoscopy disclosed a circumferential lesion at 1.5 cm below the vocal cord.

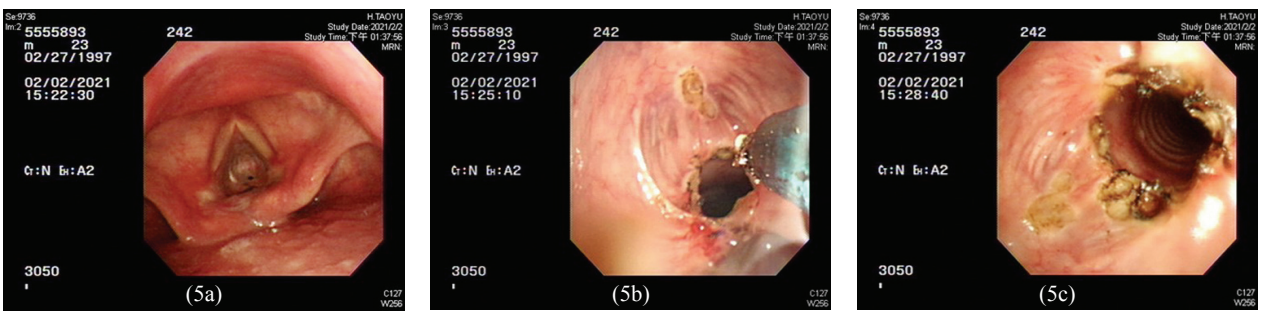

Fig. 5. Therapeutic bronchoscopy. (5a).The lesion was located below the vocal cord. Before electrocautery, we administered midazolam to achieve light sedation, and used lidocaine spray to decrease the cough reaction. (5b). We used 3000 Hz for 3-5 seconds to cut the lesion evenly at 3 quadrants. (5c). The widened trachea after electrocautery.

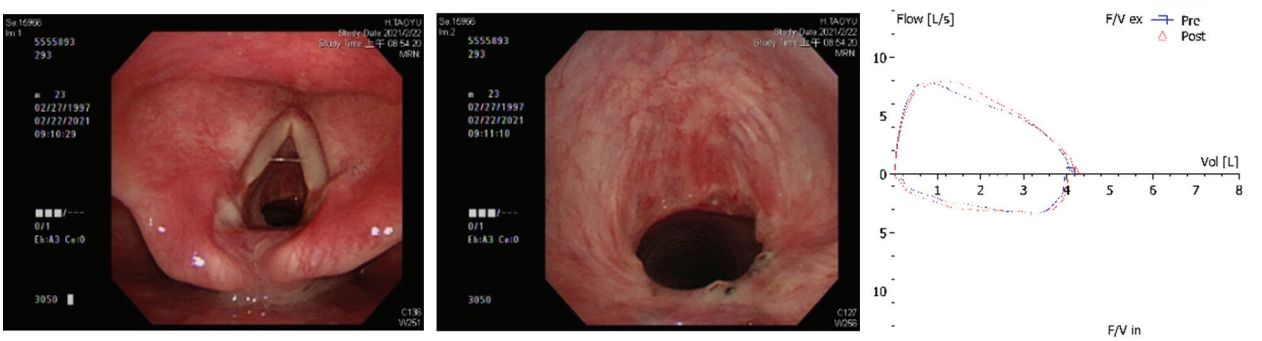

Fig. 6. Follow-up bronchoscopy 2 weeks after electrocautery. Stenosis was improved, and has not recurred. The flow-volume loop showed improvement in expiration and inspiration, compatible with symptom relief.

mg) was used to achieve light sedation before scope insertion, and local lidocaine spray was used at the vocal cord to diminish the cough response. There was no desaturation during the procedure. The patient was discharged 2 days after electrocauterization. No evidence of lesion recurrence was observed 1 month following bronchoscopy and spirometry (Figure 6), and there was significant improvement in his symptoms.

Discussion

Here, we reported the case of a 24-year-old healthy male presenting with an acute onset of stridor and dyspnea on exertion. The initial chest radiograph and chest CT findings were not specific. Due to his past medical history of acute respiratory failure after endotracheal intubation, upper airway obstruction was suspected. Spirometry revealed typical findings of severe upper airway obstruction, and this was confirmed by bronchoscopy. The subglottic tracheal stenosis was successfully treated with bronchoscopic electrocautery in the ICU.

Post-intubation tracheal stenosis rarely occurs more than 1 year after intubation. However, our patient was young and did not notice his upper airway obstruction until he developed audible stridor, which made him dyspneic. In some cases, this process could take several years.

The subglottis is the area within the cricoid ring from the bottom of the vocal folds to the top of the first tracheal ring. The subglottis is particularly prone to injury due to surgical manipulation or intubation. Injury to the mucosa can lead to inflammation, scar tissue formation, and subsequent stenosis. Bronchoscopy is an important tool for diagnosing upper airway stenosis. In a previous report, we analyzed bronchoscopic findings in patients with suspected upper airway obstruction [1]. The most common obstruction location was the trachea, followed by the vocal cords. A laryngeal lesion was found in 7 (7.7%) patients. The most common etiology was a tracheostomy tube still in place (27.3%), followed by post-translaryngeal intubation (16.5%), and direct extension of the neoplasm (13.2%). A combination of 2 types of stenosis was observed. Frequent symptoms included dyspnea (75.9%), stridor (27.5%), hoarseness (12.1%), cough (12.1%), and wheezing (5.5%). The present case was consistent with the above findings.

Stridor is a high-pitched continuous sound produced by turbulent flow in the extrathoracic airway. In contrast to wheezing, it is louder and longer during inspiration than during expiration. Flow-volume curves in spirometry may be especially helpful in identifying tracheal or other upper airway lesions. Central airway obstruction (i.e., proximal to the tracheal carina) located within the thorax produces a plateau during forced exhalation, instead of the usual rise to and descent from the peak flow. Conversely, tracheal lesions located outside of the thorax can cause decreased airflow during inhalation; during inhalation, the tracheal membrane is sucked in, and this is usually associated with stridor. If the lesions involve the vocal cord, the patient typically complains of voice change, which differs from the manifestations of glottic or subglottic lesions. In our case, the critical orifice was located at the subglottis, so its area was not affected by flow pressure during both inhalation and exhalation. Our patient's flow-volume loops showed a pattern of fixed upper airway obstruction. The spirometry curve improved significantly after bronchoscopic electrocautery.

Diagnosis of upper airway obstruction can be confirmed using laryngoscopy and bronchoscopy [2]. Spiral CT and 3-dimensional reconstructions are useful for an overall understanding of the tracheobronchial tree before bronchoscopy [3]. Over 90% of cases of stenosis at the stricture site resulted in stridor and dyspnea. The morphological classification of laryngotracheal stenosis is circumferential; the length of the lesion was less than 1 cm and the vertical

extent was ????.

Possible treatments include surgical resection, laser-assisted mechanical dilation for simple lesions, or stent insertion for complex lesions. Surgical resection of hypertrophic stenotic tissues is the procedure of choice for many patients with benign tracheal strictures. However, severe comorbidities, stricture location (e.g., high subglottic), or long vertical extent (> 4-6 cm) may preclude open surgical intervention [4]. We agree that balloon dilatation is a good modality and has fewer complications than electrocautery in some situations. However, there is limited data for a thin lesion, as in our patient. The mean length of stenosis in patients who underwent balloon dilatation was 9.1 mm to 26 mm [5-6], which was much longer than that in our patient. In addition, there are complications, including hypoxia, trachea rupture, and vocal fold laceration, when the lesion is located in the subglottic area [6-7]. Electrocautery and argon-plasma and Nd-YAG lasers are used in palliative or curative interventions for intraluminal tumors. The advantages of electrocautery are the rapid hemostasis, mechanical debulking of the obstruction, and cost-effectiveness [8]. In addition, in patients undergoing lung transplantation, electrosurgery can also be used for web-like airway strictures.

Electrocautery is precise and limits tissue vaporization. However, extreme caution must be exercised because the airway wall can easily be cut through during the procedure. This method of mucosal sparing is safe and is most beneficial when used for short (<1 cm) circumferential stenosis without significant associated malacia [9]. The most common surgical procedure is tracheal resection with an anastomosis. Laryngotracheal resections are performed in cases of subglottic stenosis. The satisfaction rate among patients who had laser or dilations before surgery was 95%–96% [10]. For central airway surgery, venovenous extracorporeal membrane oxygenation (v-v ECMO) may play a role because it provides airway security during the lifesaving procedure[11].

In patients who receive electrocautery-aided tracheal stenosis treatment, re-stenosis is a major problem. Follow-up 1 month after the procedure was not adequate. We arranged our patient's regular follow-up at our outpatient department, during which regular spirometry would be performed. We also explained the following treatment options: repeat electrocautery, balloon dilatation, and surgical resection.

In conclusion, tracheal stenosis is an important problem after intubation or tracheostomy, and history-taking and physical examination, especially breathing sounds, should be carefully considered. Characteristic spirometry findings are extrapulmonary or intrapulmonary, based on flow-volume curves. Bronchoscopy is still the gold standard for the diagnosis and for determining the stenosis location. High-resolution CT and 3-dimensional reconstruction may be helpful before bronchoscopy. Tracheal resection and reconstruction are useful, and v-v ECMO should be considered in central airway surgery. On the other hand, electrocautery ablation would be an easier option for conservative treatment, and can be performed safely in the ICU setting.

References

1. Fang WF, Wu CC, Wang YH, *et al*. Analysis of bronchoscopic findings in patients suspected of having upper airway obstruction. Thorac Med 2003; 18: 402-8.
2. Eskander A, de Almeida JR, Irish JC. Acute upper airway obstruction. N Engl J Med 2019; 381: 1940-1949.
3. Lee KS, Yoon JH, Kim TK, *et al*. Evaluation of

tracheobronchial disease with helical CT with multiplanar and three-dimensional reconstruction: correlation with bronchoscopy. Radiographics 1997; 17: 555-67.

4. Murgu SD, Egressy K, Laxmanan B, *et al*. Central airway obstruction: benign strictures, tracheobronchomalacia, and malignancy-related obstruction. Chest 2016; 150: 426-41.
5. Zias N, Chroneou A, Tabba MK, *et al*. Post-tracheostomy and post-intubation tracheal stenosis: report of 31 cases and review of the literature. BMC Pulm Med 2008; 8: 18.
6. Parker NP, Bandyopadhyay D, Misono S, *et al*. Endoscopic cold incision, balloon dilation, mitomycin C application, and steroid injection for adult laryngotracheal stenosis. Laryngoscope 2013; 123: 220-5.
7. Heyes R, Cervantes SS, Matthaeus J, *et al*. Balloon dilation causing tracheal rupture: endoscopic management and literature review. Laryngoscope 2016; 126: 2774-7.
8. Bolliger CT, Sutedja TG, Strausz J, *et al*. Therapeutic bronchoscopy with immediate effect: laser, electrocautery, argon plasma coagulation and stents. Eur Respir J 2006; 27: 1258-71.
9. Santacruz JF, Mehta AC. Airway complications and management after lung transplantation: ischemia, dehiscence, and stenosis. Proc Am Thorac Soc 2009; 6: 79-93.
10. Wright CD, Li S, Geller AD, *et al*. Postintubation tracheal stenosis: management and results 1993 to 2017. Ann Thorac Surg 2019; 108: 1471-7.
11. Hong Y, Jo KW, Lyu J, *et al*. Use of venovenous extracorporeal membrane oxygenation in central airway obstruction to facilitate interventions leading to definitive airway security. J Crit Care 2013; 28: 669-74.

Endometrial Metastasis of Lung Adenocarcinoma Mimicking Uterine Leiomyoma: A Case Report and Literature Review

Chieh-Yung Wang[1], Nien-Tzu Liu[2], Li-Fan Lin[3], Chen-Liang Tsai[1], Chung-Kan Peng[1], Chi-Hao Shen[1]

The female genitourinary tract is a rare site of distant metastasis from the lung-- most cases of distant metastases have originated from breast cancer. Here, we report an extremely rare case of metastatic endometrial cancer of lung origin, and present an extensive literature review. A 67-year-old woman with a history of uterine leiomyoma was diagnosed with adenocarcinoma of the right upper lung with left adrenal gland and visceral pleura metastases (stage T2aN0M1c). The positron emission tomography/computed tomography image during staging disclosed an abnormal uptake in the uterine region that was initially considered to be a leiomyoma. Intermittent vaginal bleeding occurred during systemic chemotherapy. Curettage of the uterus was performed, with samples demonstrating adenocarcinoma with metastasis from her known primary lung adenocarcinoma. Local radiation therapy to the endometrial metastasis was arranged; however, the disease progressed, and she died from aspiration pneumonia 11 months after the initial diagnosis of lung cancer. In conclusion, despite its rarity, the occurrence of endometrial metastasis is still possible for patients with lung cancer. The incidental accumulation of fluorodeoxyglucose in the uterus or the presence of postmenopausal vaginal bleeding must be considered malignancy until proven otherwise. ***(Thorac Med 2022; 37: 313-320)***

Key words: endometrial metastasis, lung adenocarcinoma, vaginal bleeding

Introduction

In Taiwan, the most frequent cause of cancer-related mortality is lung cancer, and the incidence has gradually increased during the past 20 years [1]. Lung cancer is also the second most common cancer among females in Taiwan [1]. Despite the substantial development of diagnostic and screening tools, approximately 75% of patients with non-small cell lung cancer

[1]Division of Pulmonary and Critical Care Medicine, Department of Internal Medicine, Tri-Service General Hospital, National Defense Medical Center, Taipei, Taiwan, 2 Department of Pathology, Tri-Service General Hospital, National Defense Medical Center, Taipei, Taiwan, 3 Department of Nuclear Medicine, Tri-Service General Hospital, National Defense Medical Center, Taipei, Taiwan.
Address reprint requests to: Dr. Chi-Hao Shen, Division of Pulmonary and Critical Care Medicine, Department of Internal Medicine, Tri-Service General Hospital, National Defense Medical Center, Taipei, Taiwan, No.325, Sec.2, Chenggong Rd., Neihu District, Taipei City, 11490, Taiwan (R.O.C)

are diagnosed at an advanced stage III or IV disease [2], indicating local or distant metastasis.

Lung carcinoma is a disease that easily spreads and disseminates. Though it may metastasize to any organ, the most commonly mentioned metastatic sites of lung cancer are reported to be the nervous system (39%), bones (34%), liver (20%), respiratory system (18%), and adrenal gland (8%) [3]. The secondary involvement of carcinoma in the female genitourinary tract is often caused by direct invasion from nearby pelvic organs or as a result of widespread peritoneal seeding. The ovary is the predominant metastatic site (50%) of extragenital tumors, followed by the vagina (22%), myometrium (10.7%), cervix (10.2%), endometrium (3.6%), and vulva (2%) [4]. Metastases from primary lung adenocarcinoma to the female genitourinary tract are not often documented, but the ovaries are the usual site of metastasis when it occurs [5]. Endometrial metastasis from primary lung malignancies is extremely rare, and can sometimes be challenging to diagnose and manage. Herein, we report a case of lung adenocarcinoma that metastasized to the endometrium and presented with clinical and radiological features that mimicked uterine leiomyoma.

Case Report

A 67-year-old postmenopausal Taiwanese lady presented with the complaints of bilateral back pain that radiated to the right anterior chest for 2 days. She was a never-smoker, with an unremarkable medical history except for a uterine leiomyoma, which was diagnosed at another hospital. The pain was persistent, stinging rather than sharp, without cold sweating, fever, dyspnea, cough, hemoptysis, or body weight loss. The contrast-enhanced computed tomography (CT) of the chest revealed a soft-tissue mass in the right upper lobe (Figure 1) that was

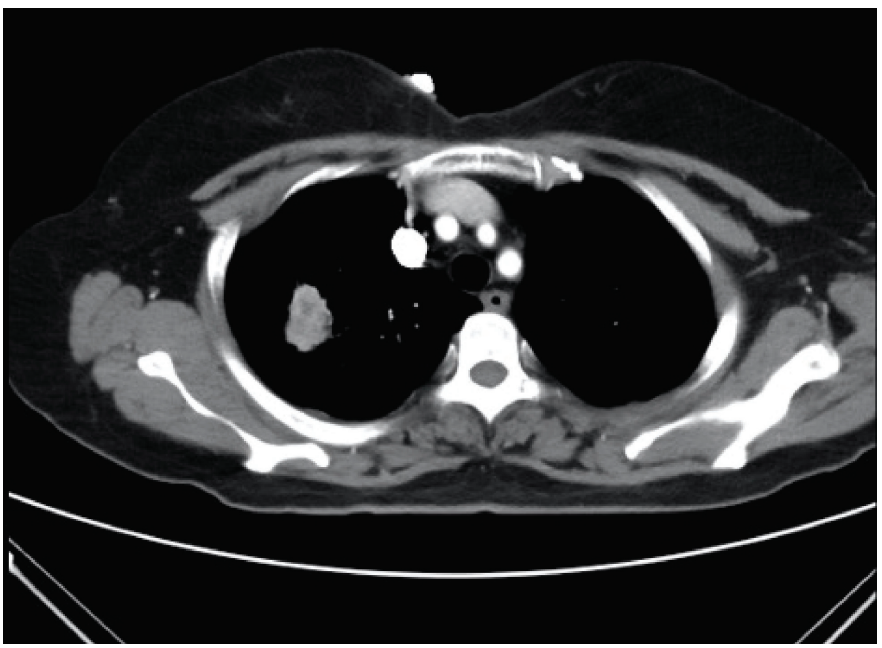

Fig. 1. Chest CT revealing a soft-tissue mass in the right upper lobe with highly suspicious lung carcinoma.

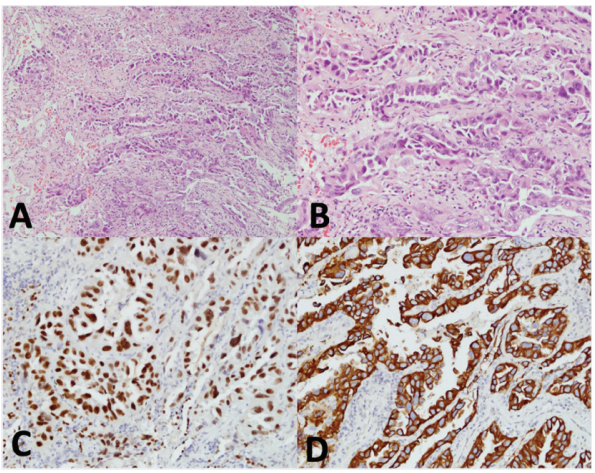

Fig. 2. Photomicrographs (A&B) showing tumor cells arranged in an acinar pattern infiltrating the pulmonary parenchyma, suggestive of an adenocarcinoma (A, H&E, ×100; B, H&E, ×200). Tumor cells exhibited immunopositivity for both TTF-1 (C, IHC, ×200) and CK7 (D, IHC, ×200).

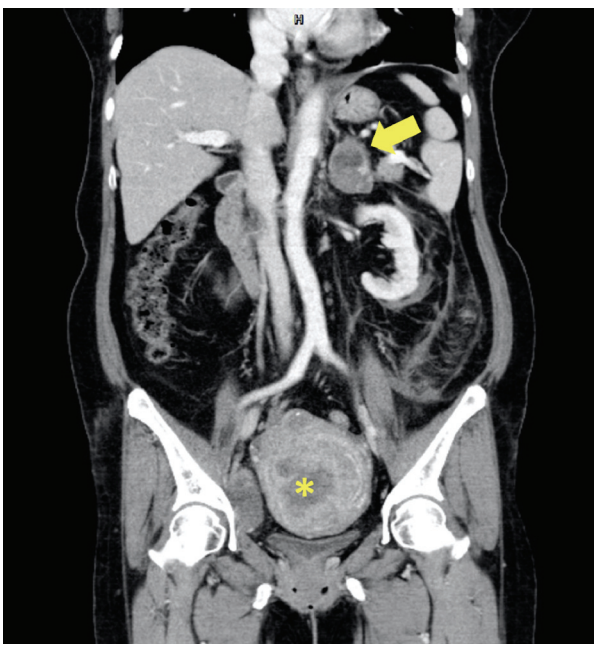

Fig. 3. Abdominal CT showing a ruptured left adrenal hematoma (arrow) and a mass lesion within the uterus (star).

highly suspicious of being lung carcinoma. No enlarged mediastinal lymph nodes were detected. A CT-guided biopsy was then performed, and the pathology revealed an adenocarcinoma with positive thyroid transcription factor-1 (TTF-1) and cytokeratin 7 (CK7) staining (Figure 2). Brain magnetic resonance imaging revealed no evidence of metastasis. However, an abdominal CT showed suspected left adrenal metastasis with a ruptured hematoma. A mass lesion within the uterus was also noted (Figure 3).

Laparoscopic left adrenalectomy was performed for the ruptured hematoma. The pathology confirmed adenocarcinoma of the lung, which had metastasized to the left adrenal gland. The tumor was staged as T2aN0M1c, stage IVB by a multidisciplinary team. Genotyping analysis of the tumor cell revealed a wild-type epidermal growth factor receptor (EGFR). Immunohistochemistry found that the specimen was negative for anaplastic lymphoma kinase (ALK) and ROS-1. The tumor proportion score was 0% for PD-L1. Whole-body positron emission tomography/CT (PET/CT) with F-18 fluoro-2-deoxy-D-glucose (FDG) was performed for complete cancer staging (Figure 4). Besides the known primary tumor lesion in the right upper lung, which showed strong FDG uptake (maximum standard uptake value [SUVmax]: 15.0), unusually intense FDG uptake within the endometrial cavity of the uterus and the right internal iliac region also was incidentally found (SUVmax: 11.7). The gynecologist was consulted for further evaluation. Based on the transvaginal ultrasound findings and her uterine leiomyoma history, the lesion was initially regarded as uterine leiomyoma.

Tri-weekly chemotherapy with cisplatin and pemetrexed was initiated. The gynecologist was consulted again 4 months later due to intermittent vaginal bleeding. Biopsy of the endometrium was done, and the histopathological exam revealed poorly differentiated adenocarcinoma characterized by pleomorphic tumor cells with

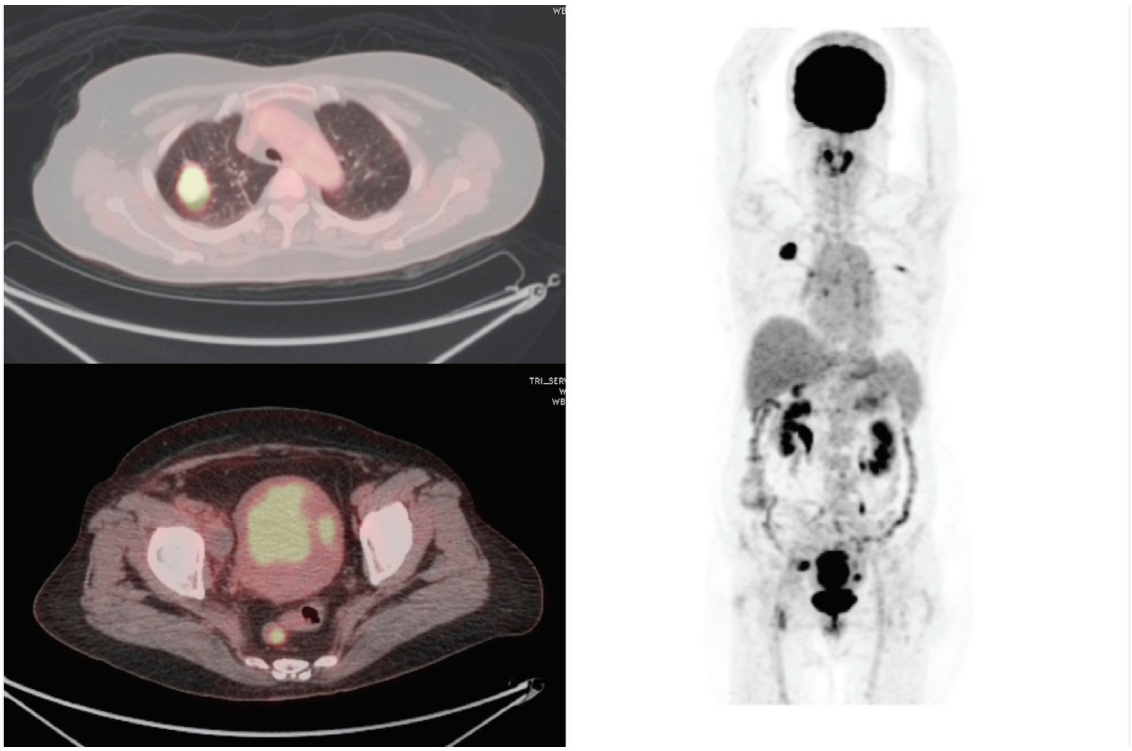

Fig. 4. PET/CT disclosed an FDG-avid tumor at the right upper lobe and abnormal uptake in the uterine region.

bizarre nuclei infiltrating the endometrial tissue, morphologically identical to the surgical lung biopsy (Figure 5, A and B). The tumor cells were positive for TTF-1, and negative for ALK, Paired-box gene 8 (PAX8), estrogen receptors (ER), and progesterone receptors (PR) (Figure 5, C–F). These results were consistent with primary lung adenocarcinoma with endometrial metastasis. Local radiotherapy was delivered to the uterus in 30 fractions to a combined total of 60 Grays. The chemotherapy regimen was shifted to tri-weekly cisplatin and docetaxel due to the left adrenal metastasis recurrence.

Two months after completing the course of radiotherapy, newly discovered metastatic sites at the right adrenal gland, left cerebellum, and bones (left ribs, left greater trochanter, and cervical and lumbar spines) revealed a progressive disease. The patient had a poor performance status, her family refused further intervention

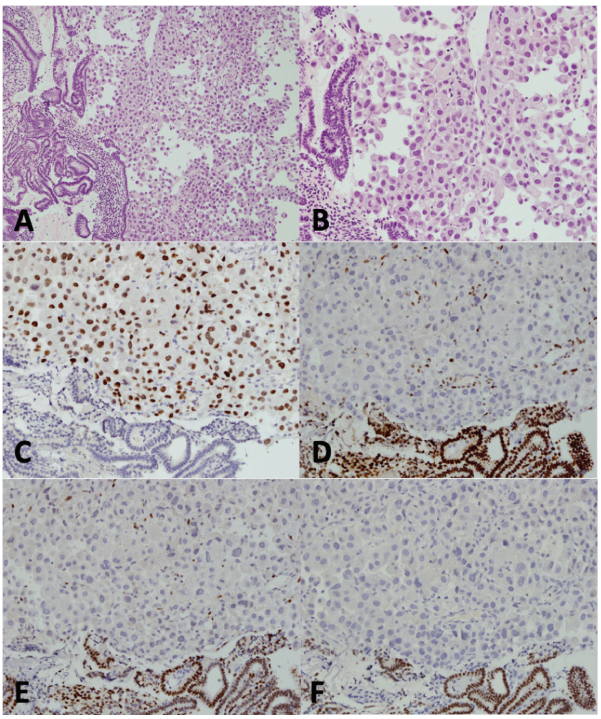

Fig. 5. Photomicrographs (A&B) from an endometrial biopsy showing adenocarcinoma infiltration (A, H&E, ×100; B, H&E, ×200). Tumor cells were immunopositive for TTF-1 (C, IHC, ×200), and negative for ER, PR, and PAX8 (D-F, IHC, ×200).

and they turned to hospice care. She died from aspiration pneumonia 11 months after the initial diagnosis of lung cancer.

Discussion

To the best of our knowledge, this is the first ever reported case of endometrial metastatic lung adenocarcinoma in Taiwan. Lung cancer with endometrial metastasis is extremely rare. The patient we reported herein presented with intermittent vaginal bleeding as an initial symptom. Her vaginal bleeding might be overlooked as related to leiomyoma because of the rareness of endometrial metastasis and her uterine leiomyoma history, which preclude surveys for true etiology.

In some cases, differentiating metastatic lesions of the endometrium from primary uterine malignancies might be challenging for pathologists and clinical physicians. Diagnostic immunohistochemistry with multiple markers provides adequate assistance to differentiate cancer origin. TTF-1 nuclear expression has been recognized as one of the most reliable immunostaining markers to differentiate primary lung adenocarcinoma from adenocarcinomas of other origins, due to its high sensitivity and specificity. From 74% to 92% of primary lung adenocarcinoma cases revealed a positive TTF-1 expression pathologically [6]. Nevertheless, approximately 19%–26% of endometrial adenocarcinomas also had expression of TTF-1 [6, 7]. Expression of ERs and PRs in endometrial adenocarcinoma ranged from 78.9% to 88.1%, and therefore often served as a traditional immunostaining marker for an endometrial origin of carcinoma [8]. PAX8 is a paired-box gene that is important in embryogenesis in several organs including the Müllerian tract, thyroid, and renal/upper urinary tracts, thus positive reactivity to PAX8 is considered in carcinomas from these sites. PAX8 is expressed in 96.3%–98% of endometrial adenocarcinomas [9, 10]. Lung cancer may harbor the receptors of estrogen and progesterone [11]; however, in our case, the combination of an absence of expression of ERs, PRs, and PAX8, and the presence of positively expressed TTF-1, supported the diagnosis of metastatic endometrial adenocarcinoma of primary lung cancer origin.

A literature review was undertaken in view of the rarity of our case, and only 5 cases were reported in the published English literature (Table 1) [12-15]. The first proven adenocarcinoma of the lung with endometrial metastasis was reported by Tiseo in 2011 [15]. The average age at initial diagnosis of lung cancer is 57.2 years (range, 37-75 years), and the duration from the initial diagnosis to identifying endometrial metastasis ranges from 5 months to 44 months, with an average of 18.7 months. The most common symptoms at initial presentation are abnormal vaginal bleeding or spotting, which occurred in 4 out of 6 cases. Regarding the diagnostic modalities of endometrial metastasis of lung adenocarcinoma, PET/CT was most common, and was utilized in 4 cases to reveal an abnormal FDG accumulation in the uterine and metastatic lesions. One study reported using ultrasound imaging to detect an increased thickness of the endometrium [15], and another reported the discovery of an enlarged uterine mass by abdominal CT [12]. The mutation status of EGFR was provided in 3 cases only, 1 patient had both an exon 19 mutation and a T790M mutation in exon 20 [13], the other had an L858R mutation in exon 21 [12], and our patient had a wild-type status.

Endometrial malignancies present as hypo-

attenuating and hypo-enhancing masses on contrast-enhanced CT. These CT imaging features are nonspecific, and a hypo-enhancing endometrial mass may be regarded as a submucosal leiomyoma, endometrial polyps, or cervical stenosis [16]. FDG PET/CT is widely used to determine metastatic malignancies. However, false-positive results may appear with a benign uterine tumor. Physiological endometrial uptake would be seen during early menstruation and the ovulatory phase in premenopausal women. Uterine tumors of a benign nature, such as uterine leiomyoma, adenomyosis, endometrial hyperplasia, malignancies including uterine cervical or endometrial cancer, leiomyosarcoma, and metastases were all documented as having increased FDG uptake at different levels [17]. Despite being more common in premenopausal women, the incidence of uterine FDG uptake in postmenopausal women still was reported to be from 1.2% to 17.6% [18-19]. Higher FDG uptake is considered suspicious for malignancy, although most leiomyomas had mild FDG accumulation. Nonetheless, Ma *et al*. [18] reported a wide range of FDG uptake for the leiomyomas in their study (SUVmax 1.74-10.81), and Chura *et al*. [20] reported high SUVs for 3 cases (SUVmax 6-16). The PET/CT image disclosed increased FDG uptake in the uterine region in our case, but leiomyoma was initially impressed due to her past history of leiomyoma and gynecological findings. Metastasis of lung cancer to the endometrium is extremely rare; however, a patient with postmenopausal vaginal bleeding, such as our patient, must be considered as potentially having cancer until proven otherwise.

Tyrosine kinase inhibitors for lung cancer with an oncogenic driver mutation, or systemic chemotherapy, have been reported as therapeutic management for endometrial metastases in previous reports (Table 1), but all 3 patients reported disease progression later. Local radiation therapy and systemic chemotherapy were administered to our patient for her advanced disease, and the treatment resolved her metrorrhagia. Hysterectomy might be considered in cases with persistent metrorrhagia to improve the patient's quality of life. However, there currently is no consensus regarding the treatment of metastatic endometrial cancer of lung origin. Therefore, further studies may help us tailor the optimal treatment for these patients.

In conclusion, despite its rarity, endometrial metastasis is still possible for patients with lung cancer. The incidental accumulation of FDG in the uterus or the presence of postmenopausal vaginal bleeding must be considered as malignancy until proven otherwise.

References

1. 衛生福利部，中華民國108年死因統計結果分析。https://dep.mohw.gov.tw/DOS/cp-4927-54466-113.html (Assessed April 3rd, 2021).
2. Blandin Knight S, Crosbie PA, Balata H, *et al*. Progress and prospects of early detection in lung cancer. Open Biol 2017; 7:170070.
3. Riihimaki M, Hemminki A, Fallah M, *et al*. Metastatic sites and survival in lung cancer. Lung Cancer 2014; 86:78-84.
4. Karpathiou G, Chauleur C, Hathroubi S, *et al*. Secondary tumors of the gynecologic tract: a clinicopathologic analysis. Int J Gynecol Pathol 2019; 38: 363-70.
5. Mazur MT, Hsueh S, Gersell DJ. Metastases to the female genital tract. Analysis of 325 cases. Cancer 1984; 53: 1978-84.
6. Zhang PJ, Gao HG, Pasha TL, *et al*. TTF-1 expression in ovarian and uterine epithelial neoplasia and its potential significance, an immunohistochemical assessment with multiple monoclonal antibodies and different secondary detection systems. Int J Gynecol Pathol 2009; 28: 10-8.
7. Siami K, McCluggage WG, Ordonez NG, *et al*. Thyroid transcription factor-1 expression in endometrial and

Table 1. Summary of Previous Cases and Characteristics of Endometrial Metastasis

Study	Age (at diagnosis)	Stage (LC)	Sites of metastases	Duration from initial diagnosis of LC to identification of EM	Signs and symptoms of EM	Diagnostic procedures	EGFR mutation of LC	Treatment for EM	Survival status
Tiseo *et al.* [12]	58	IV (T2N0M1)	Rib, brain, subcutaneous, liver, adrenal glands, endometrium	10 months	Vaginal bleeding	Ultrasound images	N/A	Chemotherapy, TKIs (erlotinib)	2 years, 1 month following the diagnosis
Zeeshan *et al.* [13]									
Case 1	55	IIIB	Hilum, endometrium	5 months	None (identified on PET)	PET/CT	N/A	N/A	N/A
Case 2	51	IV	Liver, endometrium	22 months	Abdominal pain and heavy vaginal bleeding	CT abdomen	Exon 21 (L858R)	N/A	N/A
Patel *et al.* [15]	75	IA (T1aN0M0)	Endometrium	20 months	Vaginal bleeding	PET/CT	N/A	Surgical resection (TAH-BAO)	N/A
Anjali *et al.* [14]	37	IVA	Pleura, breast, bones, brain, peritoneum, endometrium	44 months	None (identified on PET)	PET/CT	Exon 19 deletion & Exon 20 (T790M)	Chemotherapy	4 years, 9 months following the diagnosis
Current report	67	IVB (T2aNoM1c)	Pleura, adrenal gland	5 months	Vaginal bleeding	PET/CT	Wild-type	Chemotherapy with local RT	Deceased, 11 months following the diagnosis

BSO, bilateral salpingo-oophorectomy; CT, computed tomography; EGFR, epidermal growth factor receptor; EM, endometrial metastasis; LC, lung adenocarcinoma; N/A, not available; PET/CT; positron emission tomographic-computed tomography; RT, radiation therapy; TAH, transabdominal hysterectomy; TKIs, tyrosine kinase inhibitor

endocervical adenocarcinomas. Am J Surg Pathol 2007; 31: 1759-63.

8. Markova I, Duskova M, Lubusky M, *et al*. Selected immunohistochemical prognostic factors in endometrial cancer. Int J Gynecol Cancer 2010; 20: 576-82.
9. Hernandez-Caballero AI, Vierkoetter KR, Ahn HJ, *et al*. Novel immunohistochemical markers in the differential diagnosis of endocervical and endometrial adenocarcinoma: the added benefit of CAIX and PAX8. Gynecol Oncol Rep 2020; 33: 100614.
10. Laury AR, Perets R, Piao H, *et al*. A comprehensive analysis of PAX8 expression in human epithelial tumors. Am J Surg Pathol 2011; 35: 816-26.
11. Hsu LH, Chu NM, Kao SH. Estrogen, estrogen receptor and lung cancer. Int J Mol Sci 2017; 18.
12. Ahmad Z, Raza A, Patel MR. Endometrial metastasis of lung adenocarcinoma: a report of two cases. Am J Case Rep 2015; 16:296-9.
13. Anjali VR, Pandey R, Srivastava A, *et al*. Sequential EGFR mutation and ALK rearrangement in adenocarcinoma lung, with rare metastasis to bilateral breast, ovary and endometrium. Respir Med Case Rep 2019; 28: 100954.
14. Patel V, Bryan C, Pharaon M, *et al*. Unexpected endometrial metastasis of a primary lung adenocarcinoma. Radiol Case Rep 2018; 13: 793-6.
15. Tiseo M, Bersanelli M, Corradi D, *et al*. Endometrial metastasis of lung adenocarcinoma: a case report. Tumori 2011; 97: 411-4.
16. Faria SC, Sagebiel T, Balachandran A, *et al*. Imaging in endometrial carcinoma. Indian J Radiol Imaging 2015; 25:137-47.
17. Kitajima K, Murakami K, Kaji Y, *et al*. Spectrum of FDG PET/CT findings of uterine tumors. AJR Am J Roentgenol 2010; 195: 737-43.
18. Ma Y, Shao X, Shao X, *et al*. High metabolic characteristics of uterine fibroids in 18F-FDG PET/CT imaging and the underlying mechanisms. Nucl Med Commun 2016; 37: 1206-11.
19. Nishizawa S, Inubushi M, Kido A, *et al*. Incidence and characteristics of uterine leiomyomas with FDG uptake. Ann Nucl Med 2008; 22: 803-10.
20. Chura JC, Truskinovsky AM, Judson PL, *et al*. Positron emission tomography and leiomyomas: clinicopathologic analysis of 3 cases of PET scan-positive leiomyomas and literature review. Gynecol Oncol 2007; 104: 247-52.

Pulmonary Cavitation Lesions from Metastasized Urothelial Carcinoma Mimicking Primary Lung Cancer: A Case Report

Kai-Chao Chang[1,3], Chun-Chieh Wu[2], Mei-Hsuan Lee[1,3], Jen-Ye Hung[1,3]

The differential diagnosis of pulmonary cavitary lesions is important for clinicians because various critical diseases can present this radiological finding, including cancer, autoimmune diseases, vascular diseases, infections/inflammation, trauma, and congenital diseases. Cancer-related pulmonary cavitary lesions can be caused by primary lung cancer or metastasized malignancies. However, pulmonary cavitary lesions are rarely caused by metastasized urothelial carcinoma. Here, we reported a case of pulmonary cavitation caused by metastasized urothelial carcinoma. ***(Thorac Med 2022; 37: 321-324)***

Key words: Lung cavitary lesions, urothelial carcinoma

Background

A pulmonary cavity is defined as "a gas-filled space, seen as a lucency or low-attenuation area, within pulmonary consolidation, a mass, or a nodule" [1]. The thickness of the wall of the lung cavitary lesion can vary and serve as an indicator for the differential diagnosis, particularly when combined with the cavitary contents and clinical symptoms and signs. The etiologies of lung cavitary lesions are varied, and can include cancer, trauma, infection, inflammation, vascular disease, or congenital lung abnormalities [2]. Pulmonary cavitation occurs in approximately 4% of cases of lung metastases [3].

Urothelial carcinoma (UC) is a potential cause of lung metastasis, and may present as pulmonary cavitary lesions. UC, also known as transitional cell cancer (TCC), of the upper urinary tract is uncommon, accounting for only 5%–10% of all UC cases and 5%−10% of all renal tumors. Some recurrent cases associated with bladder UC have been reported after

[1]Division of Pulmonary and Critical Care Medicine, Department of Internal Medicine, Kaohsiung Medical University Hospital; [2]Department of Pathology, Kaohsiung Medical University Hospital, Kaohsiung Medical University; [3]Department of Internal Medicine, School of Medicine, College of Medicine Kaohsiung Medical University, Kaohsiung, Taiwan.
Address reprint requests to: Dr. Jen-Ye Hung, Division of Pulmonary and Critical Care Medicine, Department of Internal Medicine, Kaohsiung Medical University Hospital, No.100, Tzyou 1st Rd., Sanmin Dist., Kaohsiung City 80756, Taiwan (R.O.C.)

long-term latency [4-5]. However, few cases of late pulmonary metastasis due to upper urinary tract UC have been reported. Here, we present a case of UC complicated with lung metastasis and pulmonary cavity lesions after 5 years of follow-up.

Case Report

In May 2015, a 50-year-old man complained of gross hematuria, occurring since November 2014. No accompanying flank pain, dysuria, or aggravating factors were reported. Abdominal sonography showed a bilateral renal cyst without hydronephrosis or renal stones. However, multiple segment stenosis of the right ureter was discovered during ureterorenoscopy. A frozen biopsy was performed during the operation, and malignancy was later confirmed. Due to this finding, a laparoscopic right nephroureterectomy with bladder cuff excision was performed, and the pathological report for the right renal pelvis showed low-grade UC. After the operation, the patient maintained annual follow-up with cystostomy.

However, during one of his regular follow-ups, the patient complained of hemoptysis. Mass lesions in the bilateral upper lungs were noted on chest X-ray. High-resolution computed tomography (CT) was arranged, which revealed a 7.8-cm soft-tissue mass at the left upper lobe (LUL) and multiple cavitary lesions at the right upper lobe (RUL) and left lower lobe. Bronchoscopic biopsy of the lesion in the RUL cavity and a CT-guided biopsy of the mass in the LUL were performed separately to confirm the etiology of the lung mass and the cavitary lesions. Pathological reports for the specimens obtained from both the LUL mass and the RUL cavity lesions revealed metastatic UC [GATA3(+); thyroid transcription factor 1, TTF-1(−)]. Abdominal magnetic resonance imaging was also performed, and no other metastasis was noted. The patient received chemotherapy consisting of gemcitabine and cisplatin for metastatic UC.

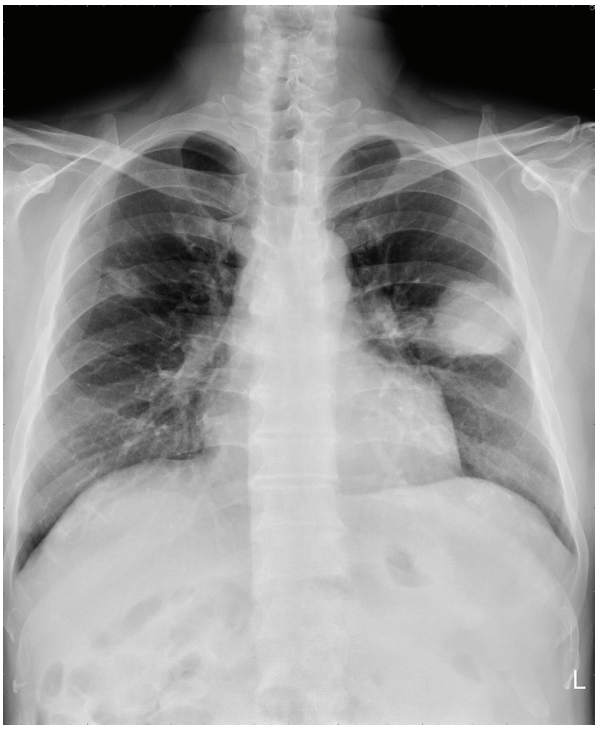

Fig. 1. Initial presentation of hemoptysis (chest X-ray, posterior-anterior view).

Discussion

The etiology of pulmonary cavitary lesions can vary, and can be cancer, autoimmune disease, vascular disease (e.g., Wegener's granulomatosis), infection (e.g., lung abscess, pulmonary tuberculosis, or pulmonary aspergilloma), trauma, or congenital disease [6]. The origins of lung cavity lesions can be determined by analyzing the wall thickness, cavitary contents, and clinical symptoms and signs. Acute onset symptoms and signs accompanied by fever might favor an acute infectious cause. The most com-

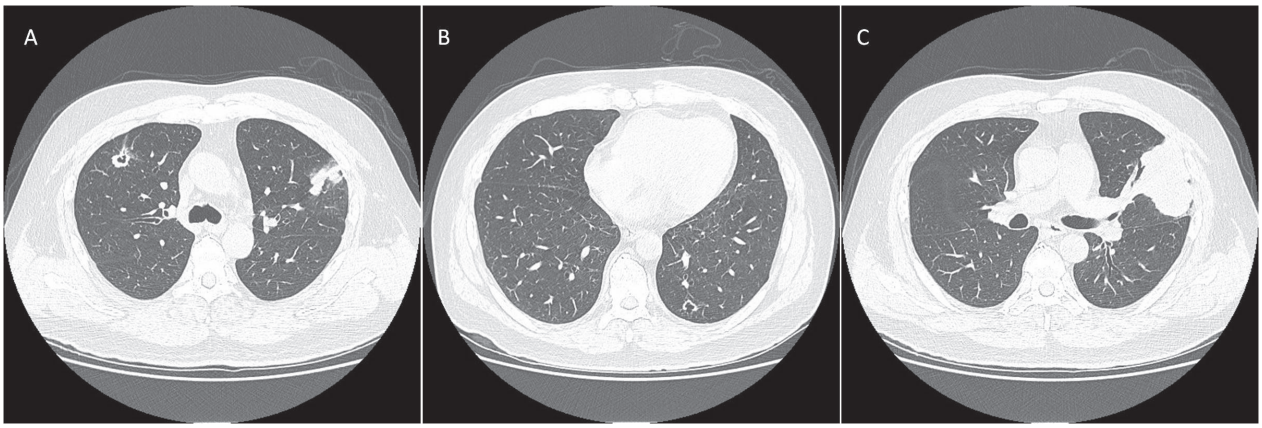

Fig. 2. Chest high-resolution computed tomography revealed bilateral lung cavitary lesions (A: right upper lobe; B: left lower lobe) and a left upper lobe lung mass (C).

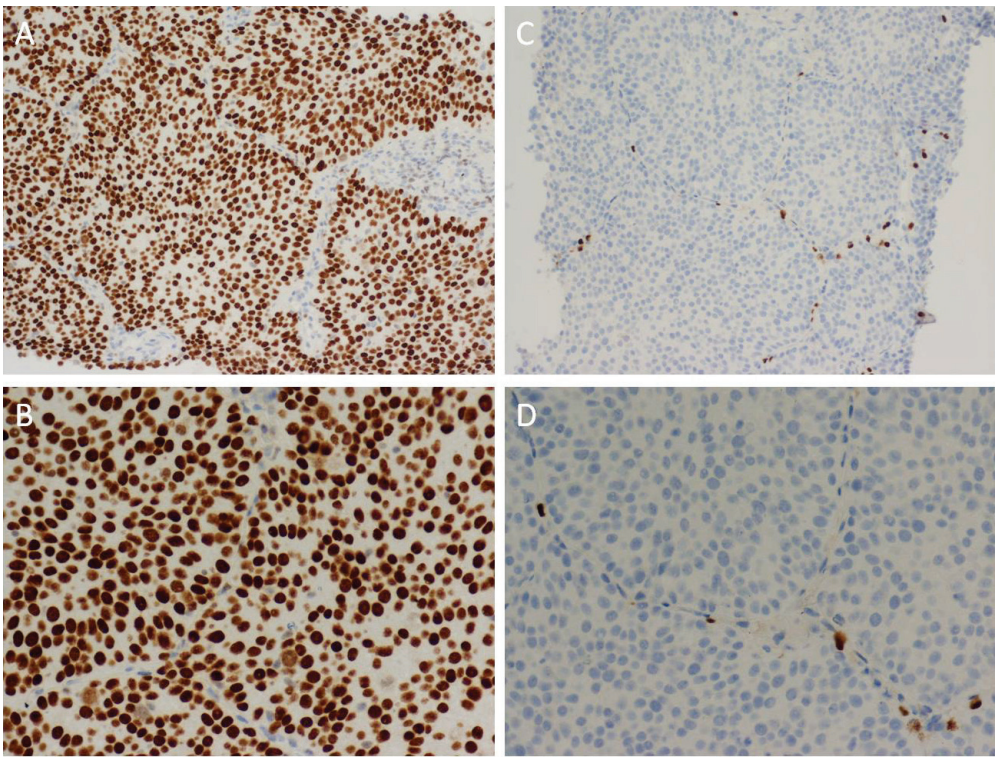

Fig. 3. Immunohistochemistry stains of tissue obtained from CT-guided biopsy of lung metastatic lesions. A: anti-GATA 100×; B: anti-GATA 200×; C: anti-thyroid transcription factor-1 (TTF-1) 100×; D: anti-TTF-1 200×.

mon microorganisms known to cause cavitary lung lesions are bacteria, such as Streptococcus pneumoniae, Staphylococcus aureus, Klebsiella pneumoniae, and Haemophilus influenzae. Chronic cough associated with fatigue and body weight loss is suggestive of potential malignancy or chronic infection, such as by typical and atypical mycobacteria, fungi (e.g., aspergillosis or Pneumocystis jirovecii), or parasites [7]. Malignancy, both primary and metastases, should

always be considered. Approximately 4% of lung metastases will develop into cavitary lesions [3]. The most common cause of metastatic lung lesions is squamous cell carcinoma, which originates from the lungs or head and neck [3], followed by gastrointestinal adenocarcinomas, UC, sarcomas, cervical cancer, and pancreatic adenocarcinoma [8-12].

The most common sites for distant metastases that originate from UCs include the liver, lungs, mediastinum, bone, and adrenal gland, in descending order [13]. Pulmonary metastases can present as multiple nodules, a solitary mass, or interstitial micronodules. When multiple nodules are present, they are typically well-circumscribed and rounded, without calcifications or cavitations. Possible mechanisms that contribute to tumor cavity formation include internal tissue necrosis, air trapping by the check valve, local extension by elastic traction, and bullae [14].

We reported a case of upper urinary tract UC with lung metastasis that presented as multiple cavity formations mimicking primary lung cancer. In clinical practice, if cavitary lung nodules are detected in a host with a history of malignancy, further survey for infections, primary lung cancer, and metastasized cancer should be considered.

References

1. Hansell DM, Bankier AA, MacMahon H, *et al*. Fleischner Society: glossary of terms for thoracic imaging. Radiology 2008 Mar; 246(3): 697-722.
2. Canan A, Batra K, Saboo SS, *et al*. Radiological approach to cavitary lung lesions. Postgrad Med J 2020 Sep 15: postgradmedj-2020-138694.
3. Boitsios G, Bankier AA, Eisenberg RL. Diffuse pulmonary nodules. AJR Am J Roentgenol 2010 May; 194(5): W354-66.
4. Lim JH, Jeon SH, Lee JM, *et al*. Late-onset distant metastatic upper urinary tract urothelial carcinoma mimicking lung adenocarcinoma. Tuberc Respir Dis (Seoul) 2013; 75(1): 32-35.
5. Kawaguchi K, Okasaka T, Fukui T, *et al*. Pulmonary metastasis from urothelial carcinoma of the upper urinary tract 29 years after nephrectomy. Surg Case Rep 2017; 3(1): 20.
6. Parkar AP, Kandiah P. Differential diagnosis of cavitary lung lesions. J Belg Soc Radiol 2016; 100(1): 100.
7. Gadkowski LB, Stout JE. Cavitary pulmonary disease. Clin Microbiol Rev 2008 Apr; 21(2): 305-33.
8. Chaudhuri MR. Cavitary pulmonary metastases. Thorax 1970; 25 (3): 375-81.
9. Alexander PW, Sanders C, Nath H. Cavitary pulmonary metastases in transitional cell carcinoma of urinary bladder. AJR Am J Roentgenol 1990; 154 (3): 493-4.
10. Seo JB, Im JG, Goo JM *et al*. Atypical pulmonary metastases: spectrum of radiologic findings. Radiographics 2001; 21 (2): 403-17.
11. Martínez-Jiménez S, Rosado-de-Christenson ML, Walker CM *et al*. Imaging features of thoracic metastases from gynecologic neoplasms. Radiographics 2014; 34 (6): 1742-54.
12. Virgilio E, Iannicelli E, Balducci G. RE: Atypical pulmonary metastases from pancreatic adenocarcinoma. Korean J Radiol 2014 May-Jun; 15(3): 399-400.
13. Kurian A, Lee J, Born A. Urothelial bladder cancer with cavitary lung metastases. Can Respir J 2011; 18(3): e46-e47.
14. Watanabe H, Uruma T, Tsunoda T, *et al*. Lung metastasis of transitional cell cancer of the urothelium, with fungus ball-like shadows closely resembling aspergilloma: A case report and review of the literature. Oncol Lett 2014; 8(1): 95-98.

Refractory Hypoxemia Caused by a Bronchoesophageal Fistula: A Case Report and Literature Review

Hao-Chung Tsai[1], Chieh-Yung Wang[1], Chen-Liang Tsai[1]

A 66-year-old man who smoked heavily initially presented with dysphagia, a huge mediastinum, and a lung mass. Adenosquamous lung cancer stage IIIC (AJCC 8th) was diagnosed, and definitive concurrent chemoradiotherapy (CCRT) was initiated when he was in partial remission. Dysphagia occurred during and after CCRT. Panendoscopy revealed radiation esophagitis. One month later, he developed pneumonia and hypoxemic and hypercapnic respiratory failure. Since the hypoxemia persisted, we performed bronchoscopy, which revealed a bronchoesophageal fistula in the right main bronchus. We reported this rare complication of CCRT in a stage IIIC non-small cell lung cancer patient and reviewed the relevant literature. ***(Thorac Med 2022; 37: 325-331)***

Key words: Lung cancer, chemoradiotherapy, bronchoesophageal fistula, tracheoesophageal fistula, adenosquamous carcinoma

Introduction

Cancer-related bronchoesophageal (BE) fistulas are rare, and in most published case reports, they are centrally located, with mediastinal or mediastinal lymph node involvement and advanced lung cancer [1-8].

Herein, we report a rare case of refractory hypoxemic respiratory failure with the complication of BE fistula formation in a lung adenosquamous carcinoma patient after chemoradiotherapy.

Case Report

A 66-year-old man who had a 20-year smoking history suffered from chronic cough for 2 months and hemoptysis for 1 month. Chest computed tomography (CT) revealed a mass of approximately 4.4 × 3.6 cm in the posterior mediastinum (Figure 1). Adenosquamous carcinoma (clinical stage T4N3M0, IIIC) of the right main bronchus and invasion of the posterior mediastinum and esophagus with the complication of external compression of the lower part of his trachea and esophagus had been con-

[1]Division of Pulmonary and Critical Care Medicine, Department of Internal Medicine, Tri-Service General Hospital, National Defense Medical Center, Taipei, Taiwan.
Address reprint requests to: Dr. Chen-Liang Tsai, Division of Pulmonary and Critical Care Medicine, Department of Internal Medicine, Tri-Service General Hospital, National Defense Medical Center, Taipei, Taiwan, No. 325, Sec. 2, Chenggong Rd., Neihu District, Taipei City 11490, Taiwan (R.O.C)

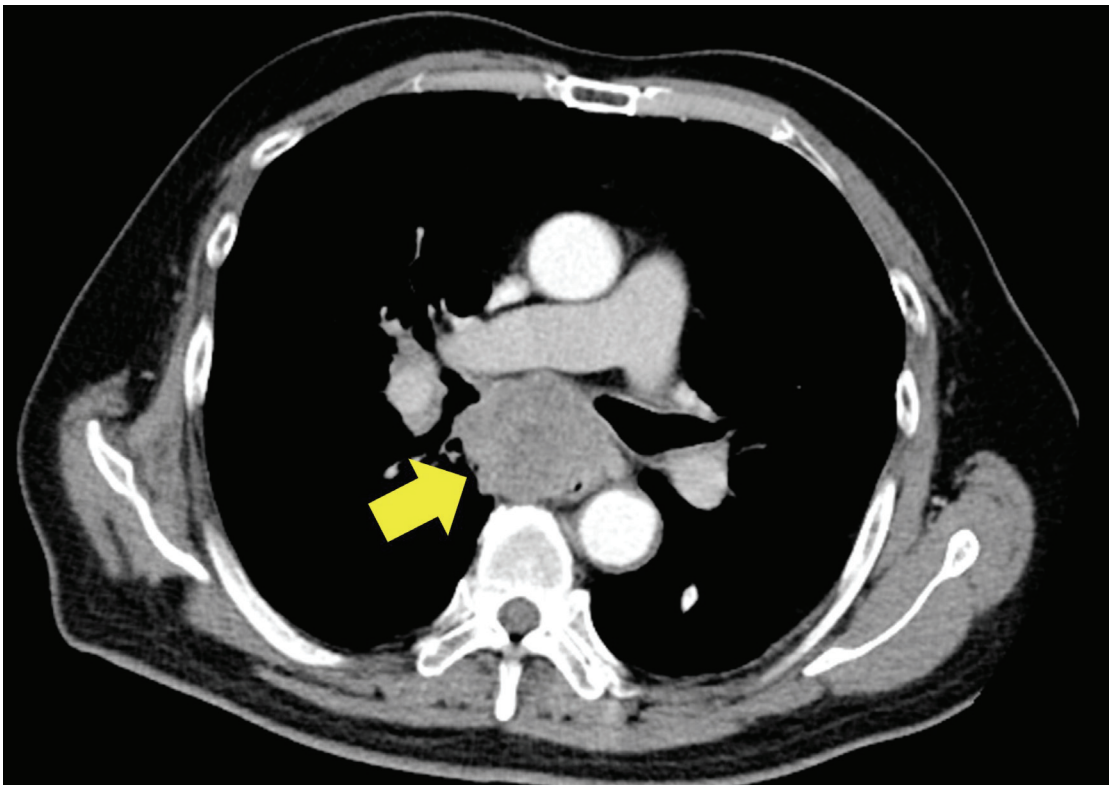

Fig. 1. An axial chest computed tomography scan showing a mass in the posterior mediastinum.

firmed 9 months before this admission.

One month later, he received concurrent chemoradiotherapy (CCRT) and showed a partial clinical response. Dysphagia occurred during and after CCRT as well as 1 month before this admission. Panendoscopy revealed circumferential ulceration and lumen narrowing, and bleeding from the upper-third to the middle-third of the esophagus, which was compatible with radiation esophagitis. A nasogastric tube was inserted for nutritional support.

After discharge, the patient visited the emergency department due to vomiting, dyspnea, and high fever. A chest plain radiograph revealed multifocal consolidations in both the lungs. His O_2 saturation was approximately 91%, even with the use of a non-rebreathing O_2 mask. For his respiratory distress, noninvasive mechanical ventilation was initiated, but no response was apparent. After endotracheal tube intubation, the hypercapnia progressed and hypoxemia persisted. The O_2 saturation decreased from 85% to 70%, and was not corrected despite a fraction of inspired O_2 of 100%. His abdomen became distended and the drainage bag of the nasogastric tube inflated after tracheal intubation. The ventilator showed an air leak and loss of positive end expiratory pressure (PEEP).

Bronchoscopy was performed immediately at bedside, and a large fistula at the posterior wall of the right main bronchus was noted (Figures 2A and 2B). A CT image revealed significant extensive ulceration at the rear wall of the right main bronchus, connected to the esophagus (Figure 3). Since his prognosis was poor, and in accordance with his will, palliative

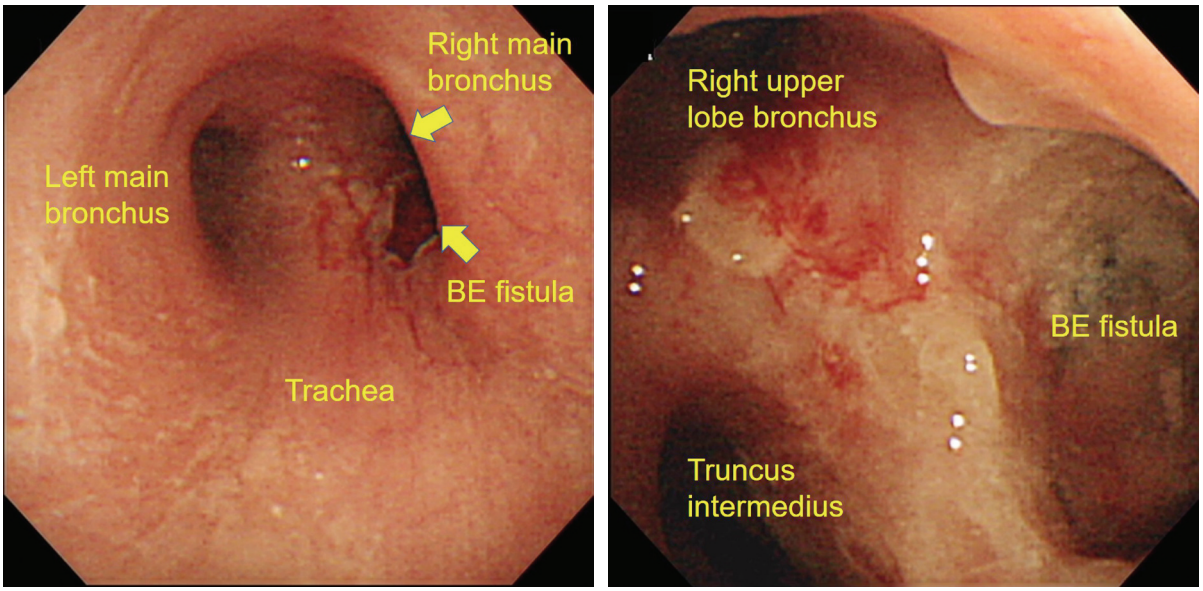

Fig. 2. (A and B): A bronchoscopy image showing a bronchoesophageal fistula in the posterior wall of the right main bronchus (A and B).

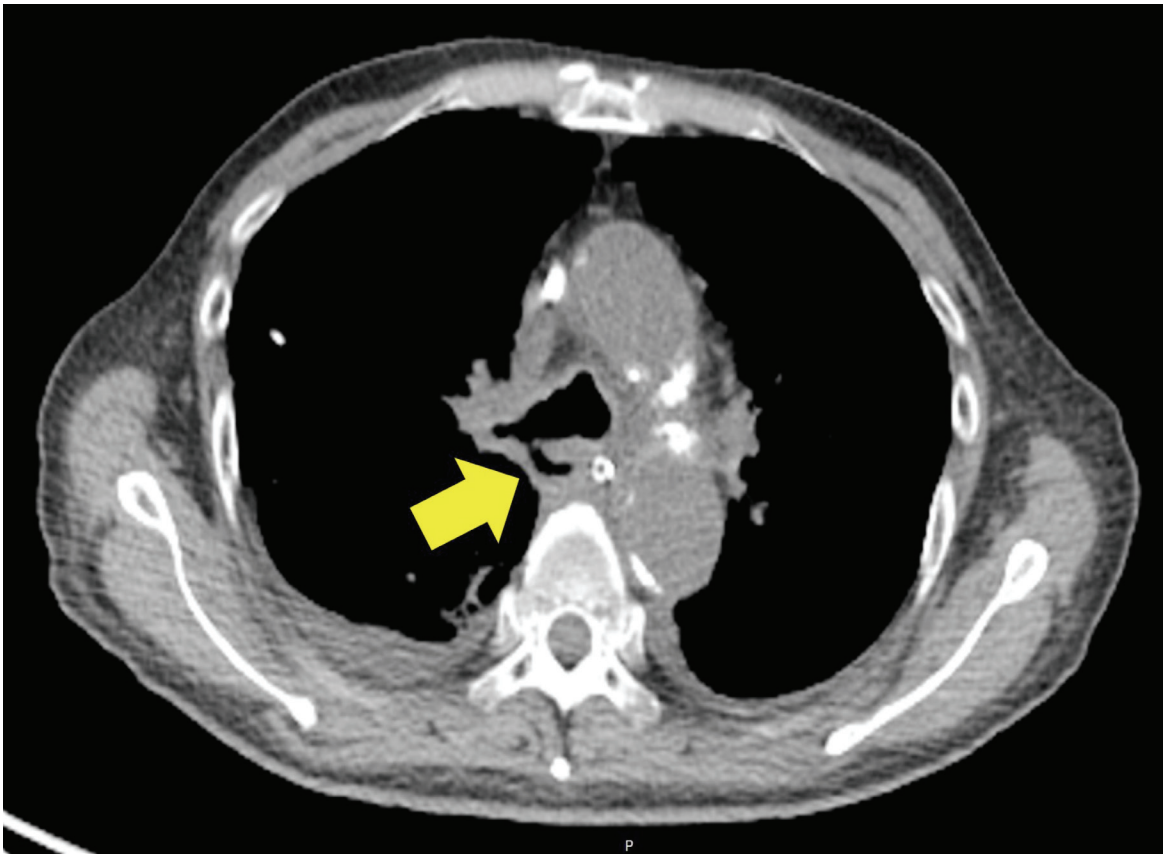

Fig. 3. A chest computed tomography scan showing a fistula between the right main bronchus and the esophagus.

hospice care was initiated. He passed away on the second day of tracheal intubation.

Discussion

The clinical scenario of persistent hypoxemia after tracheal intubation and eventual development of a BE fistula is rare in patients with lung cancer. Post-intubation hypoxia has many causes, and these can be summarized as "DOPES": where D stands for displacement of an endotracheal tube, O: obstruction of an endotracheal tube, P: pneumothorax/pulmonary embolism/pulmonary edema/pneumonia, E: equipment malfunction, and S: stacked breaths [9].

However, in our patient, none of these causes was present. In clinical practice, large air leaks, PEEP loss, increased abdominal distension, and an inflated drainage bag of the nasogastric tube should prompt physicians to consider esophageal intubation [10-11]. We reviewed previous studies and listed the causes of air leakage during mechanical ventilation (Table 1) [12-17], and then performed bronchoscopy to expand the differential diagnoses.

Table 1. Causes of Airway Leaks during Mechanical Ventilation

Equipment
A. Leaks with a properly functioning endotracheal tube:
Under-inflation of the cuff
High peak airway pressure
Wide discrepancy between the diameters of the endotracheal tube and the trachea
Placement of a nasogastric or orogastric tube in the trachea or bronchus
Cephalad migration of the endotracheal tube
B. Leaks caused by structural defects of the endotracheal tube:
Puncture of the pilot balloon, inflation line, or cuff
Defect of the inflation valve or inflation line
Asymmetrical cuff
Structure of the trachea and bronchus
Tracheocele, tracheomegaly, tracheomalacia
Tear or rupture of the trachea and bronchus caused by intubation
Tracheoesophageal fistula or bronchoesophageal fistula
Bronchopleural fistula
Blunt or penetrating trauma
Lung resection
Lung cancer after antineoplastic therapy
Parenchymal-pleural fistula
Laceration of the visceral pleura (by central catheter placement, thoracentesis, biopsy, or tube thoracostomy)
Spontaneous disruption of the distal airway
Alveolar rupture associated with mechanical ventilation

Pathological connections between the esophagus and trachea, and those between the esophagus and major bronchi are termed tracheoesophageal fistulas (TEFs) and bronchoesophageal fistulas (BEFs), respectively [18]. The incidence of cancer-related TEFs varies according to the origin of cancer: 14.76% for cases of tracheal cancer, 4.94% for cases of esophageal cancer, and 0.16% for cases of lung cancer [18]. We reviewed the reported cases [1-7] (Table 2) and found that a TEF tended to form more often with centrally located advanced lung cancer, mediastinal involvement, and mediastinal lymph node involvement; these occurrences corresponded to the anatomy between the trachea and esophagus and that between the bronchus and esophagus.

The most common symptoms of a fistula include cough (56%), aspiration (37%), fever (25%), and dysphagia (19%) [19]. According to previous studies on esophageal cancer-related fistulas [20-23], patients with T4 stage and N3 stage cancer, and those with maximum thickness of the tumor had an increased risk of esophageal fistula formation [20,23].

Wound healing requires a coordinated interaction of keratinocytes, fibroblasts, and endothelial cells. These cells form a scaffold in a healing wound and induce neovascularization [24]. Chemotherapeutic agents interfere with cell metabolism [24], and radiation injury disrupts the interactions of keratinocytes, fibroblasts, and endothelial cells, thereby impairing the capacity for tissue repair [24-25]. A tumor with a larger size and greater invasion depth involves more surrounding tissue. When a tumor regresses faster after therapy than regular tissue repair, fistulas can form easily [20,23]. This scenario is consistent with the condition of our patient.

In recent years, sequential case reports have highlighted the possibility that treatment with angiogenesis inhibitors or immune checkpoint inhibitors increases the risk of TEF formation in patients with lung cancer [6–8]; however, more cases must be studied to confirm this hypothesis.

Conclusion

According to the reported cases we reviewed, centrally located lung cancer and mediastinal involvement after CCRT increased the probability of TEFs. All of those patients had more than 1 typical symptom (cough, aspiration, fever, and dysphagia). When patients with lung cancer show such typical symptoms, imaging should be performed to diagnose potentially fatal complications.

References

1. Buemi L, Stefanelli S, Bichard P, *et al*. Esophageal pulmonary fistula - a rare complication of radiation therapy: a case report. J Med Case Rep 2018 May 2; 12(1): 116.
2. Ozeki T, Asano M, Fujimoto N, *et al*. Esophagobronchial fistula in a patient with squamous cell carcinoma of the lung: a case report. Case Rep Oncol 2017 Jun 22; 10(2): 553-557.
3. Honda T, Tsuzaki Y, Mitaka K, *et al*. Tracheoesophageal fistula closed by chemoradiotherapy in lung cancer. Case Rep Oncol 2011; 4(2): 350-7.
4. Abe T, Nagai T, Murakami K, *et al*. Esophago-pulmonary fistula caused by lung cancer treated with a covered self-expandable metallic stent. J Clin Gastroenterol Treat 2016; 2(4).
5. Sugimoto H, Yoshihara A, Obata D, *et al*. Bronchooesophageal fistula after lung cancer treatment. BMJ Case Rep 2020 Mar 25; 13(3).
6. Nishie K, Yasuo M, Kitaguchi Y, et al. Bevacizumab-induced tracheoesophageal fistula in a patient suffering from lung cancer with bulky subcarinal lymph node: a

Table 2. Summary of Previous Cases and Characteristics of Cancer-related Tracheoesophageal Fistula

Study	Age and gender	Cancer type	Site of primary cancer	Treatment for cancer	Symptoms	Diagnostic procedures	Location of fistulas	Treatment for TEFs	Survival status after the diagnosis of TEFs
Buemi, *et al.* [1]	72/M	SqCC	Left upper lung lobe with mediastinal invasion	CBP + GEM & mediastinal RT	Fever, dyspnea	Videofluoroscopy	Left upper lung	Esophageal stenting	7 weeks
Ozeki, *et al.* [2]	73/M	SqCC	Posterior mediastinum	CCRT with CBP + DOC	Cough, sore throat	Chest CT, PES, bronchoscopy	1st LMB 2nd RMB	Esophageal stenting	111 days
Honda, *et al.* [3]	45/M	Poorly differentiated lung carcinoma	Pancoast tumor with mediastinal invasion	CCRT with CBP + DOC	Cough, aspiration	PES, bronchoscopy	Trachea	CRT	N/A
Abe, *et al.*[4]	71/M	SqCC	Right lower lobe	1st line: CDDP + TS-1 + RT 2nd line: CBP + nab-PTX + RT	Fever, chest pain	Chest CT, PES, esophagography	Right lower lobe	Esophageal stenting	N/A
Sugimoto, *et al.*[5]	67/M	SqCC	Central location of right lower lobe	CCRT with CBP + PTX	Cough, dysphagia	Esophagography	Truncus intermedius	Esophageal stenting	N/A
Nishie, *et al.*[6]	66/M	NSCLC	Left lower lobe	CBP + pemetrexed + BEV & palliative RT	Fever, cough, dysphagia, aspiration	Chest CT, PES, bronchoscopy	LMB through a bulky subcarinal metastatic LN	Esophageal stenting	3 months
Nishiyama, *et al.* [7]	59/M	SqCC	Unknown primary	1st line: CBP + nab-PTX 2nd line: CBP + ramucirumab 3rd line: S-1 4th line: nivolumab	Fever, cough	Chest CT, bronchoscopy	Truncus intermedius	Esophageal stenting	N/A
Our case	66/M	Adenosquamous carcinoma	RMB	CCRT with CDDP + NVB	Fever, dyspnea, dysphagia	Chest CT, bronchoscopy	RMB	Hospice	1 day

LMB, left main bronchus; RMB, right main bronchus; TEF, tracheoesophageal fistula; LN, lymph node; SqCC, squamous cell carcinoma; NSCLC, non-small-cell lung cancer; RT, radiotherapy; CT, computed tomography; PES, panendoscopy; CCRT, concurrent chemoradiotherapy; CRT, chemoradiotherapy; CBP, carboplatin; CDDP, cisplatin; NVB, vinorelbine; GEM, gemcitabine; DOC, docetaxel; PTX, paclitaxel; BEV, bevacizumab

case report. Nagoya J Med Sci 2018 Feb; 80(1): 129-134.
7. Nishiyama A, Sakaguchi H, Yanagimura N, *et al*. Bronchoesophageal fistula formation after three courses of nivolumab for carcinoma of unknown primary with a subgroup of lung squamous cell carcinoma. Oxf Med Case Reports 2020 Dec 28; 2020(12): omaa116.
8. Spigel DR, Hainsworth JD, Yardley DA, *et al*. Tracheoesophageal fistula formation in patients with lung cancer treated with chemoradiation and bevacizumab. J Clin Oncol 2010 Jan 1; 28(1): 43-8.
9. Myrianthefs P, Kouka C, Giannelou E, *et al*. Acute desaturation in intubated patients. Crit Care 2011; 15(Suppl 1): P157.
10. Birmingham PK, Cheney FW, Ward RJ. Esophageal intubation: a review of detection techniques. Anesth Analg 1986 Aug; 65(8): 886-91.
11. Neeraj K, Amarjeet K, Prakash K, *et al*. Delayed detection of esophageal intubation: Nasogastric tube was the cause? Saudi Med J 2018 Oct; 2(2): 27.
12. El-Orbany M, Salem MR. Endotracheal tube cuff leaks: causes, consequences, and management. Anesth Analg 2013 Aug; 117(2): 428-34.
13. Valluri K, Jiwani A. A curious case of persistent air leak. Chest 2018 Oct; 154(4): 382A.
14. Singh S, Gurney S. Management of post-intubation tracheal membrane ruptures: A practical approach. Indian J Crit Care Med 2013 Mar; 17(2): 99-103.
15. Parker RJ, Rechner IJ, Parke TJ. Tracheo-oesophageal fistula and upper airway leak in the intensive care unit. Br J Anaesth 2008 Jan; 100(1): 139-40.
16. Kempainen RR, Pierson DJ. Persistent air leaks in patients receiving mechanical ventilation. Semin Respir Crit Care Med 2001 Dec; 22(6): 675-84.
17. Frytak S, Lee RE, Pairolero PC, *et al*. Necrotic lung and bronchopleural fistula as complications of therapy in lung cancer. Cancer Invest 1988; 6(2): 139-43.
18. Martini N, Goodner JT, D'Angio GJ, *et al*. Tracheoesophageal fistula due to cancer. J Thorac Cardiovasc Surg 1970 Mar; 59(3): 319-24.
19. Burt M, Diehl W, Martini N, et al. Malignant esophagorespiratory fistula: management options and survival. Ann Thorac Surg 1991 Dec; 52(6): 1222-8; discussion 1228-9.
20. Hu B, Jia F, Zhou H, *et al*. Risk factors associated with esophageal fistula after radiotherapy for esophageal squamous cell carcinoma. J Cancer 2020 Mar 31; 11(12): 3693-3700.
21. Zhang Y, Li Z, Zhang W, et al. Risk factors for esophageal fistula in patients with locally advanced esophageal carcinoma receiving chemoradiotherapy. Onco Targets Ther 2018 Apr 23; 11: 2311-2317.
22. Xu Y, Wang L, He B, *et al*. Development and validation of a risk prediction model for radiotherapy-related esophageal fistula in esophageal cancer. Radiat Oncol 2019 Oct 22; 14(1): 181.
23. Zhu C, Wang S, You Y, *et al*. Risk factors for esophageal fistula in esophageal cancer patients treated with radiotherapy: a systematic review and meta-analysis. Oncol Res Treat 2020; 43(1-2): 34-41.
24. Deptuła M, Zieliński J, Wardowska A, *et al*. Wound healing complications in oncological patients: perspectives for cellular therapy. Postepy Dermatol Alergol 2019 Apr; 36(2): 139-146.
25. Haubner F, Ohmann E, Pohl F, *et al*. Wound healing after radiation therapy: review of the literature. Radiat Oncol 2012 Sep 24; 7: 162.

Successful Treatment of Iatrogenic Tracheal Injury with Stent Placement and Extracorporeal Membrane Oxygenation – A Case Report

Hsien-Chi Liao[1], Jen-Hao Chuang[2], Wei-Ling Hsiao[3], Ke-Cheng Chen[4]

Tracheobronchial injuries are infrequent but potentially life-threatening. Iatrogenic tracheal rupture after endotracheal intubation is extremely rare. In this report, we present the case of a 16-year-old male who suffered an iatrogenic tracheobronchial injury during multiple trauma treatment after a traffic accident, and who was treated successfully with stent placement and extracorporeal membrane oxygenation. In addition to a literature review, we also discuss post-intubation injuries to the trachea and bronchi and treatment possibilities. ***(Thorac Med 2022; 37: 332-338)***

Key words: Iatrogenic Tracheal Injury, Stent Placement, Extracorporeal Membrane Oxygenation

Introduction

Tracheobronchial injuries are infrequent but potentially life-threatening [1]. Iatrogenic tracheal rupture after endotracheal intubation is extremely rare. In this report, we present the case of a 16-year-old male who suffered an iatrogenic tracheobronchial injury during multiple trauma treatment after a traffic accident, and who was treated successfully with stent placement and extracorporeal membrane oxygenation. We also discuss post-intubation injuries to the trachea and bronchi in detail.

Case presentation

A 16-year-old male with a history of attention-deficit hyperactivity disorder was admitted to our emergency department after a severe traffic accident. His Injury Severity Score was 26, and initial consciousness was assessed as 4 on eye-opening, 4 on verbal response, and 5 on motor response on the Glasgow Coma Scale (GCS) (E4V4M5), with agitation. Physical

[1]Department of Traumatology, National Taiwan University Hospital and National Taiwan University College of Medicine, No. 7 Chung Shan South Road, Taipei 100, Taiwan, [2]Department of Surgery, National Taiwan University Hospital and National Taiwan University College of Medicine, No. 7 Chung Shan South Road, Taipei 100, Taiwan, [3]Department of Nursing, National Taiwan University Hospital and National Taiwan University College of Medicine, No. 7 Chung Shan South Road, Taipei 100, Taiwan, [4]Department of Surgery, National Taiwan University Hospital and National Taiwan University College of Medicine, No. 7 Chung Shan South Road, Taipei 100, Taiwan.
Address reprint requests to: Dr. Ke-Cheng Chen, National Taiwan University Hospital and National Taiwan University College of Medicine, No. 7 Chung Shan South Road, Taipei 100, Taiwan

examination on arrival showed bilateral chest wall contusions and lower limb deformities. Endotracheal intubation was performed immediately to protect his airway and administer sedation during further examination. However, difficult ventilation and abnormally high airway pressure were noted from the beginning. Since the patient's respiratory situation continued to worsen, the emergency physician tried to replace the endotracheal tube and rechecked its location on a chest radiograph. At the same time, chest tubes were inserted bilaterally because the poor vital signs raised suspicion of a tension hemopneumothorax. Persistent hemoptysis from the endotracheal tube was also noted.

Despite the resuscitation measures, the clinical condition of the patient did not improve notably. Instead, progressive subcutaneous emphysema was observed. After transfer to the intensive care unit, computed tomography (CT) of the patient's chest confirmed diffuse subcutaneous emphysema and showed severe pneumomediastinum with heart compression (Figure 1(a)). It also revealed air within the bilateral chest wall, shoulder, neck, and even the subdiaphragmatic area, so pneumoperitoneum was diagnosed (Figure 1(b)). The abdomen and pelvis CT showed a pneumoperitoneum and retroperitoneum, and air within both scrotums and thighs subcutaneously.

Therefore, we performed bronchoscopy, which revealed a significant tracheal defect at the carina level with exposure of the subcarinal soft tissue (Figure 2). Based on this finding, we suspected his carina was damaged by the endotracheal tube stylet protruding out of the distal end of the tube during intubation. Unfortunately, the patient suffered from desaturation and progressive subcutaneous emphysema for 2 days after admission, despite ventilator support with high FiO_2. In order to restore sufficient hemodynamics and oxygenation, veno-venous extracorporeal membrane oxygenation (V-V ECMO) was begun. A Dumon® Y-shaped, 150*320 mm silicone stent (Novatech®, La Ciotat, France) (Figure 3) was trimmed to shape, and then placed into his trachea through a rigid bronchoscope. The patient's respiratory status

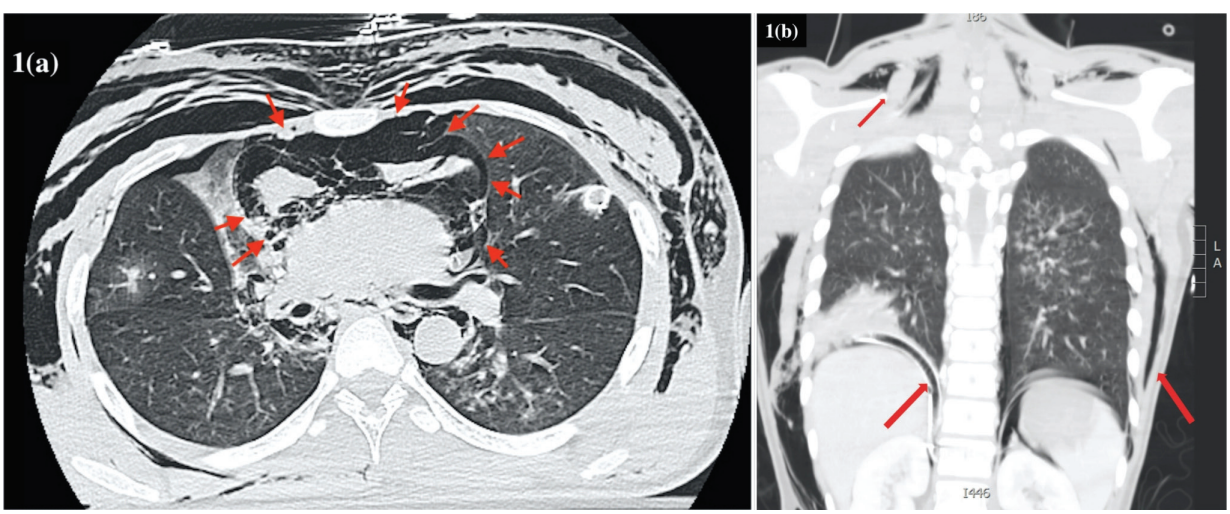

Fig. 1. (a). Computed tomography (CT) of the chest. Day 2 chest CT in the ICU showing diffuse subcutaneous emphysema and severe pneumomediastinum with heart compression (see arrows). (b). Computed tomography (CT) of the chest Day 2 chest CT in the ICU showing air within the bilateral chest wall, shoulder, neck and subdiaphragmatic areas (arrows), which led to a diagnosis of pneumoperitoneum.

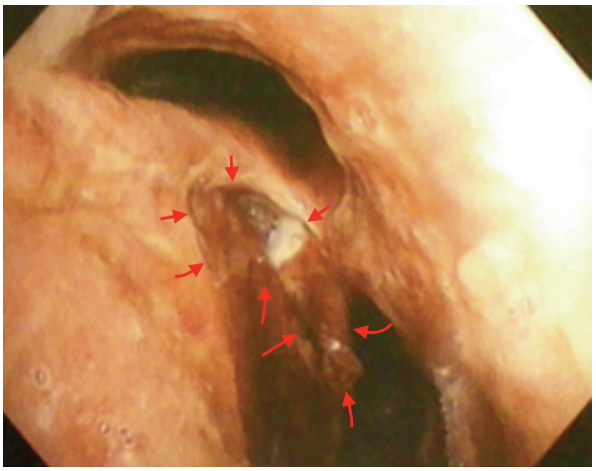

Fig. 2. Bronchoscopic view of the trachea Bronchoscopic examination revealed a significant tracheal defect at the carina level (see arrows) with exposure of the subcarinal soft tissue.

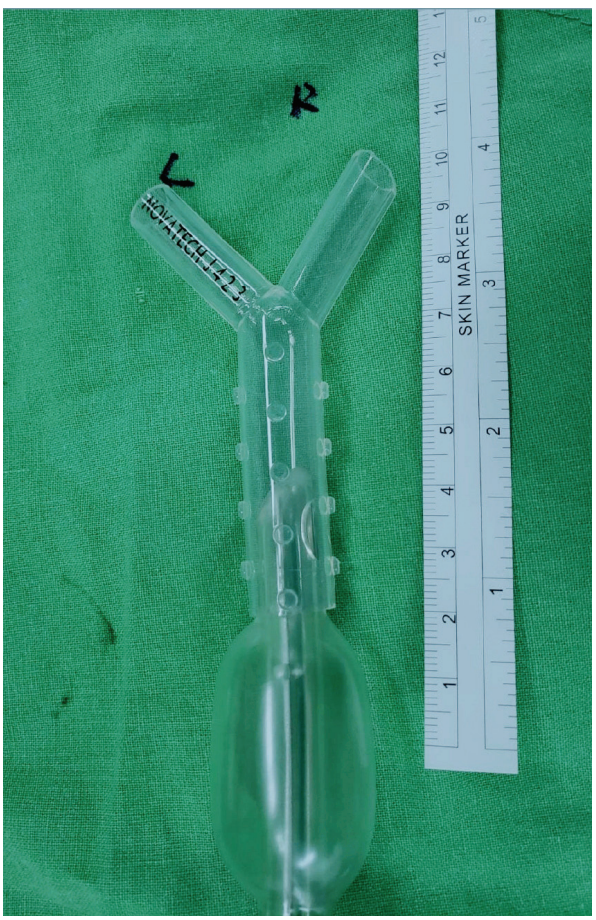

Fig. 3. The Dumon® stent. The Dumon® 150*320 mm Y-shaped silicone stent (Novatech®, La Ciotat, France), which accommodates the 7 Fr endotracheal tube (ETT) tip. Slipping the ETT tip into the stent can avoid permanent injury to the tracheal fistula from persistent positive air pressure from the ventilator.

improved afterward, and he was weaned off ECMO 4 days later.

However, the follow-up chest radiograph 1 day after ECMO removal showed right lung haziness, and an increased oxygen demand was noted again. Bronchoscopic examination revealed a tissue mass obstructing the right distal end of the Dumon® Y-stent. This occurred because the right branch of the Y-stent was inadvertently trimmed too short in attempting to prevent RUL bronchus occlusion. Consequently, we implanted a new stent with an oblique right branch cut, which entirely covered the right main bronchus defect and maintained the RUL bronchus outlet. The patient's respiratory condition was much improved after the new stent implantation.

Once his condition was stabilized, the chest tubes were removed. Endotracheal extubation was performed with bronchoscopic assistance on the tenth postoperative day, after the weaning parameters indicated that the patient was ready to breathe spontaneously. The patient's vital signs and hemodynamics remained stable, allowing us to remove the Dumon® Y-stent after 14 days and discharge him without further complications (Figure 4, 6(a) & 6(b)).

Discussion

Was endotracheal intubation necessary for this patient?

We generally acknowledge that endotracheal intubation should be performed in a patient with impaired consciousness, difficult airways, respiratory failure, or cardiac arrest in the emergency department. In our case, the patient met current guidelines for tracheal intubation in trauma patients [2-3]. The patient had good oxygen saturation (SpO_2 >95 %) and

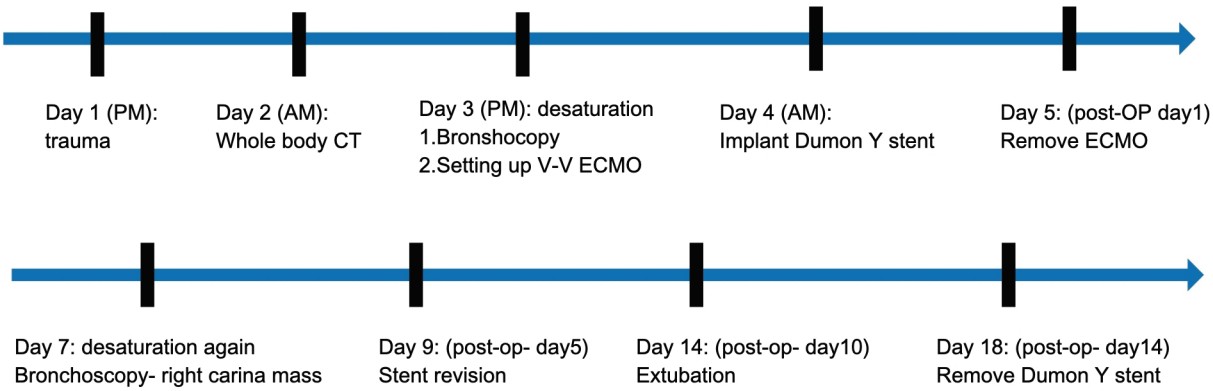

Fig. 4. The timeline of events.

a moderate GCS score (E4V4M5), but he was agitated and disorientated. In order to evaluate the severity of his sustained injuries, further imaging scans were necessary, and emergency surgical treatment could have been required. Further, endotracheal intubation would be helpful in the prevention of vomiting and aspiration [4]. Therefore, we concluded that endotracheal intubation was necessary for this patient.

Emergency intubation may lead to tracheal and bronchial injuries

Tracheal and bronchial injuries (TBIs) are rare but may be life-threatening [1]. TBIs occur between the cricoid cartilage and the tracheal bifurcation into the right and left mainstem bronchus [1]. Traumatic injuries are more common than iatrogenic injuries [5]. The most common causes of iatrogenic TBIs are intubation and tracheotomy. The incidence of iatrogenic injuries is 1 in 20,000 intubations, and is higher in cases with double-lumen intubation, where it occurs in around 0.5% to 1% of cases [6-8].

Risk factors for TBIs can be roughly divided into categories [9], such as gender (female), age >50 years, operator errors (multiple attempts, inexperienced physicians, emergency intubation), errors in equipment selection and use (inappropriate use of stylets, cuff overinflation, malposition of the tube, improper tube size), patient actions (abrupt movements, excessive coughing), and some clinical and anatomical factors (long-term steroid therapy, chronic obstructive pulmonary disease, tracheomalacia, kyphosis, or kyphoscoliosis). All of these factors may increase the risk of tracheal injury.

Clinical manifestations of TBIs include dyspnea, cyanosis, hemoptysis, irritative cough, and subcutaneous and mediastinal emphysema, and their extent is dependent on TBI severity. 5 In cases of pulmonary contusion, obstruction of the airways by blood, secretion, bronchial mucosa edema, and dyspnea may be present. A progressive pneumothorax may block venous return and lead to heart failure. Hemoptysis is usually mild, but can be massive if there is concomitant bronchial artery injury, tracheal fistula, or hemorrhagic shock. Subcutaneous and mediastinal emphysema implies airway perforation and may spread to the abdomen, perineum, and lower extremities. Moreover, air embolism may cause pneumomediastinum and result in compression of the vena cava, which may contribute to heart failure and be life-threatening.

Based on the above, we highly suspected his trachea wall was damaged by the endotracheal tube or the stylet protruding out of the distal end of the tube during intubation.

Timing of diagnostic fiber bronchoscopy

As described above, there are many clues that can be used to identify TBIs. The diagnostic work-up includes history, physical examination, and imaging studies. To identify an injury to the trachea or bronchus, diagnostic imaging in the acute stage is necessary. Depending on availability, a chest radiograph is usually performed first, and can reveal tracheal disruption [5]. A chest CT provides a more characteristic image, but the diagnosis can be masked by pulmonary edema, hemorrhage, or secretions blocking the airway. Bronchoscopy is a good alternative tool to confirm subtle airway injuries that are difficult to perceive, because it facilitates a more accurate injury location than imaging, an exact assessment of injury size and type, and more precise treatment than other imaging tools [5,10,11]. Moreover, if the patient has difficult ventilation that is noticed initially, bronchoscopy should be done as soon as possible to avoid an extension of the emphysema. If there is no conclusive finding in any of these examinations, CT reconstruction may be indicated, under a suspicion of bronchial injury.

Bronchoscopic examination is not available in all health facilities, so it is not a routine examination in the ATLS guideline. Besides, when we perform bronchoscopic examination, a higher oxygen saturation of the patient is required. For these reasons, after careful assessment and evaluation, we decided not to perform bronchoscopy with our patient during the first 3 days.

Early repair of TBIs

In treating TBIs, first aid has to ensure airway patency and support the collapsed trachea. Chest or mediastinal decompression has to be performed. One-lung ventilation with endotracheal tube placement under flexible bronchofiberscopic guidance may sometimes be required. Controlled positive pressure ventilation should be used simultaneously [1]. In cases with difficult airways, emergency tracheostomy or thoracotomy may be considered. With continuous monitoring and management, it should be possible to prevent a deterioration of the clinical condition and reduce the need for ECMO support.

Many studies show that conservative treatment of TBIs after prompt diagnosis can yield a good prognosis. However, the indication for conservative treatment is limited to small injuries with mild symptoms and signs. The tear should be less than 2 cm in length or less than 1/3 of the diameter of a major airway [5]. Another non-surgical intervention consists of endotracheal stent placement, which is traditionally used for airway obstruction. Though short-term symptomatic relief is excellent, there are some long-term complications, including granulation tissue formation, stent migration, infection, and chronic cough.

A silicon Y-stent is used mainly in the distal trachea and mainstem bronchus. Nevertheless, surgical intervention would be appropriate if the stent fails, or if the tear is longer than 4 cm in length. Surgical options include repair, end-to-end anastomosis, a sleeve, lobectomy, and reconstruction. When the length of the tear is between 2 and 4 cm, either conservative treatment or surgery is possible, and the indication should be based on the operators' experience and the patient's condition.

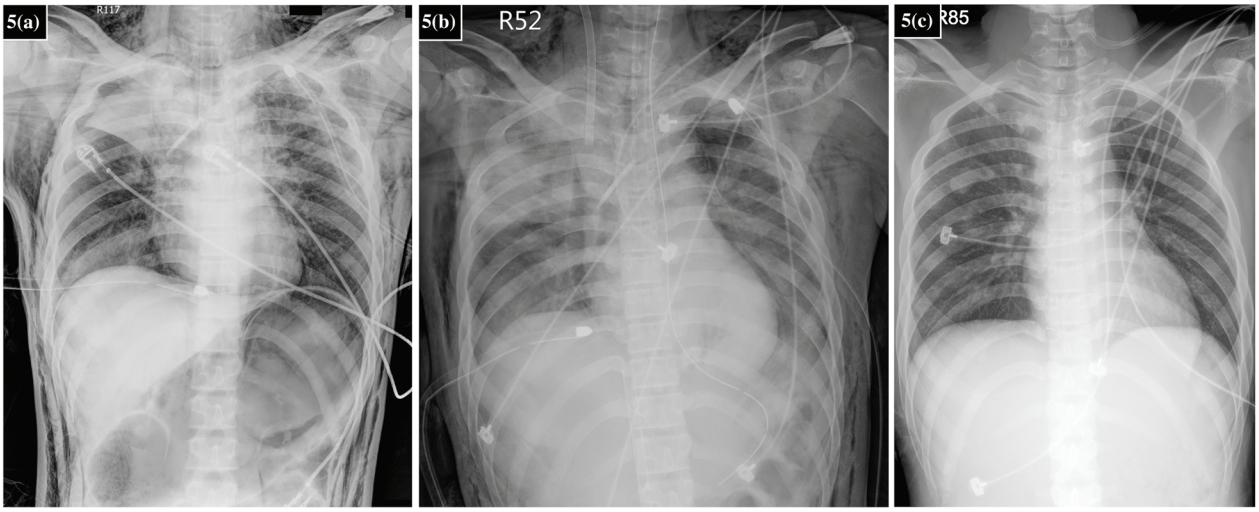

Fig. 5. (a). Chest radiograph after initial resuscitation. The chest radiograph showed severe collapse of the right upper lung, and diffuse subcutaneous emphysema on both sides of the neck, chest wall, and abdominal area, and even in mediastinal sites. (b). Chest radiograph after ECMO. The follow-up chest radiograph showed not only confluent opacities in the right lung and left perihilar region, but also persistent subcutaneous emphysema and pneumomediastinum. (c). Chest radiograph after stent placement. The postoperative chest radiograph showed no emphysematous changes, atelectasis, or further infiltration of the lungs.

Treatment with Dumon® Y-stent

In our case, the chest radiograph after the initial resuscitation showed severe collapse of the right upper lung, and diffuse soft tissue emphysema on both sides of the neck, chest wall, and abdominal area, and even mediastinal sites (Figure 5(a)). Given the continuous deterioration of the patient's respiratory condition, including desaturation (SpO_2 < 80%), 100% oxygen use, tachypnea (respiratory rate > 30 breaths/min), and respiratory acidosis, we decided to use V-V ECMO. Although his respiratory status improved temporarily, the follow-up chest radiograph showed not only confluent opacities in the right lung and left perihilar region, but also persistent subcutaneous emphysema and pneumomediastinum (Figure 5(b)). Since conservative treatment has shown good results recently [12-13], we inserted a Y-stent to bridge the airway defect.

We selected the Dumon® Y-shaped, 150*320 mm silicone stent (Novatech®, La Ciotat, France) based on the CT scan for measuring his trachea diameter and length. In addition, the Y-shaped stent can fully cover the carina defect.

This treatment resulted in improvement of the patient's condition, and the postoperative chest radiograph showed no emphysematous changes, atelectasis, or further infiltration of the lungs (Figure 5(c)). Consequently, we considered that the stent implantation was a successful and timely management. The patient's respiratory parameters had improved compared to the pre-stent period.

Fortunately, the Dumon stent is available in Taiwan, and use of the silicone material will not cause a severe tissue reaction, such as with metal stents. For this reason, this type of stent is suitable for use with patients who have suffered from airway injury during the recovery stage.

The Dumon stent is suggested to be removed around 6 to 8 weeks after implantation. All patients who submit to stent removal should

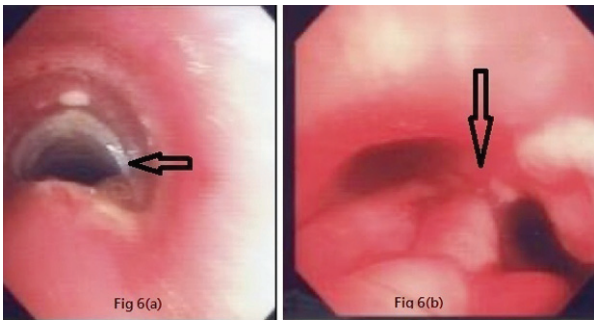

Fig. 6. (a). Bronchoscopic examination on the day of stent removal. The arrow shows the Y-shaped silicone stent in the carina area. (b). Bronchoscopic examination on the day of stent removal. After removal of the stent, we found that the carina defect was healing, and there was some granulation tissue covering the defect area.

undergo periodic clinical and endoscopic examinations. The decision to remove the stent should be based on the operators' experience and the patient's condition. The clinical symptoms and signs, the severity of airway injury, and the patient's age and wound recovery status could also lead to a different timing for stent removal.

Conclusion

In conclusion, if there is pneumomediastinum with or without subcutaneous emphysema following blunt chest trauma or intubation, a high degree of suspicion of TBIs is warranted. CT and bronchoscopy are used in the initial assessment. Management of TBIs includes conservative stent placement and surgical intervention, depending on the length of the tear and the patient's clinical condition. A good prognosis is possible with early diagnosis and treatment.

References

1. Altinok T, Can A. Management of tracheobronchial injuries. Eurasian J Med 2014; 46(3): 209-215.
2. Higgs A, McGrath BA, Goddard C, et al. Guidelines for the management of tracheal intubation in critically ill adults. Br J Anaesth 2018; 120(2): 323-352.
3. Mayglothling J, Duane TM, Gibbs M, *et al*. Emergency tracheal intubation immediately following traumatic injury: an Eastern Association for the Surgery of Trauma practice management guideline. J Trauma Acute Care Surg 2012; 73(5 Suppl 4): S333-340.
4. Sise MJ, Shackford SR, Sise CB, *et al*. Early intubation in the management of trauma patients: indications and outcomes in 1,000 consecutive patients. J Trauma 2009; 66(1): 32-39; discussion 39-40.
5. Zhao Z, Zhang T, Yin X, *et al*. Update on the diagnosis and treatment of tracheal and bronchial injury. J Thorac Dis 2017; 9(1): E50-E56.
6. Borasio P, Ardissone F, Chiampo G. Post-intubation tracheal rupture. A report on ten cases. Eur J Cardiothorac Surg 1997; 12(1): 98-100.
7. Schneider T, Volz K, Dienemann H, *et al*. Incidence and treatment modalities of tracheobronchial injuries in Germany. Interact Cardiovasc Thorac Surg 2009; 8(5): 571-576.
8. Harney TJ, Condon ET, Lowe D, *et al*. A novel technique for repair of iatrogenic tracheal tear complicating three-stage oesophagectomy. Ir J Med Sci 2009; 178(3): 337-338.
9. Gil T, Warmus J, Wlodarczyk J, *et al*. Iatrogenic injuries to the trachea and main bronchi. Kardiochir Torakochirurgia Pol 2016; 13(2): 113-116.
10. Singh S, Gurney S. Management of post-intubation tracheal membrane ruptures: a practical approach. Indian J Crit Care Med 2013; 17(2): 99-103.
11. Barrett E. Management of a traumatic tracheal tear: a case report. AANA J 2011; 79(6): 468-470.
12. Yopp AC, Eckstein JG, Savel RH, *et al*. Tracheal stenting of iatrogenic tracheal injury: a novel management approach. Ann Thorac Surg 2007; 83(5): 1897-1899.
13. Chaaban S, Simoff M, Ray C, *et al*. Posterior tracheal laceration treated with a stent. Ann Am Thorac Soc 2017; 14(7): 1224-1226.

Conservative Management of Tracheal Laceration after Blunt Chest Trauma: A Case Report

Yen-Lin Wu[1], Hwai-Luh Chang[1], Yei-San Hsieh[1]

Tracheal injuries are rare but fatal. Although the prevalence rate is not high, many patients have died before arriving at the hospital. The sooner a tracheal laceration can be diagnosed, the sooner the likelihood of complications and mortality can be reduced. So far, there is no treatment guideline for tracheobronchial injury. In the past, the treatment of tracheal laceration was based mainly on surgical repair. In this case, the patient was diagnosed with chest contusion, tracheal laceration, rib fractures on both sides combined with pneumothorax, and a 4th thoracic vertebral fracture. We observed that the subcutaneous emphysema and pulmonary air leakage improved after placing chest tubes in both sides. Therefore, we chose tracheotomy as conservative treatment. Through active oral cleaning, secretion suction, and administration of broad-effect antibiotics, the patient's damaged trachea showed significant wound healing. After the airway was completely healed, the patient underwent spinal surgery, and was then discharged from the hospital. Therefore, we suggest conservative treatment for spontaneous wound healing as an alternative for patients who refuse surgery or who are at high risk of complications or mortality due to surgery. ***(Thorac Med 2022; 37: 339-343)***

Key words: tracheal laceration, blunt chest trauma

Introduction

Tracheal lacerations can be caused by blunt trauma, penetrating trauma, or iatrogenic injuries such as acute endotracheal intubation [1]. Acute posttraumatic tracheobronchial injuries are rare but potentially life-threatening events, and prompt recognition and treatment are essential to limit morbidity and mortality [1-2]. Subcutaneous emphysema, pneumothorax, and hemoptysis are the most common signs after tracheal injury. Hoarseness and dysphonia are other symptoms that accompany tracheal injury [3]. Herein, we present a case of tracheal perforation after blunt chest injury.

Case report

A 47-year-old male (height, 168 cm; weight, 70 kg) with no significant medical history presented to the emergency room. He suffered from neck pain, chest pain, tachypnea,

[1]Division of Thoracic Surgery, Department of Surgery, Taoyuan General Hospital, Ministry of Health and Welfare, Taoyuan, Taiwan.
Address reprint requests to: Dr. Yen-Lin Wu, Division of Thoracic Surgery, Department of Surgery, Taoyuan General Hospital, Ministry of Health and Welfare, No.1492, Zhongshan Rd., Taoyuan Dist., Taoyuan City 330, Taiwan.

and paraparesis after blunt chest injury. His vital signs were as follows: heart rate: 85 beats/min; respiratory rate: 24 breaths/min; blood pressure: 110/50 mmHg; and initial pulse oximetry saturation of 93%. His Glasgow Coma Scale score was E4V2M4. Significant subcutaneous emphysema at the neck and bilateral anterior chest area was diagnosed.

Computed tomography (CT) examination showed tracheal perforation, pneumomediastinum, multiple rib fractures, bilateral lung contusion with hemopneumothorax, and fourth thoracic vertebra transected fracture (Figure 1, Figure 2 and Figure 3).

We first inserted chest tubes into both lungs for the hemopneumothorax. With rapid worsening of the desaturation and the patient's hemodynamic instability, emergency endotracheal intubation was performed. Then, bronchoscopic examination was carried out, and tracheal laceration was noted at the posterior aspect of the carina. The size and depth of the tracheal injury were less than 2 cm and there was a partial

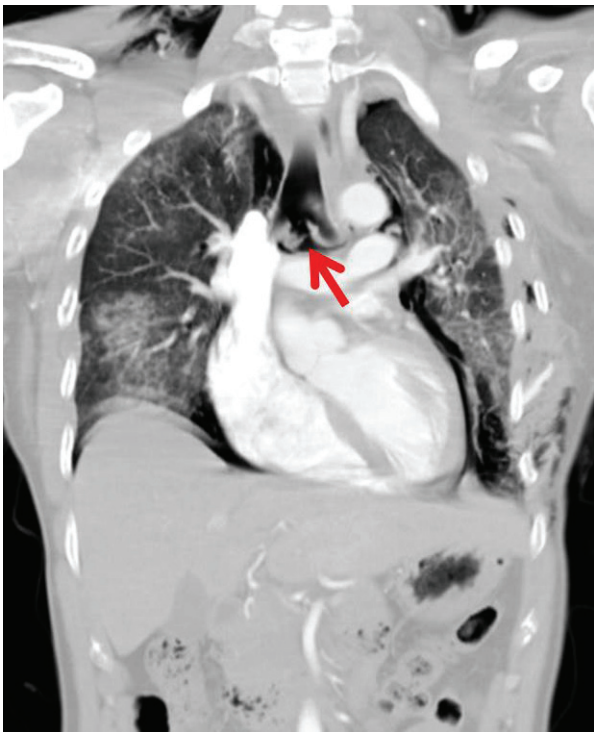

Fig. 2. Initial chest CT (axial view). Red arrow: tracheal perforation (carina area).

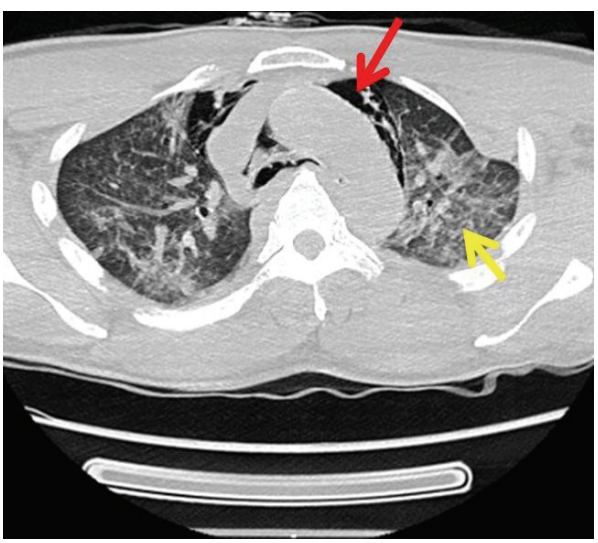

Fig. 1. Initial chest CT (axial view). Red arrow: pneumomediastinum. Yellow arrow: lung contusion.

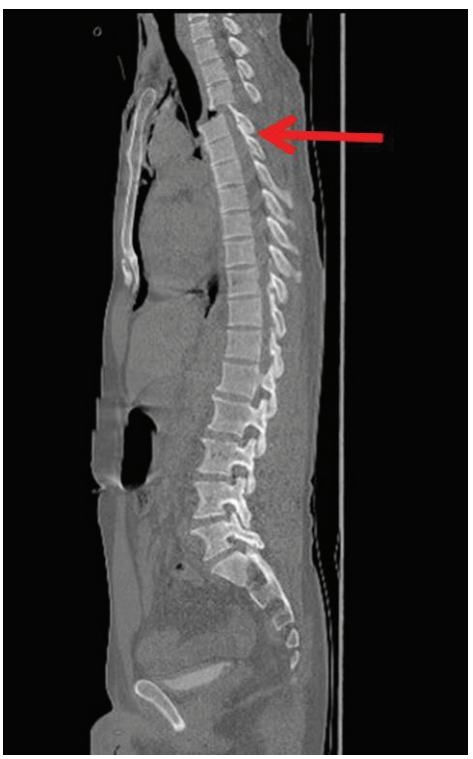

Fig. 2. Initial thoracic spine CT (sagittal view). Red arrow: fourth thoracic vertebra transected fracture.

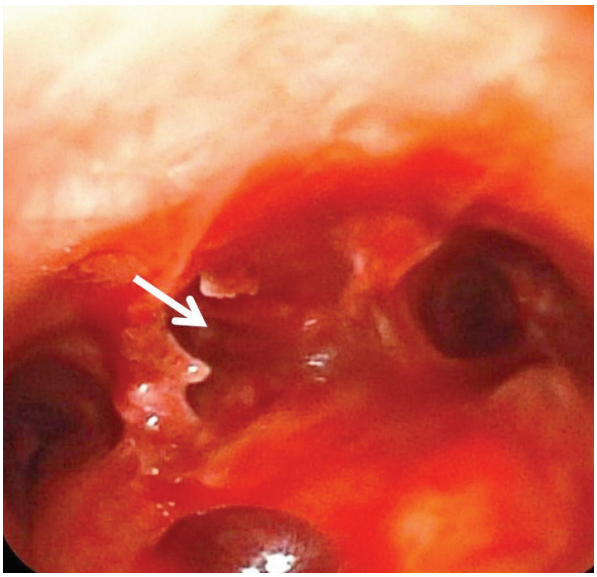

Fig. 4. Initial bronchoscopy examination finding: tracheal laceration at the posterior aspect of the carina. White arrow: the laceration wound at the carina.

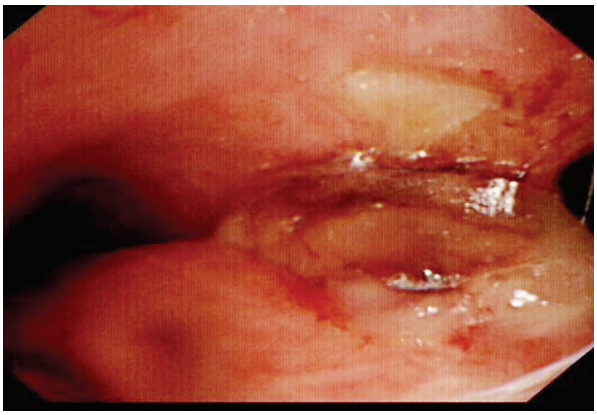

Fig. 5. Day 14 after chest injury: significant wound healing with a slight scar remaining.

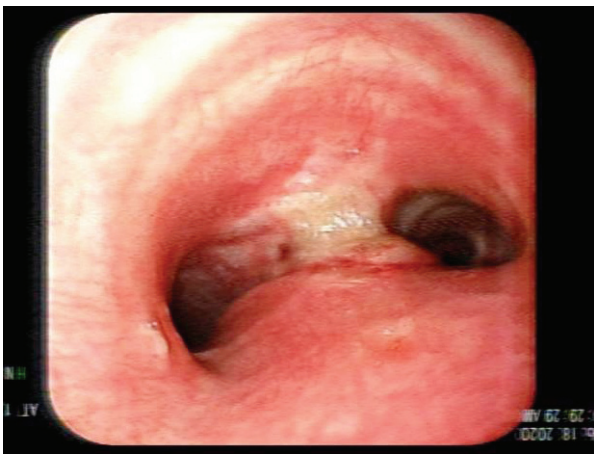

Fig. 6. Day 25 after chest injury: wound is almost healed with scar resolution and no airway stenosis.

full-thickness tear (Figure 4). Under the impression of tracheal laceration, we decided to perform tracheostomy to build a stable airway and facilitate wound healing with active secretion suction. Fortunately, spontaneous wound healing improved without the need for surgical repair. On day 7 after the blunt chest injury, the mechanical ventilator was weaned smoothly. On day 14, the wound was healing with scar formation (Figure 5). By day 25, wound healing was complete and there was no airway narrowing (Figure 6).

Discussion

Tracheal laceration is a rare but life-threatening injury. Timely recognition and treatment are important to reduce morbidity and mortality [1]. However, there is little series data available to establish a guideline for the treatment of tracheobronchial injury. Surgery has been the traditional choice of treatment. A previous study reported that mortality and morbidity are not higher in surgical repair than in conservative treatment for more severe tracheal rupture [4]. Most institutes determine the treatment modality based on the criteria of size, vital signs, spontaneous breathing, adjacent organ injury, subcutaneous emphy¬sema, and sepsis.

So far, there is no definitive guideline for using surgical or conservative treatment for tracheal injury. Still, reports have shown that conservative treatment plays a critical role in

some selected patients with tracheal injury. For example, a previous report showed that conservative management was an effective treatment, particularly for patients with iatrogenic lesions [5]. Other reports found that spontaneous wound healing of tracheobronchial injuries in patients with non-esophageal injury showed a good prognosis [6, 7]. In addition, Leoncinii, G., et al. suggested that conservative treatment can play a significant role, even in cases with wide tracheal lacerations [8]. Conservative treatment is also particularly indicated in patients with stable respiratory parameters independent of the size and depth of the lesion [9, 10]. Based on the literature, we have compiled several indications for conservative treatment, as follows: 1) hemodynamic stability, 2) spontaneous ventilation, 3) no esophageal injury, 4) non-progressive pneumomediasti¬num with/without subcutaneous emphysema, and 5) no signs of sepsis [11-14].

With our case, we decided to use conservative treatment because the subcutaneous emphysema and air leak were improved after chest tube insertion. The wound size was less than 2 cm, and there was no wound gap during ventilation. Vital signs were stable with no sepsis. Thus, we implemented conservative treatment by providing a proper wound bed with the use of adequate broadly effective antibiotics, complete oral hygiene, and secretion suction. On day 25 after the blunt chest injury, wound healing was complete with no airway narrowing. We succeeded in treating the patient through spontaneous wound healing.

Tracheal injury after blunt chest injury is not common, but it has a high rate of mortality. Early diagnosis can reduce mortality and morbidity. In addition to clinical symptoms, image surveys such as CT and bronchoscopy can help confirm the tracheal laceration.

Although the choice of management is controversial, we suggest that conservative treatment is an alternative choice for patients who are determined to have small lacerations, an absence of signs of an ongoing infection, stable vital signs, decreasing subcutaneous emphysema post-chest tube implantation, and no esophageal injury. Moreover, complete oral hygiene, proper section suction, and adequate broadly effective antibiotics therapy are essential for tracheal injury patients when undergoing wound healing with conservative treatment.

References

1. Minard G, Kudsk KA, Croce MA, et al. Laryngotracheal trauma. Am Surg 1992; 58(3): 181-7.
2. Kiser AC, O'Brien SM, Detterbeck FC. Blunt tracheobronchial injuries: treatment and outcomes. Ann Thorac Surg 2001; 71(6): 2059-65.
3. Karmy-Jones R, Wood DE. Traumatic injury to the trachea and bronchus. Thorac Surg Clin 2007; 17(1): 35-46.
4. Lee SK, Kim DH, Lee SK, et al. Does surgical repair still have a role for iatrogenic tracheobronchial rupture? Clinical analysis of a thoracic surgeon's opinion. Ann Thorac Cardiovasc Surg 2016; 22(6): 348-53.
5. Carretta A, Melloni G, Bandiera A, et al. Conservative and surgical treatment of acute posttraumatic tracheobronchial injuries. World J Surg 2011; 35(11): 2568-74.
6. Conti M, Pougeoise M, Wurtz A, et al. Management of postintubation tracheobronchial ruptures. Chest 2006; 130(2): 412-8.
7. Minambres E, Buron J, Ballesteros MA, et al. Tracheal rupture after endotracheal intubation: a literature systematic review. Eur J Cardiothorac Surg 2009; 35(6): 1056-62.
8. Leoncinii G, Iurilli L, Boni L, et al. Treatment of iatrogenic and traumatic tracheal disruptions. Monaldi Arch Chest Dis 2008; 69(3): 119-27.
9. Gomez-Caro Andres A, Ausin Herrero P, Moradiellos

Diez FJ, et al. [Medical and surgical management of noniatrogenic traumatic tracheobronchial injuries]. Arch Bronconeumol 2005; 41(5): 249-54.
10. Kuhne CA, Kaiser GM, Flohe S, et al. Nonoperative management of tracheobronchial injuries in severely injured patients. Surg Today 2005; 35(7): 518-23.
11. Jougon J, Ballester M, Choukroun E, et al. Conservative treatment for postintubation tracheobronchial rupture. Ann Thorac Surg 2000; 69(1): 216-20.
12. Beiderlinden M, Adamzik M, Peters J. Conservative treatment of tracheal injuries. Anesth Analg 2005; 100(1): 210-4.
13. Martin de Nicolas J, Gomez-Caro Andres A, Moradiellos Diez FJ, et al. [Importance of routine mediastinal staging in women with non-small cell lung cancer]. Arch Bronconeumol 2005; 41(3): 125-9.
14. Cardillo G, Carbone L, Carleo F, et al. Tracheal lacerations after endotracheal intubation: a proposed morphological classification to guide non-surgical treatment. Eur J Cardiothorac Surg 2010; 37(3): 581-7.

Dilemma of Difficult Airway Management in a Patient with COVID-19: Case Report and Literature Review

Suey-Haur Lee[1], Wen-Feng Fang[1]

Aerosol and fomite transmission of SARS-CoV-2 is possible, since the virus can remain infectious in aerosols for hours. This dangerous situation exists, especially, during the intubation and extubation of patients with COVID-19. However, many modalities used for difficult airway management are not suitable for use during the current pandemic. Herein, we report on the dilemma and our experience with difficult airway management in a patient with COVID-19. ***(Thorac Med 2022; 37: 344-350)***

Key words: Difficult airway; Covid-19

Case Report

A 63-year-old man with a medical history of hypertension and newly diagnosed diabetes mellitus traveled to Turkey from March 4 to March 13, 2020. Upon his return, he was quarantined in our airborne infection isolation rooms with negative room pressure, according to Taiwan Centers for Disease Control guidance, because of close contact with confirmed COVID-19 cases. The patient tested positive for severe acute respiratory syndrome coronavirus 2 (SARS-CoV-2) using real-time reverse transcriptase-polymerase chain reaction (rRT-PCR) with an oropharyngeal swab after admission. His body mass index was 29 (body weight: 80 kilograms, height: 166 centimeters) and he had a short neck (Figure 1).

The patient had been well until 4 days after admission. He then began experiencing fever off and on, fatigue, and malaise. Dyspnea progressed rapidly on day 10, despite non-rebreather oxygen mask support. Chest radiography and arterial blood gas confirmed acute respiratory distress syndrome. Laboratory tests revealed white blood cell count: 11.5x1000/uL, lymphocyte count: 14.7%, D-dimer: 1.31 mg/L (<0.5, PE & DVT exclusion), ferritin: 1508.1

[1]Division of Pulmonary and Critical Care Medicine, Kaohsiung Chang Gung Memorial Hospital, Kaohsiung, Taiwan. Address reprint requests to: Dr. Wen-Feng Fang, Division of Pulmonary and Critical Care Medicine, Kaohsiung Chang Gung Memorial Hospital, Kaohsiung, No. 123, Dapi Rd., Niaosong Dist., Kaohsiung City 833401, Taiwan (R.O.C.).

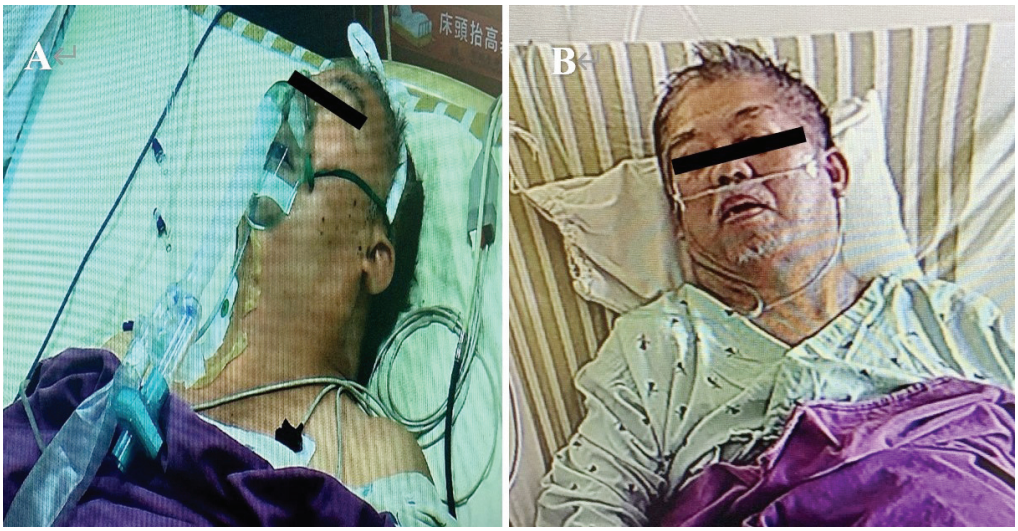

Fig. 1. External look after extubation. Difficult airway with restricted mouth opening and short thyromental distance. (Panel A) First day of extubation (Panel B) One week after extubation.

ng/mL (22-322), CRP level: 132.1 mg/L (<5), and LDH: 321 U/L (135-225). Blood gas analysis disclosed hypercapnic acidosis (pH 7.299, pCO_2 64.2 mmHg, pO_2 64.4 mmHg, HCO_3 30.8 mmol/L) and a PF ratio of 107.3 mmHg. Therefore, he was transferred to an intensive care unit (ICU) equipped with negative room pressure, a remote-control panel and a monitor of the mechanical ventilator for intubation.

Intubation was attempted by an experienced anesthesiologist with full personal protective equipment (PPE) including an N95 mask with face shield. Rapid sequence intubation was performed with a video-assisted laryngoscope and avoidance of Ambu bagging due to possible aerosol spreading. Medication used for rapid sequence intubation included propofol as an induction agent and recuronium as a neuromuscular blocking agent. However, intubation attempts failed due to an anatomically difficult airway accompanied with severe laryngeal edema. During each of 4 failed attempts, the hypoxia period was partially corrected using a laryngeal mask temporarily to support the oxygen. However, due to paralysis as a result of sedation and the muscle relaxant, temporary ventilatory support was urgently warranted. Therefore, a laryngeal mask airway (LMA) was initiated for bridging until further airway management was established (tracheal intubation or tracheostomy).

Even though this maneuver maintained temporary mechanical ventilation, the tidal volume could not be secured, and a nasogastric tube could not be used (these are important for antiviral medicine administration). Emergency cricothyroidotomy was considered with a prepared surgery team, but aerosol spreading during the operation and wound care after the procedure would be quite dangerous. We decided to use a fiber-optic bronchoscope to assist in intubation, although this is not suggested in the guideline for intubation of COVID-19 patients for fear of aerosol production during the procedure. Due to severe laryngeal edema and severe hypoxemia in this patient with an LMA in situ, a 6.5-mm inner diameter endotracheal tube was successfully inserted via the nose with fiber-optic bron-

Fig. 2. Equipment used with endotracheal intubation. (Panel A) Video-assisted laryngoscope (Panel B) Fiber-optic bronchoscope (Panel C) Training intubation with Pentax AWS and 'intubation' box (Panel D) Personal protective equipment with a powered air-purifying respirator worn by the team during intubation and extubation.

choscope guidance (Figure 2).

Because of persistent hypercapnia due to a low tidal volume and small-sized endotracheal tube, we tried to emplace a larger-sized endotracheal tube via the oral route using fiber-optic bronchoscopic guidance 4 days after nasotracheal intubation. The attempt failed due to persistent laryngeal edema. After 3 weeks of ventilator support, the patient's condition improved. Prior to tracheal extubation, a modified cuff

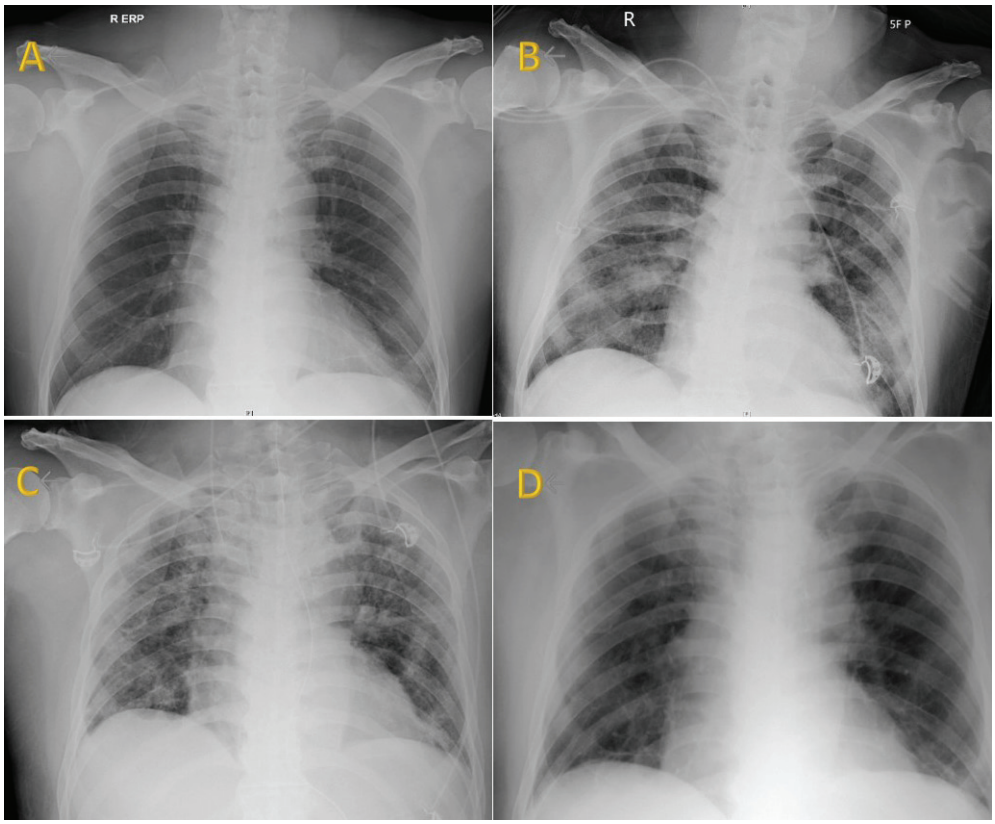

Fig. 3. Serial chest plain films during the disease course (Panel A) First day of admission (Panel B) 10 days after admission (Panel C) Extubation after 22 days of mechanical ventilator support (Panel D) After 2 months.

leak test was performed to exclude the possibility of immediate upper airway obstruction and avoid the risk of aerosol-generation. The cuff pressure was not routinely checked. However, we kept the cuff pressure as low as possible to reduce possible laryngeal edema. We also prescribed low-dose corticosteroid before extubation, for this patient with exceedingly difficult airway management. We allocated the use of a powered air-purifying respirator (PAPR) to our staff during tracheal extubation, and also made equipment for high-flow nasal oxygen (HFNO) and cricothyroidotomy available in the ICU. The patient was extubated successfully and finally was able to tolerate oxygen mask support. The SARS-CoV2 PCR did not turn negative during extubation, but it did 9 days later. The series of chest plain films during the disease course are presented in Figure 3.

Discussion

Intubation of critically ill patients with COVID-19 is associated with a high risk of transmission to the healthcare worker. The procedure should be attempted by the most skilled person using a rapid sequence intubation technique to optimize success. Our patient`s short thyromental distance and restricted mouth opening predicted a difficult airway for intubation. Even though the procedure was performed by a most experienced operator, the course was not smooth. Since we lowered the threshold for intubation of patients with COVID-19 infec-

tion, we had enough time to deal with the difficult airway. Use of a video laryngoscope with a separate screen that enables the operator to stay farther from the orifice of the airway is recommended [1].

Flexible bronchoscopy techniques are likely to be aerosol-generating and therefore more potentially infectious, but they are recommended in the COVID-19 Taiwan Critical Care Consensus Guideline. Difficult intubation prediction should be individualized, and various preventive measures should be prepared in advance [2-3]. The situation is complicated in patients with a difficult airway and COVID-19 infection, because we need to care for patients and protect health workers at the same time. Patients with COVID-19 infection may be predisposed to laryngeal edema, as in our case, although no direct evidence is available. In addition, performing cricothyroidotomy can increase the risk of virus exposure to the surgical team and the nurses during post-tracheostomy care.

In this case, and after failed trials, we chose the minimized aerosol-generating procedure, nasotracheal intubation with flexible bronchoscopy techniques. Remaining with the patient for more than a half hour during intubation was worrisome, but our colleague tested negative for SARS-CoV-2 with an oropharyngeal swab after the procedure.

Our institution allocated PAPR to staffs, so as not to expose them to risk under any circumstance. We suggest all personnel caring for these patients must use appropriate airborne/droplet PPE, including a fit-tested N95 mask and PAPR. During the intubation procedure, especially, this helps to avoid the misting up of the glasses of medical personnel when wearing a face shield. We should avoid aerosol-generating procedures (e.g., bag-valve-mask (BVM) bagging) during intubation. In our experience, a supraglottic airway device (e.g., LMA) for airway rescue is appropriate, if the first tracheal intubation fails.

After this difficult intubation event that we experienced, our institution prepared more equipment for us to use, such as an 'intubation' box and Pentax Airway Scope (AWS) video laryngoscope; however, we need time to become familiar with this equipment.

Endotracheal intubation is frequently complicated by laryngeal edema, which may present as post-extubation stridor or respiratory difficulty, or both [4-6], but no evidence of SARS-CoV-2 as the cause of laryngeal edema has been reported. Use of a high-flow nasal cannula (HFNC) for hypoxemic COVID-19 patients may avoid intubation, and reduce the need for invasive ventilation and escalation of therapy compared with conventional oxygen therapy. This benefit must be balanced against the unknown risk of airborne transmission [7-8].

A study suggested that an HFNC significantly reduces the need for intubation and subsequent invasive mechanical ventilation, but does not affect case fatality [9]. We prepared an HFNO because it could also provide positive end expiratory pressure to overcome upper airway obstruction due to laryngeal edema after extubation, although it was not used in the end. Two randomized trials led by Hernandez *et al*. [10-11] found that HFNC was superior to conventional oxygen (nasal cannula or facemask) in low-risk patients, and not inferior to noninvasive ventilation in high-risk patients in preventing post-extubation respiratory failure in a general ICU, so an HFNC may be used if the SARS-CoV2 RT-PCR is negative when the patient is extubated.

One of our hospital branches also encoun-

tered a difficult intubation, and that patient with confirmed COVID-19 underwent urgent cricothyroidotomy. Our case suggests that intubation with the aid of a fiberscope may prevent that complication.

As for predicting upper airway obstruction after extubation, our team found that a reduced cuff-leak volume may signal the presence of severe laryngeal edema in patients on long-term mechanical ventilation [12]. However, deflating the tube cuff should be considered an aerosol-generating procedure, and should be performed safety with PPE and PAPR support.

Professional society guidelines discouraged bronchoscopy in patients with COVID-19, because bronchoscopy exposes healthcare workers by generating aerosols, but this recommendation was based only on expert opinion [13-15]. A study suggested that the risk of transmitting COVID-19 to providers performing bronchoalveolar lavage (BAL) is low, and they also found that bronchoscopy was not associated with increased seropositive rates [16]. While the optimal role for COVID-19 BAL remains to be determined, these data suggest that BAL can be safely performed in intubated COVID-19 patients if experienced providers take precautions to limit aerosol generation and wear PPE. Another study also suggested that intubation of COVID-19 patients can benefit from specific bronchoscopic management, of which, guided mini-BAL can be of help to confirm a clinical suspicion of superinfection [17].

In conclusion, we must prepare well in advance for difficulties during tracheal intubation and extubation. A supraglottic airway device can be used for bridging, and flexible bronchoscope-assisted intubation may be helpful with difficult airway management in patients with COVID-19.

References

1. Lewis SR, Butler AR, Parker J, *et al*. Videolaryngoscopy versus direct laryngoscopy for adult patients requiring tracheal intubation: a Cochrane Systematic Review. Br J Anaesth 2017; 119: 369-383.
2. Cook TM, El-Boghdadly K, McGuire B, *et al*. Consensus guidelines for managing the airway in patients with COVID-19: Guidelines from the Difficult Airway Society, the Association of Anaesthetists the Intensive Care Society, the Faculty of Intensive Care Medicine and the Royal College of Anaesthetists. Anaesthesia 2020; 75: 785-799.
3. Wax RS, Christian MD. Practical recommendations for critical care and anesthesiology teams caring for novel coronavirus (2019-nCoV) patients. Can J Anaesth 2020; 67: 568-76.
4. Pluijms WA, van Mook WN, Wittekamp BH, *et al*. Postextubation laryngeal edema and stridor resulting in respiratory failure in critically ill adult patients: updated review. Crit Care 2015; 19: 295.
5. McGrath BA, Wallace S, Goswamy J. Laryngeal oedema associated with COVID-19 complicating airway management. J Anaesthesia 2020; 75: 972.
6. Brodsky M, Levy MJ, Jedlanek E, *et al*. Laryngeal injury and upper airway symptoms after oral endotracheal intubation with mechanical ventilation during critical care: a systematic review. Crit Care Med 2018; 46: 2010-7.
7. Li J, Fink JB, Ehrmann S. High-flow nasal cannula for COVID-19 patients: low risk of bio-aerosol dispersion. Eur Respir J 2020; 55: 2000892.
8. Agarwal A, Basmaji J, Muttalib F, *et al*. High-flow nasal cannula for acute hypoxemic respiratory failure in patients with COVID-19: systematic reviews of effectiveness and its risks of aerosolization, dispersion, and infection transmission. Can J Anaesth 2020; 67: 1217-1248.
9. Demoule A, Vieillard Baron A, Darmon M, *et al*. High-flow nasal cannula in critically III patients with severe COVID-19. Am J Respir Crit Care Med 2020; 202: 1039-1042.
10. Hernandez G, Vaquero C, Colinas L, *et al*. Effect of postextubation high-flow nasal cannula vs noninvasive ventilation on reintubation and postextubation respiratory

failure in high-risk patients: a randomized clinical trial. JAMA 2016; 316: 1565–1574.
11. Hernandez G, Vaquero C, Gonzalez P, *et al*. Effect of postextubation high-flow nasal cannula vs conventional oxygen therapy on reintubation in low-risk patients: a randomized clinical trial. JAMA 2016; 315: 1354–1361.
12. Chung YH, Chao TY, Chiu CT, *et al*. The cuff-leak test is a simple tool to verify severe laryngeal edema in patients undergoing long-term mechanical ventilation. Crit Care Med 2006; 34: 409-14.
13. Tran K, Cimon K, Severn M, *et al*. Aerosol generating procedures and risk of transmission of acute respiratory infections to healthcare workers: a systematic review. PLoS One 2012; 7.
14. Wahidi MM, Lamb C, Murgu S, *et al*. American Association for Bronchology and Interventional Pulmonology (AABIP) Statement on the Use of Bronchoscopy and Respiratory Specimen Collection in Patients with Suspected or Confirmed COVID-19 Infection. J Bronchol Interv Pulmonol 2020; 27: 52-54.
15. Wahidi MM, Shojaee S, Lamb CR, *et al*. The use of bronchoscopy during the Coronavirus disease 2019 pandemic: CHEST/AABIP Guideline and Expert Panel Report. Chest 2020; 158: 1268-1281.
16. Walter JM, Coleman JM, Malsin ES, *et al*. Bronchoscopy on intubated COVID-19 patients Is associated with low infectious risk to operators. Ann Am Thorac Soc 2021; 18: 1243-1246.
17. Torrego A, Pajares V, Fernández-Arias C, *et al*. Bronchoscopy in patients with COVID-19 with invasive mechanical ventilation: a single-center experience. Am J Respir Crit Care Med 2020; 202: 284–287.